DEVELOPMENT AND EVALUATION OF SUPERCONDUCTING CIRCUIT ELEMENTS

FINAL REPORT

to

National Aeronautics and Space Administration
Langley Research Center
Hampton, VA 23665-5225

Principal Investigator:
Gene Haertling

Co-Investigator:
Burtrand Lee

Supporting Investigators:
Dennis Hsi
Vibhakar Modi
Matt Marone

Contract No. NAG-1-820   October 31, 1990

College of Engineering

DEPARTMENT OF CERAMIC ENGINEERING

CLEMSON
UNIVERSITY

DEVELOPMENT AND EVALUATION OF SUPERCONDUCTING CIRCUIT ELEMENTS

FINAL REPORT

to

National Aeronautics and Space Administration
Langley Research Center
Hampton, VA 23665-5225

Principal Investigator:
        Gene Haertling

Co-Investigator:
        Burtrand Lee

Supporting Investigators:
        Dennis Hsi
        Vibhakar Modi
        Matt Marone

Contract No. NAG-1-820   October 31, 1990

Table of Contents

SUMMARY

A new approach to the application of high Tc ceramic superconductors to practical circuit elements was developed and demonstrated. This method, known as the rigid-conductor process (RCP), involves the combinaton of a pre-formed, sintered and tested superconductor material with an appropriate, rigid substrate via an epoxy adhesive which also serves to encapsulate the element from the ambient environment. Emphasis of the effort focused on the practical means to achieve functional, reliable and reproducible components. Although all of the work described in this report involved a $YBa_2Cu_3O_{7-x}$ high Tc superconducting material, the techniques developed and conclusions reached are equally applicable to other high Tc materials.

The specific accomplishments for FY-90 are:

1. Developed, tested and evaluated the rigid superconducting/ substrate concept as a new technique for fabricating practical superconducting components such as conducting links, coils and hybrid circuit elements.

2. Established (1) an oxide process capable of producing homogeneous and reproducible $Yba_2Cu_3O_{7-x}$ (123) high Tc ceramic materials, (2) a tapecasting technique for fabricating the flexible pre-forms and (3) a sintering method to reliably produce the rigid superconducting material diplaying the Meissner effect and possessing a Tc greater than $90^\circ K$.

3. Demonstrated techniques for splicing and/or joining the 123 superconductor with no loss in superconducting properties.

4. Developed methods for terminating the high Tc superconducting ceramic with very low electrical resistivity (2×10^{-9} ohm-cm^2) contacts and connectors.

5. Evaluated and selected epoxy encapsulants suitable for protecting the high Tc ceramic superconductor from the environment and also capable of providing additional rigid support to the circuit element.

6. Developed flexible high Tc superconducting composites which could be applied to electromagnetic shielding and Meissner magnetic bearing applications

7. Demonstrated the achievement of a melt textured 123 superconducting material with a critical current in excess of 1000 A/cm^2.

8. Developed an acetate-derived, chemically processed, sol-gel process for fabricating high Tc superconducting thin films.

I. Introduction

This report details work that was carried out over the period from July 1, 1989 to September 30, 1990 in the ceramic engineering department of Clemson University under NASA contract no. NAG-1-820. The work is part of the final phase of a three-year program entitled "Superconducting Wire Fabrication." In the period covered by this report, the emphasis of work shifted away from a flexible-wire approach to a rigid-conductor concept. Consequently, the work reported here deals exclusively with the various aspects of this promising new technology.

In principle, the rigid-conductor (RCP) concept is quite simple and is tailor-made to take advantage of the inherent desirable properties of the superconducting ceramics while at the same time recognizing the fundamental brittleness of these materials. This is accomplished by pre-forming, sintering and testing the ceramic superconductor prior to bonding it to a rigid supporting substrate which is then totally encapsulated for further support and environmental protection. This approach has the advantages of (1) pre-testing of the superconducting material separate from the substrate, (2) optimization of the superconductivity development (oxygen stoichiometry) in the ceramic without temperature limitations imposed by the substrate, (3) wider selection of substrate materials, particularly those of low thermal conductivity, since the high temperature processing step precedes mounting to the printed circuit board, (4) freedom from firing shrinkage and other material compatibility problems and (5) high anticipated reliability because of its simplicity, rigid design and total encapsulation from the environment.

All of the superconducting materials work covered in this report involved the high Tc (95K) ceramic superconductor composition $Yba_2Cu_3O_{7-x}$ (designated as 123). This material was selected because it was judged to be the most fully characterized of all the ceramic superconductors developed in the industry; i.e., it has been the most researched of all the materials within the last two years and has been found to have a readily attainable, relatively stable and reasonably reproducible superconducting phase. Research work on the two other known high Tc oxide superconducting systems (Bi-Sr-Ca-Cu-O and Tl-Ba-Ca-Cu-O) will be carried out under a separate contract effort.

II. Objectives

The objectives of the proposed work are to develop and demonstrate the feasibility of fabricating rigidly supported, environmentally protected superconducting circuit elements such as (1) conductors, (2) coils, (3) connectors and (4) crossovers on dielectric substrates for microelectronic applications.

(2)

One such application toward which a major effort has been directed during this period is in the development of a low-noise, superconducting, grounding link for a remote infrared detector (SAFIRE). The technology developed under this project, however, should be applicable and adaptable to a wide range of devices.

III. Scope of Work

The overall scope of the work carried out during this period is given below. It is divided into two major areas; i.e., (A) superconducting material fabrication and (B) grounding link device development with a special section (C) describing special work on composites and thin film superconductors. As can be seen, there are numerous facets to this endeavor and these will be discussed under separate headings.

Rigid Superconducting Circuit Elements

A. 123 Superconducting Material Fabrication

    1. 123 Composition
       a. Basic Composition ($Y_1Ba_2Cu_3O_{7-x}$)
       b. Additives (Ag_2O)
       c. Raw Material Qualification

    2. 123 Powder Processing
       a. Mixed Oxide and Chemical Processing
       b. Calcining Schedule and Oxygen Atmosphere

    3. Tapecast Technology
       a. Binder Type and Binder Loading
       b. Study of Release Agents for Tape/Glass System

    4. Special Firing Techniques
       a. Firing Circuit Patterns
       b. Coil Firing Techniques (1" dia.)
       c. Splicing and Lamination

B. Grounding Link Device Development

    1. Component Design
    2. Substrates (Alumina, Plexiglas, Fiber reinforced epoxy)
    3. Electrodes/Connectors (Ag paste; Ag, Au, Pd, Pt foil)

4. Encapsulants (Envirotex Epoxy, UV Curing, RTV)
            5. Performance Testing (Resistance, Tc, Thermal cycle, Drop,
                                    Water immersion, Long term in LN$_2$)

C. Special Studies

            1. Composites
            2. Thin Films

        Although some of the grounding links have been fabricated as
long ago as one year ago and some real time results can be
extracted from them, it is anticipated that the long term effects
(vacuum outgassing, superconducting phase stability, radiation
hardness, resistance change, etc.) on this material, and
particularly this device, will be studied in detail under separate
contract work.

        In addition to the major thrust of the work mentioned above,
two areas of particular interest were singled out for more in-depth
research. These are (1) development of practical, low resistance
contacts to the 123 material and (2) development of high Jc
(critical current) tapecast 123 material They are included in this
report as special topics and are appended to the report as separate
sections.

                        IV. Experimental

A. Material Fabrication

1. YBa$_2$Cu$_3$O$_{7-x}$ Superconducting Materials

        Since the objectives of this work were to emphasize the
fabrication and evaluation of superconductor components rather than
the development of new compositions, it was decided to select the
123 material as the base composition for all of the subsequent
work. This material was selected because, to date, it has been
thoroughly researched by many investigators and much is already
known about its chemical composition and stoichiometry (oxygen
content), its X-ray structure, its mechanical properties, and its
electrical and superconducting behavior. In addition, quite a
number of institutions have also demonstrated that this composition
can be prepared relatively easily and with reproducible
characteristics. Several properties of interest for the 123
material are given in Table I.

                            (4)

Table I.

Properties of Bulk 123 Superconductor

Composition: $YBa_2Cu_3O_{6.7-6.9}$
Crystal Structure: Orthorhombic
Unit Cell: a = 3.83, b = 3.88,
                                      c = 11.71 Angstroms
Theoretical Density: 6.38 g/cc
Nominal Fired Density: 5.53 g/cc (86.7%
                                                theo.)
Thermal Expansion (50-500°C):   11.5/°C
Thermal Conductivity (77K)   2.7 W/m-K
Specific Heat   0.431 J/g-K
Transition Temperature (Tc)   92 K
Critical Current   1000 A/cm^2

Note: Data taken from product literature of ICI Advanced
       Ceramics, ICI Americas, Inc., Wilmington, DE, 19897

The special effects and properties of many electronic ceramic
materials are often significantly influenced by the raw materials
(particle size, distribution, reactivity, impurities, etc.) used in
their preparation. This has been found to be the case also with
the high Tc superconducting ceramics where the existence or non-
existence of superconductivity can sometimes be a fleeting
phenomena. With this in mind, several products from various
vendors were checked in regard to their suitability (Meissner
effect) and availability as raw material sources of the Y_2O_3, $BaCO_3$
and CuO. The results showed that Fisher Scientific, Johnson
Matthey, Molycorp, Chemical Products Corp. and Alfa all qualified
as sources of their respective products; however, Aldrich did not
and was subsequently eliminated as a vendor.

A typical batch consisted of 500 grams of oxides and
carbonates blended in the following proportions:

Material	Weight
Y_2O_3	85.8 g
$BaCO_3$	299.8
CuO	181.3

Note: The total weight of the raw batch is greater than 500 g
       because barium carbonate loses CO_2 during calcining.

In addition to the above, selected batches of 123 were
prepared with various amounts (7.5 and 15 m/o) of Ag_2O added as a
second phase in order to (1) enhance the sintering of the 123
material, (2) improve the electrode contact to the superconductor

(5)

and (3) increase the Jc characteristics of the material.

The composition targeted as the insulating crossover material for the superconductor was a 211 formulation; i.e., Y_2BaCuO_{5-x}, the so-called green phase, which is not superconducting but in most every other way was is compatible with the black superconducting 123 phase. Its batch formulation was:

Material	Weight
Y_2O_3	246.2 g
$BaCO_3$	215.2
CuO	86.7

2. Process Description

A flowsheet description of the rigid-conductor process, as it is presently being employed in the fabrication of the superconducting grounding links, is given in Figure 1. The process shown in the figure involves all of the major steps, starting from the basic raw materials and finishing with a tested element. All of the steps through sintering are included in the Scope of Work (A) section above while the remaining steps are associated with (B) above. Although a mixed-oxide process for powder preparation (before tapecasting) is presented in the flowsheet, a chemically prepared powder could also be used with similar results.

The flowsheet of Figure 1 shows that the starting materials for the preparation of the superconducting powders are composed of yttrium and copper oxide in combination with barium carbonate. After drying in an oven for several hours at 100°C to remove adsorbed moisture, the materials are weighed, wet blended with distilled water, oven dried and calcined (a high temperature reaction process) at 900°C for 5 hours in air or oxygen. The calcined powder is then ground in a mortar and pestle or ball milled in order to break apart the agglomerated particles. This two-step operation of calcining and milling is repeated two additional times for maximum homogeneity of the chemical composition of the powder. Visually, this homogenizing operation is quite easy to detect since there is a progressive change in the color of the powder from dark green (non-superconducting 211 tetragonal phase) to jet black (superconducting 123 orthorhombic phase). After three calcines, the existence of the desirable 123 orthorhombic phase is definitely confirmed by means of X-ray diffraction analysis. Following the third calcine, the powder is ball milled for one hour in trichloroethylene with alumina grinding media, oven dried and stored for subsequent use.
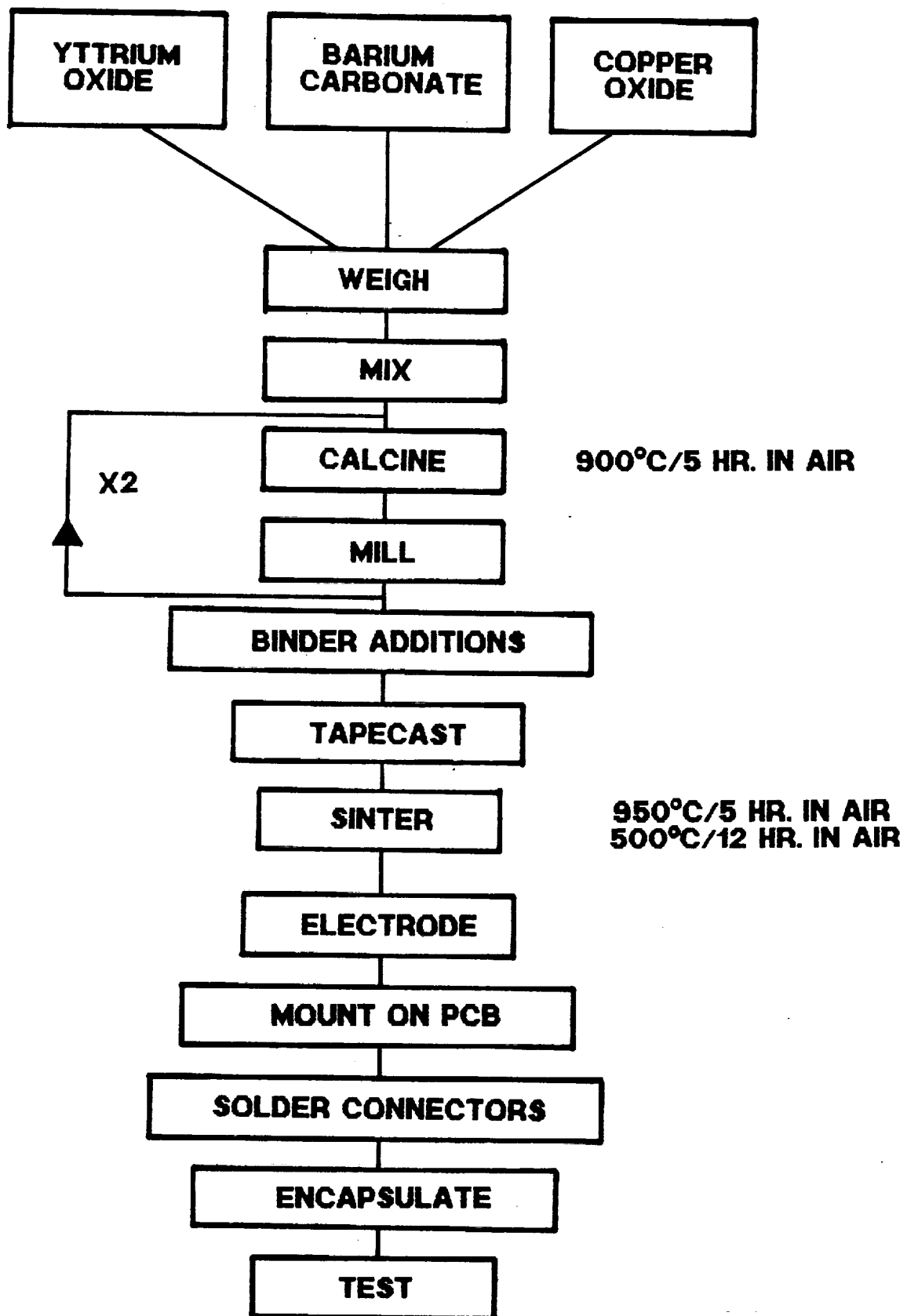
(6)

Figure 1. Flowsheet for processing and fabrication of $YBa_2Cu_3O_{7-x}$ superconducting circuit element.

Prior to the tapecasting operation, appropriate polymeric binders, dispersants and solvents are added to the ceramic powder to form a moderately viscous but freely flowing liquid mixture which is cast onto a glass, metal or plastic surface by means of a doctor blade with an adjustable gap for precisely controlling the thickness of the cast tape. After drying, the flexible tape is stripped from the casting surface and stored or it is cut into strips or other desired shapes for subsequent processing.

A typical firing setup consists of placing the 123 superconductor parts on a clean, porous zirconia setter plate inside the furnace chamber which is sufficiently large to allow for free exchange of air and/or oxygen. The firing schedule involves an initial heating rate of $5^{\circ}C$/minute to $920^{\circ}C$, a 12 hour hold at temperature, a $5^{\circ}C$ cooling rate to $450^{\circ}C$, a 12 hour hold at $500^{\circ}C$ and a final cool in the furnace at its natural rate with the power off. When superconducting elements other than simple strips are fired, it has been found to be beneficial to fire the elements on green tape of the same composition in order to compensate for the simultaneous length and width shrinkage.

The 123 superconductor material is very sensitive to the sintering process; i.e., heating rate, sintering temperature, hold time, sintering atmosphere (oxygen is desirable), cooling rate and oxygen anneal at $450^{\circ}C$ on cooling. If sufficient oxygen is not available on sintering and annealing, superconductivity (as evidenced by the Meissner effect and resistance vs. temperature) will not be achieved.

After sintering, the parts (e.g., thin strips) are brittle and relatively fragile but generally do exhibit enough flexibility for ordinary handling purposes. The strips are then cut to length with a diamond scribe and electroded on both ends with fired-on, high density conductive silver paint (Heraeus/Cermalloy #8710) which is subsequently fired at $900^{\circ}C$ for 12 minutes. Producing low resistivity electrical contacts to the 123 material has proven to be a real challenge, requiring special techniques and careful consideration for cleanliness. The 8710 silver electrode material possesses a minimum of sintering aids yet still achieves an excellent ohmic contact to the 123 material. Contact resistivities of 1×10^{-7} or better are now routinely obtained. Similar contact resistivities are also obtained with silver foil pads which are fired on during the sintering of the 123 material; however, the differential shrinkage between the foil and the 123 causes bowing of the part in the contact area and makes this technique somewhat less appealing.

At this stage in the process, evaluation of the fired material for superconductivity consists of two tests; i.e., (1) a 1"x1"x1/4" thick pressed part is checked for the Meissner (magnetic levitation) effect and (2) a tapecast strip is tested for critical

(7)

current (Jc) using a 4-point probe technique. Examples of the Meissner test for superconductivity and various photomicrographs of the fired 123 materials are given in Figure 2. Selected results of tests conducted on parts sent to R. Caton, Christopher Newport College, are given in Figure 3 and Table II. More recent data on critical current shows that Jc values of 200-300 A/cm2 are now more standard.

The end-electroded superconductor strips are temporarily mounted onto pre-cut printed circuit board (uncoated PCB) strips to which gold-plated connectors are attached. Once in place, the end electrodes are permanently joined to the gold-plated connectors with a low melting Pb-Sn solder. Care must be exercised at this state in order to prevent overheating of the fired-on Ag pads which can eventually lead to leaching and debonding of the Ag electrode from the superconductor.

The last step in the fabrication process is the encapsulation operation. This involves the slow and careful application of a bead of bubble-free epoxy (or other encapsulant) along the length of the printed circuit board. Capillary action then causes the epoxy to impregnate the superconductor and to flow between the superconductor and the circuit board as well as above the superconductor such that a bubble-free envelope of the superconductor is obtained. In this case, the epoxy encapsulant serves both to seal the superconductor from the environment and also to bond the superconductor to the PCB. A final cure of the epoxy at 110°C/1hr. then produces an integral, rigid structure.

Testing of the parts is carried out as part of the final evaluation of the device. In general, these tests consist of:

1. Resistance vs. Temperature - Tc
2. Critical current - Jc at 1 uV/mm
3. Thermal shock - room temperature to 77K for 10 cycles
4. Extended Exposure at 77K - immersion in LN_2 for 2 days
5. Drop testing - on to a concrete floor from 3 feet
6. Moisture sensitivity - immersion in water for 24 hours
7. Inspection for visual flaws and cosmetics

Typical examples of various superconductor element configurations are shown in Figure 4. These include the various lengths of grounding links, coils, Ag contact pads, connnector configurations, superconductor splice, tapecast and cut strip, bare 123 fired strips, pressed and sintered parts, surface mounted capacitor on a superconductor hybrid circuit, and superconductor/polymer parts (upper right) for future magnetic/superconducting bearing applications.

(8)
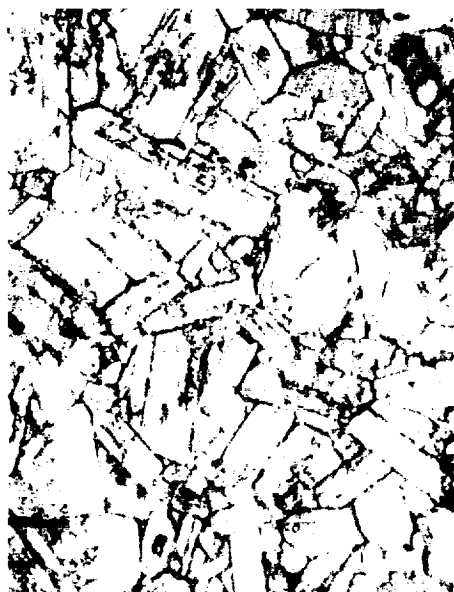
FIRED SLUG (OPTICAL, x1000)

FIRED SLUG (SEM, x700)

MEISSNER EFFECT

FIRED TAPE (SEM, x700)

Figure 2. Meissner effect and microstructures of superconducting materials. The microstructures show that very little grain orientation is present in the fired tapes.
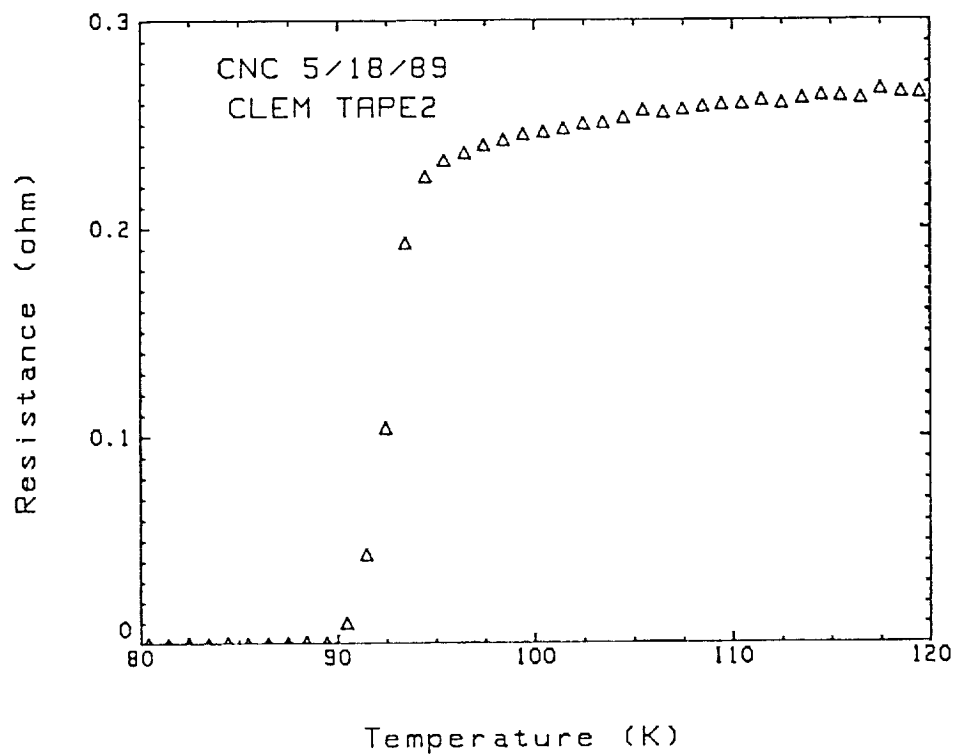
CNC 5/18/89
CLEM TAPE2

Figure 3. Tc curve for 123 fired tape measured by R. Caton at Christopher Newport College.
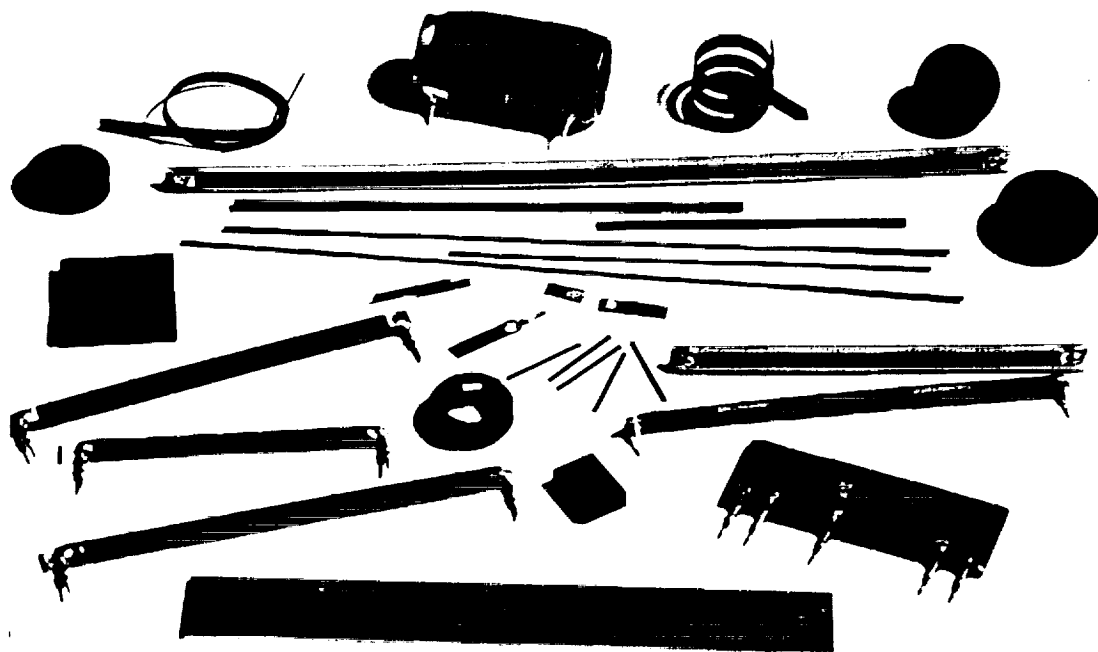
Figure 4. Typical examples of 123 superconducting circuit elements.

Table II.

Selected Results of Tests on 123 Tapecast Superconductor
(measurements by R. Caton, CNC)

SAMPLE	DESCRIPTION	Jc(A/cm2)BEFORE	Tc(K)BEFORE	TREATMENT	Jc(A/cm2)AFTER	Tc(K)AFTER
1 A	FROM 12 BARS	1.3	9 0	O2 (950 °C)	2.2	89.5
1 B	FROM 12 BARS	NOT MEASURED	NOT MEASURED	O2 + Au BEAD	2.7	8 4
2 A	SPLICE	0.2	9 1	O2 (950 °C)	4.8	8 8
2 B	SPLICE	1.5	88.5	O2 + Au BEAD	1 2	8 7
3 A	Ag CONTACT	1.4	87.5	O2 (700 °C)	1.8	8 9
3 B	Ag CONTACT	1.3	8 5	O2 (700 °C)	1.9	8 9
4 A	123 WITH Ag	2.1	9 0	O2 (950 °C)	13.8	89.5
4 B	123 WITH Ag	NOT MEASURED	NOT MEASURED	O2 + Au BEAD	BROKEN	BROKEN
5 A	Ag/SPLICE	NOT MEASURED	8 8	O2 (950 °C)	BROKEN	BROKEN
5 B	FROM 5A	NOT MEASURED	NOT MEASURED	O2 + Au BEAD	9 4	89.5
5 C	FROM 5A	1.6	90.5	NOT TREATED		

3. Tapecast Technology

The successful application of the tapecasting technique to a particular materials technology depends to a large extent on the specific binders selected for the tape, itself, as well as the solvents, dispersants and plasticizers used to modify the properties of the tape. Factors of concern here are:

1. Powder wetting by the binder
2. Powder suspension (deflocculation) by the binder
3. Wet tape viscosity
4. Dry tape flexibility
5. Powder/binder loading
6. Tape separation from the casting surface
7. Binder burnout characteristics (temperature, residue).

Several binders were evaluated in the course of the work carried out under this contract. These were typical binders normally used in the multilayer capacitor industry, which consisted of polyvinyl butyrate (Metoramics 73305, 73210, 73171), PMMA (polymethyl methcrylate) and acrylic (Rohm and Haas B72). The first group of binders from Metoramic Sciences, Inc. are industrially prepared, proprietary formulations which already contain the necessary dispersants, plasticizers and solvents. The latter two groups consist of only the binder, and consequently, the complete formulation is prepared in house. A typical in-house formulation is:

B72 (50% solids)	30 parts by weight
Santicizer 160 (Monsanto plasticizer)	7
Toluene	30
Mehadan Fish Oil	1
123 Superconductor powder	150

This tape strips very well when cast on a teflon surface, it dries to a thickness of 29 mils when cast at a thickness of 50 mils. It is very flexible and easy to handle. It has a solids/total binder loading ratio of 69.1 percent by weight.

The prepared binders from Metoramics are also quite easy to use and produce a consistently good product. The 73305 formulation is specially made to be used for casting relatively thick substrates such as we are attempting under this contract. A typical batch formulation for this binder is:

Binder 73305	80 parts by weight
123 Superconducting powder	150

The tapecasting operation is shown schematically in Figure 5 and in practice in Figure 6. A thin layer of wet, ceramic tape
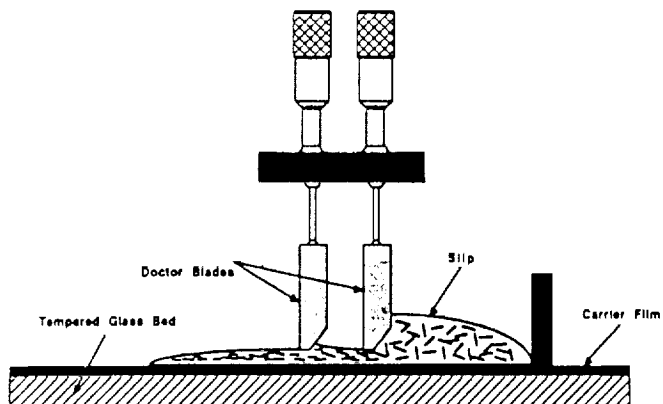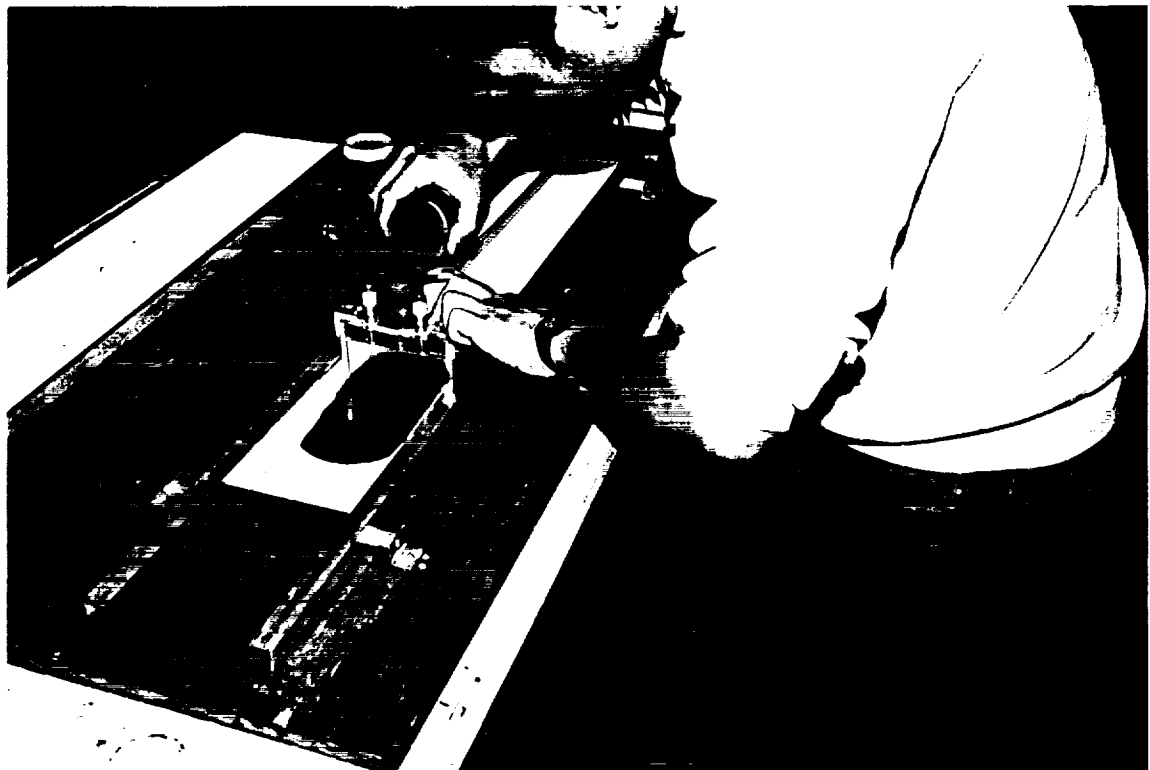
(9)

Figure 5. Schematic illustration of the tapecasting operation.

Figure 6. 123 superconducting material being tapecast.

(about the viscosity of molasses) is laid down on a casting surface by moving the doctor blade assembly containing the ceramic slip over the casting surface in a slow and uniform manner. The thickness of the tape in its wet form containing all of the solvents and in its dry form with the solvents evaporated is directly dependent on the gap between the doctor blade and the flat casting surface. In general, the dry tape thickness will be approximately 55-60% of the as-cast (wet) thickness. A 50-mil thick tape will usually be dry enough after 6 hours to remove from the casting surface.

The stripping characteristics of the dry tape from the casting surface is a very real concern when casting on glass. Glass is a popular (it is cheap, flat and scratch resistant) and convenient (readily available) casting surface, but unfortunately, most binder/ceramic formulations tend to adhere quite firmly to the glass after drying. A parting agent is often beneficial but not always totally successful. It can sometimes be added to the binder formu-lation, but most often, is more effective when applied as a very thin coat to the casting surface. Our studies with the Metoramic and Rohm & Haas binders have shown that a dilute solution of Mehadan fish oil in trichloroethylene is effective for the Metoramic 73305 and a dilute solution of silicone grease in trichloroethylene works well with the Rohm & Haas B72. It has also been demonstrated that either binder can be used without a parting agent when a teflon casting surface is employed. It should be remembered, however, that in the case of teflon, troublesome scratches can readily occur in the casting surface.

Polyethylene and mylar films were also evaluated in regard to their suitability as casting surfaces for the binders used in this study. Neither of these were judged to be suitable because of a reaction between the binder solvent and the film which caused unde-sirable warping of the tape.

4. Special Firing Techniques

a. Firing Circuit Patterns

As mentioned previously under the section on Process Description, the flexible tape, after casting and drying, can be cut into any desired shape with a suitable instrument such as a knife, shears or punch. For the grounding link, this shape is a simple strip cut to a uniform width; however, in the case of hybrid circuits, a more complex set of conductor patterns is usually required.

In such an instance as a two-dimensional hybrid circuit pattern, special care must be exercised in the firing operation in order to preserve the length-to-width aspect ratio of the element

(10)

as well as to prevent any warping during the firing when shrinkages in the order of 15-20% are experienced. A technique which is commonly used to address this problem is to fire the circuit pattern on an additional piece of unfired tape which shrinks in all directions identically to the pattern, itself, thus preserving the geometry of the pattern after firing. This technique was successfully employed to produce a sample hybrid circuit with a surface mounted capacitor as part of the element.

b. Coil Firing Techniques

Coils (1-inch diameter) were fabricated by first cutting the flexible, unfired tape into long strips and then winding the strip at a selected pitch around a high density alumina tube acting as a mandrel. The tube/tape assembly was placed in the furnace and supported in a elevated position such that the tape was free to shrink around the alulmina mandrel during firing. A slight tension was imparted to the tape during firing by allowing the two extended ends of the tape to hang a couple of inches below the centerline of the alumina mandrel.

When initially winding the flexible tape on the alumina mandrel, it is important to do it in a uniform manner with a minimum of tension. Each succeeding winding can be placed immediately adjacent to the preceding one since the eventual firing shrinkage will insure that a gap between the coils develops after firing.

Subsequent to final cooling of the furnace, the now rigid coil is removed from the alumina mandrel by simply slipping it carefully off the end of the tube. After triming the ends, the coil is ready for electroding, mounting and encapsulation.

An example of a fired coil prior to electroding and mounting is shown in Figure 7. Also included in the figure is a multi-turn flat coil which was fired with a tapecast insulating layer (211 green composition as the crossover material) in between the superconducting layers. This latter coil was fired as one integral element with connections to the 123 material via Ag foil pads; however, the 211 insulating material was observed to have cracked in several places, probably due to differential firing shrinkage.

Although this technique appears simple in concept, it is somewhat difficult to put into practice with a high yield. Often, the coil will break into two or more sections during firing because too little allowance was made for the firing shrinkage or the coil will distort on the mandrel during firing because of gravitational effects. Altogether, the method was judged to be practical only for small, simple, one-layer coils.
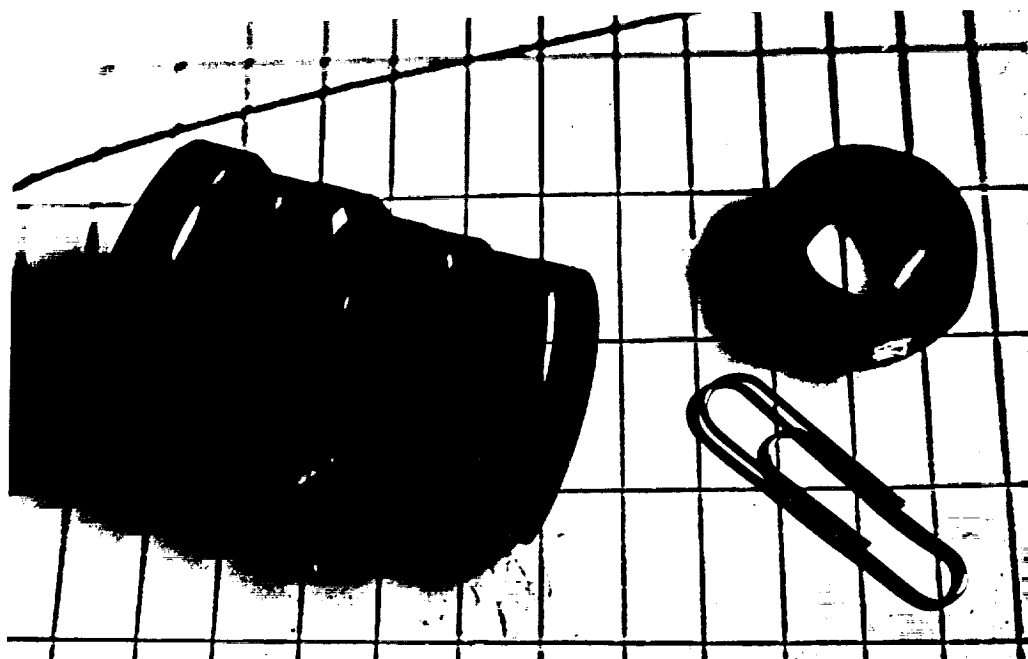
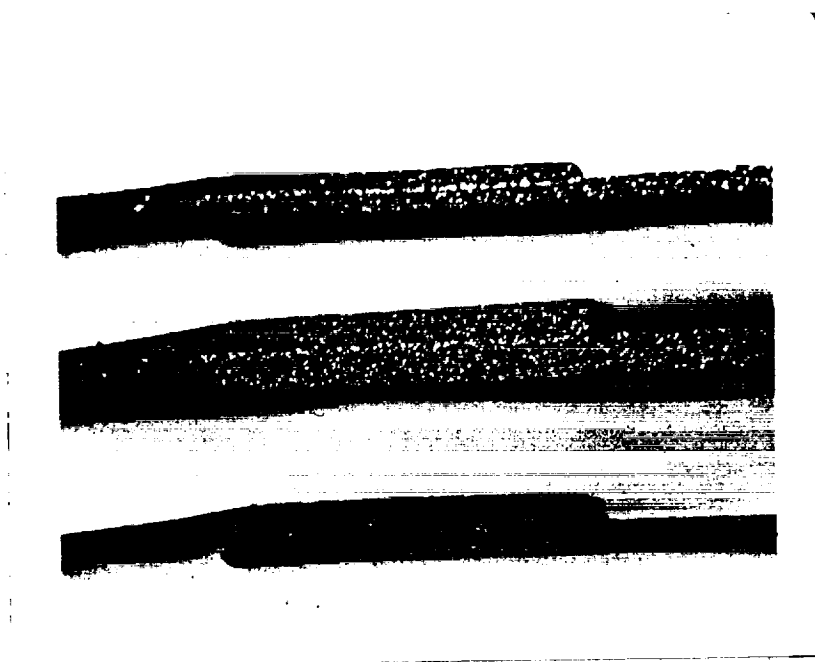Figure 7. Typical coils fabricated from 123 superconducting tape.

Figure 8. Fired lap joints of 123 superconducting tapes - the top
two tapes contained Ag_2O additive whereas the bottom
tape was pure 123 material.

c. Splicing and Lamination Techniques

As the techniques for producing superconductor elements are developed, there is an accompanying need to develop methods for splicing and repairing these conductors in the field. As a first step in this process, it was decided to test for the presence of superconductivity across a simple lap joint formed from two tapecast superconducting strips which were joined in the green state with the aid of a small amount of trichloroethylene solvent, dried and then fired as usual. Cross sections of the 123 joints after firing, as shown in Figure 8, revealed little or no distinguishable line of demarcation in the joint area for the pure 123 material, but there did appear to be some segregation of the Ag along the join line for the two Ag_2O containing tapes. From a microstructural strandpoint, these results are very promising. Attempts to laminate two or more layers of tapes together with subsequent firing resulted in equally promising results.

The electrical results from the lap joint of the pure 123 (Figure 8) material is given in Figure 9. As can be seen, the lap joint alone is very similar in behavior to the pure tape, itself, which is shown in Figure 10, with the exception that the joint displays a slight "tail" at the transition temperature resulting in a slightly lower Tc temperature for complete loss of resistance; i.e., 88K vs. 92K.

Attempts were also made to splice together two fired strips of 123 material by sandwiching a small strip of unfired tape between the two fired strips in the lap joint area and then refiring the joined part. This also worked quite well with similar electrical results.

B. Device Development

1. Component Design

The superconducting gounding link is very simple in design and structure, consisting of a fired and electroded, straight element which is soldered to gold-plated or silver foil termination connectors, mounted to a substrate and encapsulated in a rigid epoxy. Figure 11 shows the various parts which go to make up the total elements as well as the finished elements themselves. Typical sizes of the conducting links are:

length = 4.35 inches
width = 0.23   "
height = 0.10   "

which utilizes a fired ceramic superconducting strip with a cross section of 0.125 inches wide x 0.015 inches thick.
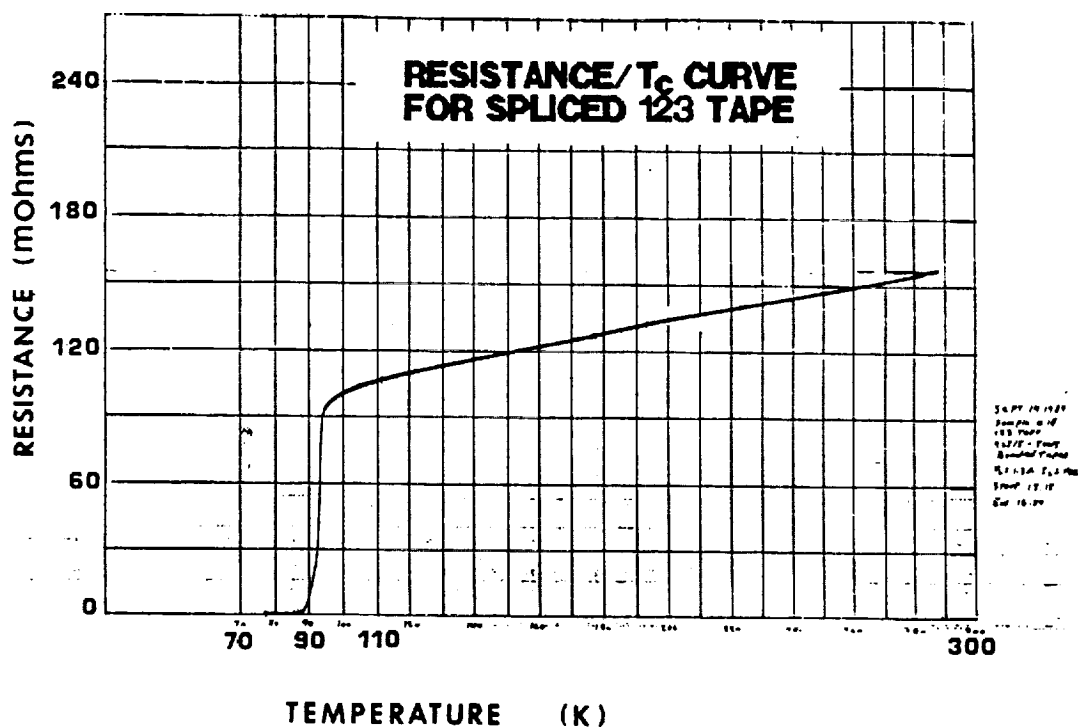
(12)

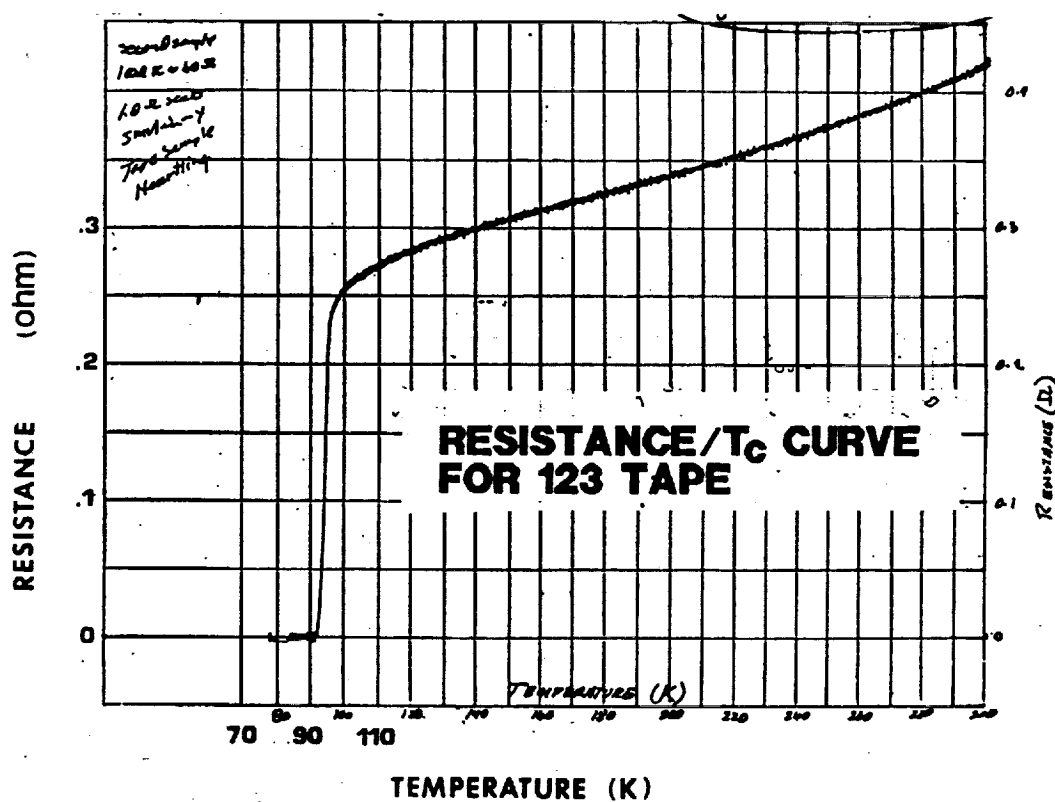Figure 9. Tc curve for spliced (lap joint) 123 superconducting tape.

Figure 10. Tc curve for pure 123 superconducting tape.

Figure 11. Various component parts of the grounding link shown in
foreground; finished grounding links in the background.

Figure 12. A close-up photograph of the various end configurations
of the electrodes and the encapsulant; the top two and
the bottom element show inverted electrodes and the
newly designed square end, the third from top shows a
normal electrode/pin configuration with square end, and
the fourth from top is the old original design.

A close-up of the various types of end electrodes and connectors is given in Figure 12. Early designs utilized a top, Ag fired-on electrode which was soldered to a Au-plated pin using a low temperature melting Pb-Sn solder, whereas, more recent styles either place the electroded pad on the bottom side of the conductor next to the substrate or the electrode connection is made via an embedded Ag foil which sandwiched and fired in between a double laminated conductor strip. These configurations are still under test but they show excellent promise and serve to eliminate a troublesome area; i.e., the Ag contact pad, which seems to initiate debonding of the encapsulant after extended exposure to liquid nitrogen.

Also shown in the close-up of Figure 12 is the recently modified encapsulant end configuration. Rather than utilizing a smooth, rounded end configuration which was often found to leave the solder/electrode pad area depleted of encapsulant, the new design consists of a squared-off end with a semicircular cross-section. This end style is considered to be an improvement over the first designs in that it provides more encapsulant where it is needed most; i.e., at the ends, for both sealing and adhesion.

2. Substrates

Several substrates were initially investigated as possible rigid support materials for the 123 superconductor. Among these were alumina, glass, Plexiglas, non-reinforced printed circuit board (PCB) and glass fiber reinforced epoxy PCB. For various and different reasons, including the primary one of thermal expansion mismatch, all of the candidate materials were eliminated as a suitable substrates with the exception of the latter; i.e., the glass fiber reinforced PCB. Its thermal expansion of $16 \times 10^{-6}/°C$ is slightly higher than that of the 123 material ($11.5 \times 10^{-6}/°C$), and this makes it ideal as a support material in that it places the 123 in slight compression on cooling down to $77°K$. Other factors which also make this material desirable are (1) high strength, (2) fairly high rigidity, (3) low thermal conductivity and (4) ready availability.

The specifications and description of the glass fiber reinforced PCB is included in Appendix A of this report. A compilation of some properties of interest are:

Source:	Westinghouse	
Tensile Strength:	36,000	psi
Flexural Strength:	60,000	psi
Flexural Modulus:	3×10^{6}	psi
Linear Thermal Expansion:	16×10^{-6}	/°C
Thermal Conductivity:	0.2	W/m-K
Dielectric Constant:	4.7	
Volume Resistivity:	1×10^{14}	ohm-cm
Water absorption (24hr/RT)	0.09	%

3. Electrodes

It is extremely important that good, minimal resistance, electrical contact be made to the superconducting material in order to prevent joule heating in the contact area which, in turn, causes the material temperature to rise above its Tc with subsequent loss of superconductivity. This can be accomplished via judicious selection of the electrode material as well as by paying careful attention to the method of application.

The first material selected as an electrode for the 123 was a DuPont fired-on Ag, composition 7095, which contained a few percent of glass frit in order to facilitate sintering of the Ag particles at a low temperature of $550°C$. Although this material produced an electrode with a good visual appearance, it proved to be inadequate because it resulted in a relatively high contact resistivity ($1x10^{-3}$ ohm-cm^2) compared to other techniques.

The second material studied was Ag foil (5 mil thick) which was applied to the ends of the 123 strips by first cutting the foil into 0.15"x0.50" tabs, drilling holes in the tabs at one end for better adhesion of the tab to the 123, setting the tabs firmly in place with the aid of trichloroethylene solvent which was used to soften the 123 strips, laying down a matching top 123 strip superimposed on the bottom one, drying, and finally, firing as usual. This laminated assembly with the end-protruding Ag tabs is shown in Figure 13. The electrical characteristics of this tape/tab assembly are quite satisfactory as given in Figure 14. The residual resistance of the element was 0.02 mohm (20 uohm) which resulted in a calculated contact resistivity of 2.9 x 10^{-6} ohm-cm^2. These data were confirmed by independent measurements made by Dr. R.Caton of Christopher Newport College and are shown in Figure 15.

An attempt was made to combine the ease of application of the fired-on silvers (painting, spraying, screening) with the excellent electrical contact characteristics of the metal foils by evaluating a special fired-on, high density Ag composition (Heraeus Cermalloy 8710) possessing only very minimal additives which are designed to achieve intimate "molecular bonding". The results of these tests exceeded our expectations in that not only was the electrode easy to apply and con-venient to fire onto the sintered 123 material ($900°C$ for 12 minutes), but it also produced lower contact resistivities (1 x 10^{-7} ohm-cm^2) than the foil which was undoubtedly due to the better penetration and contact of the Ag to the 123 superconductor.

Recent results by C-S Hsi, as described in Part II of this report, show that this method, as well as the previous one utilizing Ag foils, can actually produce contact resistivities in the range of 2 x10^{-9} ohm-cm^2. Also reported in Part II are the results of the work on Au, Pt and Pd electrodes. In general, these

Figure 13. Ag tab technique for end-electroded 123 superconducting tape. Left photo shows the Ag tab with holes and the fired assembly, top right - cross section of fired assembly, bottom right - detail of the cross section.

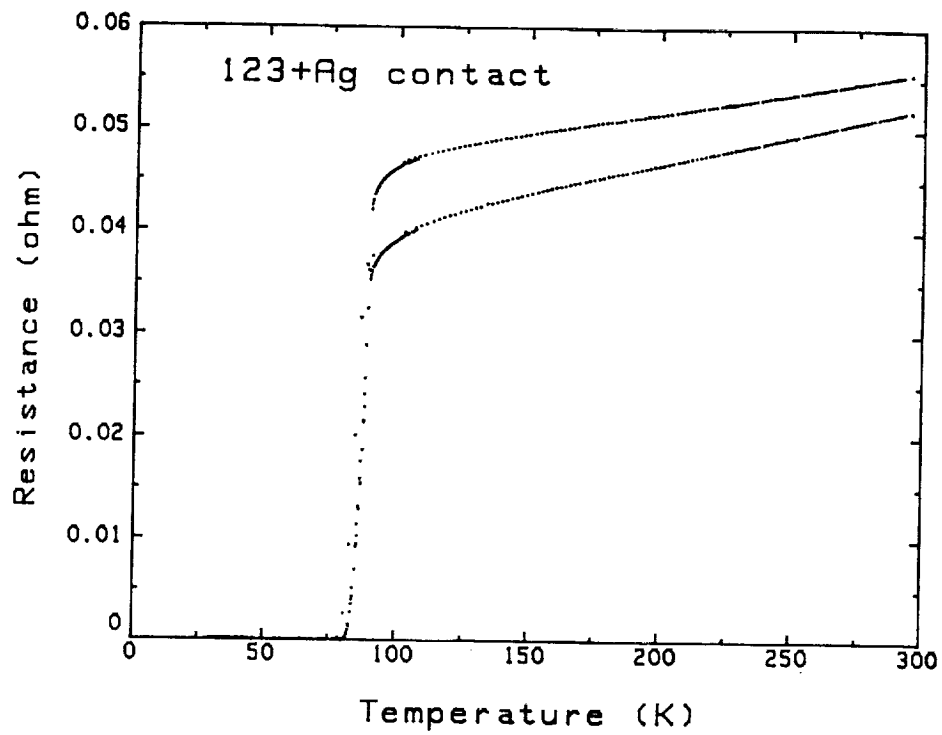Figure 14. Tc curve of 123 tape/tab electrode assembly.

Figure 15. Tc curve for 123 tape/tab assembly. (Courtesy of R. Caton, CNC).
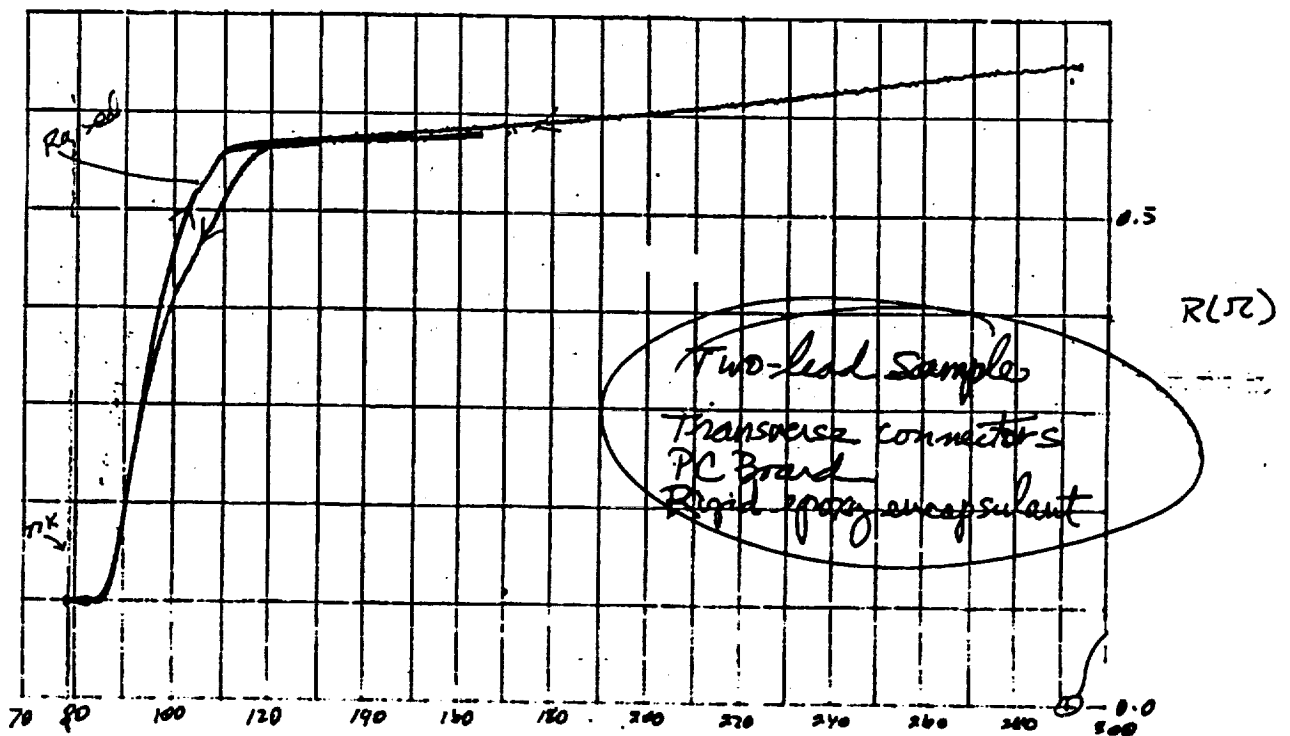
Figure 16. Tc curve for conducting link with original design.

latter materials do not produce electrodes with as low a contact resistivity as that of Ag, and hence, are not recommmended for further investigation.

4. Encapsulants

The 123 superconducting materials are well known to be sensitive to the environment and especially to water vapor. As a consequence, it is necessary to protect them from the atmosphere via encapsulation. Ideally, one needs an encapsulating material which would hermetically seal the 123 from its surroundings, but it should also provide additional structural support, be applied by a process compatible with the temperature limitations for the substrate and should not interact with the 123 so as to destroy or alter its superconducting properties. Other important consider- ations involve (1) thermal expansion compatibility between the encapsulant, 123 and the substrate, (2) adhesion of the encapsulant to the superconductor and the substrate, (3) the hardness of the encapsulant surface finish and its resistance to abrasion and (4) its impermeability to water vapor.

Several materials were selected for evaluation in this study. They included:

1. Envirotex thermosetting epoxy
2. Behr thermosetting epoxy
3. Norland UV curing epoxy
4. General Electric RTV
5. Dow Corning RTV Sylgard 186

This investigation is still in progress and a final selection will depend on the results of long term testing which has now begun (Westinghouse/Savannah River) under a separate contract. Preliminary evaluations, however, have shown that the Envirotex epoxy is superior in regard to strength, adhesion, and surface hardness and satisfactory with respect to thermal expansion compatibility and thermal shock. All of the other materials were judged to be less acceptable for one or more reasons. The EnviroTex Lite encapsulant was obtained from:

Environmental Technology Inc.
P.O. Box 365
Fields Landing, CA 95537
(707) 443-9323

Specific information on the EnviroTex Lite epoxy resin is very limited, however, listed below are some average values for epoxy resins:

Tensile Strength:	12,000	psi
Flexural Strength:	18,000	psi

(15)

Modulus of Elasticity: 0.45×10^6 psi
Thermal Expansion: 50×10^{-6} /°C
Volume Resistivity 1×10^{16} ohm-cm
Dielectric Constant   3.8
Water Absorption (24hr/RT) 0.14%

Note: Data selected from: Epoxy Resins by H. Lee and
K. Neville, McGraw-Hill, New York, 1957.

5. Performance Testing

Performance evaluation tests were conducted on selected samples from various groups of elements fabricated during the last year. As mentioned under section A-2, these include:

                 a. Resistance vs. temperature (Tc)
                 b. Thermal cycling
                 c. Extended immersion in LN_2
                 d. Immersion in water
                 e. Drop testing
                 f. Visual Inspection

A typical resistance vs. temperature curve of a 4-inch grounding link is given in Figure 16. As can be seen, the transition from metallic behavior to the superconducting state was less abrupt than normal (compare Figure 10 for the 123 material characteristics after sintering), and the transition temperature (Tc) has dropped several degrees to approximately 86K. In addition, for this particular sample measured as a two-port device several months ago, it can be observed that the resistance did not drop to zero but reached a value equal to the sum of the contact resistances of the two Ag electrodes plus the lead resistances. In this case, a less than optimum value of 0.1 ohm was obtained since the DuPont 7095 fired-on Ag does not generally produce a low resistance contact with the 123 material. A more recent and improved Tc curve, as shown in Figure 17, was obtained with the better, high density Ag (Cermalloy #8710) electrodes. This curve shows a RT resistance of 1.56 ohms going down to 1.2 mohms below the Tc of 86K (measured with 10 ma constant current).

For the thermal cycling test, five samples were randomly selected and monitored for change in room temperature resistance as the samples were cycled ten times from room temperature to liquid nitrogen (77K) in an eight minute period per cycle (3 minutes at LN_2 and 5 minutes at RT). Table III summarizes the results. As can be noted, there is no noticeable change in element resistance as a result of the test. Several samples were also tested to 30 cycles with similar results.
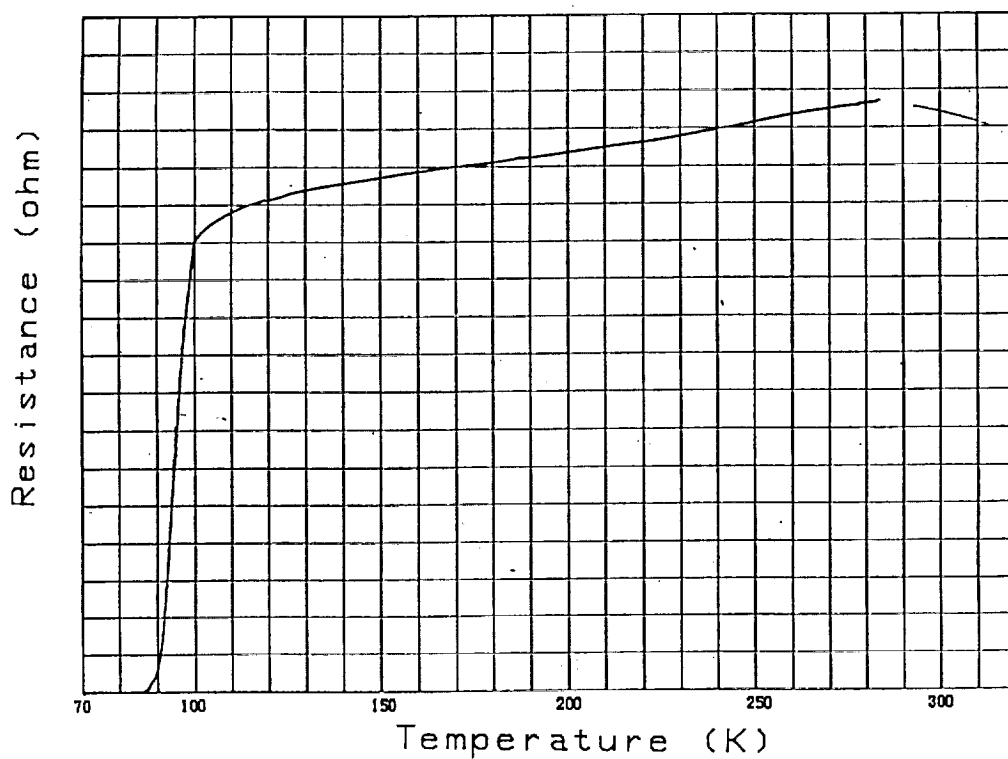
Figure 17. Tc curve for conducting link with new design.
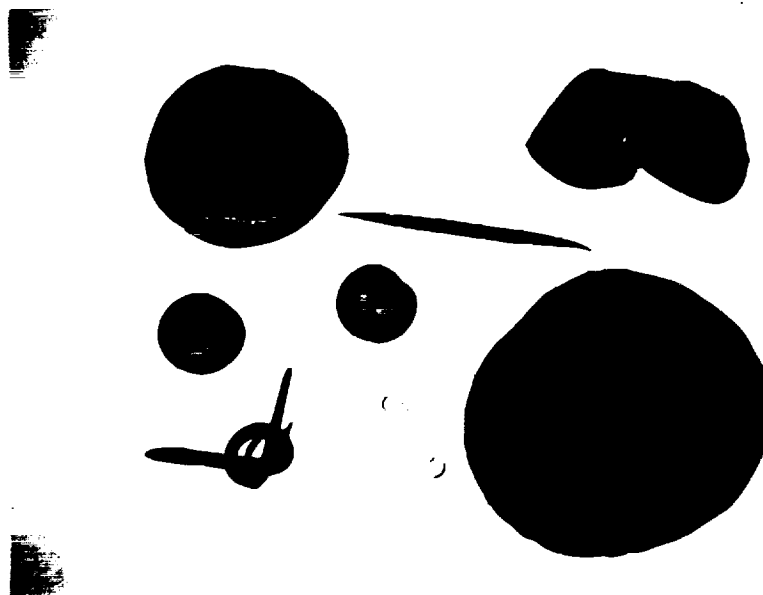
Figure 18. Examples of 123/polymer composite shapes illustrating variety and flexibility.

Table III.

Thermal Cycling Test of Grounding Link Element

Sample No.	Original Resistance	1 Cycle	5 Cycles	10 Cycles
1	1.60 ohms	1.61	1.62	1.60
2	1.72	1.72	1.71	1.70
3	1.54	1.55	1.54	1.54
4	1.56	1.50	1.58	1.56
5	1.65	1.66	1.65	1.65

For the long term LN_2 exposure, an additional five samples were randomly selected and monitored for change in room temperature resistance as the samples are immersed in liquid nitrogen for extended periods of time. These results are given in Table IV. They show that up to 12 days there is no measurable change in resistance.

Table IV.

Long Term LN_2 Exposure Test of Grounding Link Element

Sample No.	Original Resistance	1 day	3 days	9 days	12 days
1	1.57 ohms	1.61	1.60	1.57	1.57
2	1.40	1.40	1.45	1.39	1.39
3	2.11	2.14	2.10	2.11	2.10
4	1.87	1.87	1.91	1.87	1.89
5	1.26	1.42	1.28	1.26	1.26

The water immersion test was conducted on another five samples which were randomly selected and monitored for change in room temperature resistance after a 24 hour immersion in distilled water. Results are given in Table V. Here again, as in the case of the two previous tests, there was no detectable change in resistance as a result of direct contact with water, indicating that the encapsulant is effective in protecting the 123 material from deterioration.

Table V.

Water Immersion Test of Grounding Link Element

Sample No.	Original Resistance	24 Hours in DH_2O
1	1.7 ohms	1.7
2	1.9	1.9
3	1.6	1.6
4	1.3	1.3
5	1.5	1.5

A final five samples were randomly selected for the drop test which monitored the change in room temperature resistance as the samples were dropped from progressively higher levels to a concrete floor. For the final 12 foot level, the samples were actually thrown up to approximately that height and allowed to impact the floor. These results are tabulated in Table VI. Unlike the other tests, this test showed that there was a progressive change in resistance of the samples as they were dropped from heights greater than 3 feet, however, none of them produced an open circuit. Visually, only one sample (sample No. 1) had a couple of slight cracks in the encapsulant which developed after the 12 foot drop level, but these cracks did not appear to extend to the 123 superconductor when view under a microscope. The reason for the progressive change in resistance is undoubtedly due to the increasing mechanical shock at the various drop levels, however, the specific failure mechanism is still under investigation. In any event, these elements in actual service would need to be designed to survive such impacts if these conditions were considered to be highly probable.

Table VI.

Mechanical Drop Test of Gounding Link Element

Sample No.	Original Resistance	3 ft.	6 ft.	9 ft.	12 ft.
1	1.5 ohms	1.5	2.4	8.5	86.9
2	2.4	2.5	3.7	7.4	18.7
3	1.5	1.6	3.6	6.7	23.8
4	1.8	1.9	2.3	11.5	21.3
5	1.8	1.8	1.9	3.0	7.7

In summary, the performance evaluation of the grounding link element, as designed, was generally better than expected and indicated that a viable and reproducible product was feasible.

C. Special Studies

1. 123/Polymer Composites

The two most characteristic features of superconducting materials are (1) the loss of all electrical resistance at Tc and (2) the exhibiting of the Meissner effect (repulsion of magnetic fields) in the superconducting state. While the first of these is of primary concern in circuit elements for magnet coils, noiseless conductors and sensors, the second one (Meissner effect) is useful in applications such as electromagnetic shielding and frictionless bearings and bearing surfaces.

Since in the Meissner effect the electrical conductivity through the element is not of primary concern, it is conceivable that a composite consisting of a superconductor powder suspended in a polymer matrix would be a satisfactory material for such devices utilizing this effect. With this in mind, formulations involving 123 superconducting powder and the encapsulants mentioned in section B(4) were prepared at various powder-to-polymer loadings. Best results were obtained with the GE RTV polymer. It permitted relatively high loading ratios, was easy to process and mold and was flexible on curing at room temperature or in an oven. A couple of examples of this material are included in the photograph of Figure 4 (upper right hand corner). Large, bulk shapes for magnetic bearing surfaces with reasonable flexibility are shown in Figure 18 as well as thin, "pizza-like" coatings which can be conformally applied to large area surfaces for magnetic shielding are feasible and have been demonstrated. The Meissner effect, floating magnet photograph in Figure 19 is produced with such a 123/polymer composite. In our first demonstration of a superconducting/polymer magnetic bearing surface, the magnet in Figure 20 was loaded down with approximately 10 grams of extra weight (besides the weight of the magnet itself) before touch down. Higher loading of the polymer or the use of more strongly superconducting powder will serve to increase the weight handling capability, but such a study would be the subject of future work.

2. 123 Thin Films

For the last couple of years a large amount of research work on high temperature oxide superconductors has been conducted on thin films. In contrast to the bulk ceramic and single crystal materials, thin films can be fabricated reasonably quickly and easily on various substrates via vacuum, chemical or laser ablation techniques. When epitaxially deposited on the appropriate substrate, thin films can be produced which contain little or none of the "weak links" which limit the bulk ceramics, and critical currents in excess of 10^6 A/cm^2 are possible.
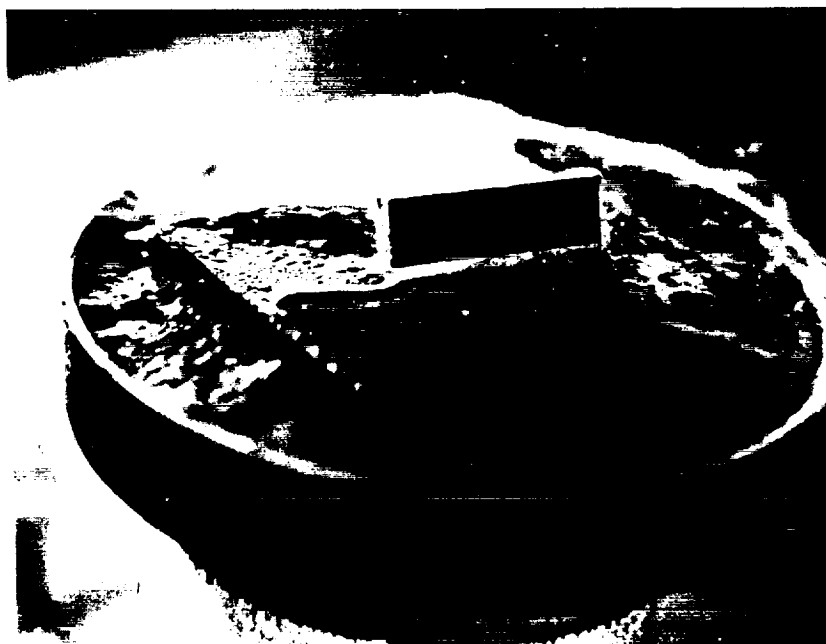
(19)

Figure 19. Meissner effect of 123/polymer composite shown floating
a Nd-Fe-B rectangular magnet.
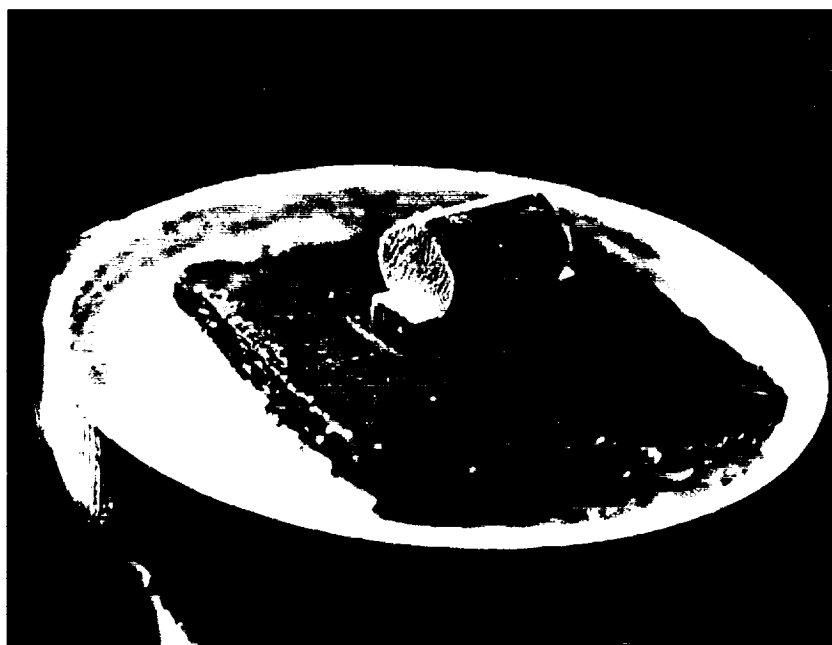

Figure 20. Same as in Figure 19 but with a 10 gram weight added to
the floating magnet.

As a preliminary investigation of the feasibility of fabricating thin films of $YBa_2Cu_3O_{7-x}$ via a chemical process, it was decided to develop a water-soluble acetate chemical process for the 123 material. Accordingly, yttrium acetate (YAc), barium acetate (BaAc) and copper acetate (CuAc) were selected as the precursors. All of these compounds were sufficiently soluble in both water and alcohol so as to make the process feasible.

Appropriate amounts of $Y(C_2H_3O_2)_3 \cdot 4H_2O$, $Ba(C_2H_3O_2)_2$ and $Cu(C_2H_3O_2)_2 \cdot H_2O$ were dissolved in distilled water and methanol, and adjusted for proper pH with either acetic acid or ammonium hydroxide. Using silver foil as a substrate, films of the solution were deposited on the substrate via a dipping process. They were then dried and fired at $900°C$ for two minutes in a simple box furnace. Although a single layer produced a black, smooth and uniform film, several layers were required in order to obtain an X-ray diffraction pattern of the film. This pattern is given in Figure 21. It indicates a proper crystalline structure for superconductivity, however, electrical measurements have not yet been made which substantiate the existence of superconductivity in these films. A photo of a two-layer film is shown in Figure 22 along with an SEM photomicrograph of its surface.

This preliminary investigation established the viability of such a process for the fabrication of 123 thin films, however, more development work would need to be accomplished to make it practical.

V. Presentations

1. Gene H. Haertling, "High Tc Ceramic Superconducting Circuit Elements," ISHM 1st Joint Technology Conference, San Diego, CA, March 26-28, 1990.

2. Chi-Shiung Hsi and Gene H. Haertling, "Low Resistivity Contacts to $YBa_2Cu_3O_{7-x}O_3$ Superconductors," American Ceramic Society Ceramic Science and Technology Congress, Orlando, FL, November 12-15, 1990.

3. V.V. Modi, B.I. Lee and G.H. Haertling, "$YBa_2Cu_3O_{7-x}$ - Ag Composites Prepared by the CoPrecipitation Route: Analysis of Physical and Superconducting Properties as a Function of Ag Content," American Ceramic Society Ceramic Science and Technology Congress, Orlando, FL, November 12-15, 1990.

4. V.V. Modi, B.I. Lee, G.H. Haertling and D.R. Dinger, "Densification of Tape Cast $YBa_2Cu_3O_{7-x}$ by Blending Powders with Varying Particle Size Distributions," American Ceramic Society Ceramic Science and Technology Congress, Orlando, FL, November 12-15, 1990.
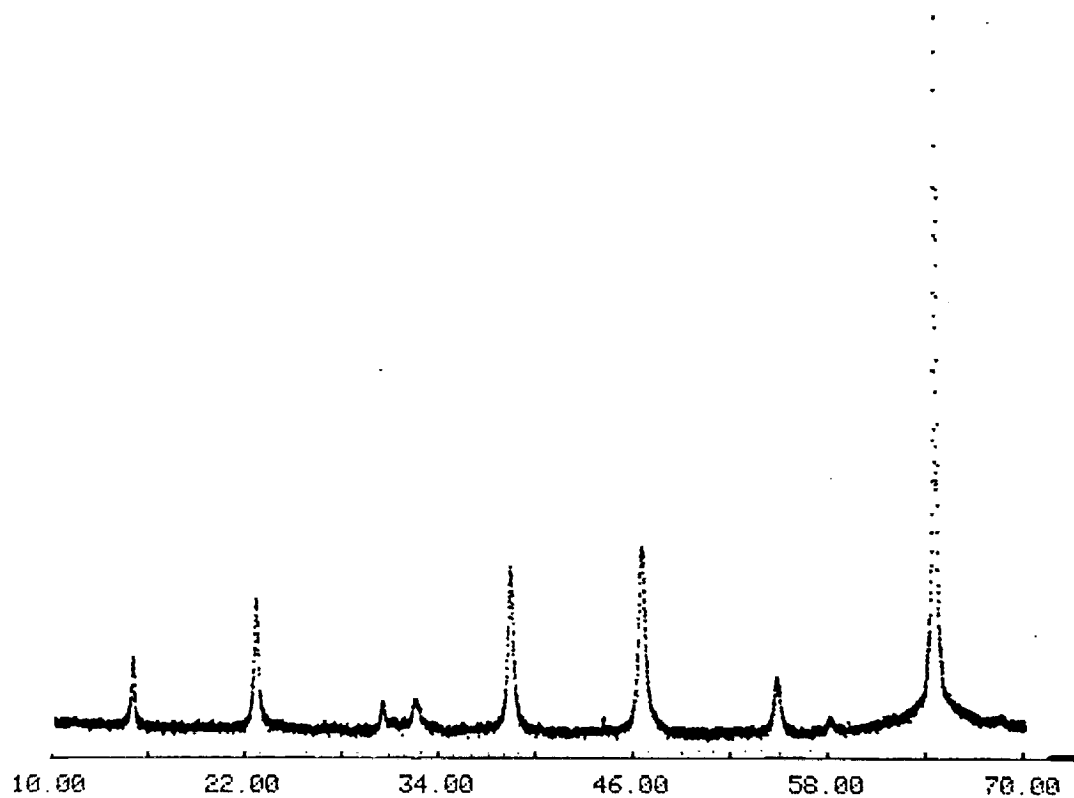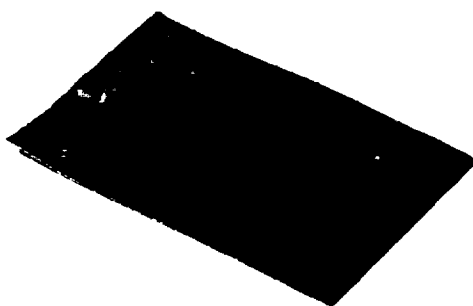
Figure 21. X-ray diffraction pattern of a 4-layer, 123 thin film.

Figure 22. Acetate-derived 123 thin film deposited on Ag foil via dipping process.

5. V.V. Modi, B.I. Lee and G.H. Haertling, "Characteristics of Co-Precipitated $YBa_2Cu_3O_{7-x}$ Powders Subjected to Varying Calcining Conditions," American Ceramic Society Ceramic Science and Technology Congress, Orlando, FL, November 12-15, 1990.

6. Gene H. Haertling, "Ceramic Superconducting Components," American Ceramic Society Ceramic Science and Technology Congress, Orlando, FL, November 12-15, 1990.

VI. Patent Disclosures

1. "Ceramic Superconducting Circuit Elements and Method of Making Same," Gene H. Haertling and John D. Buckley, NASA-LaRC, August, 1990.

2. "Ceramic Superconducting Composites and Method of Making Same," Gene H. Haertling and John D. Buckley, NASA-LaRC, August, 1990.

3. "Acetate Process for Preparing $YBa_2Cu_3O_{7-x}$ Superconducting Thin Films," Gene H. Haertling, NASA-LaRC, August, 1990.

Appendix A

Westinghouse
Copper Laminates Division

RIGID EPOXY LAMINATE GRADE 65M38

Grade 65M38 is a high reliability epoxy rigid laminate line consisting of 7628 and 7642 glass cloth constructions. Our 65M38 laminates are designed to sustain temperatures above the melting point of solder without warpage or delamination. Their high resin to glass ratio permits cleaner drilling and easier punching with reduced tooling wear.

Grade 65M38 laminates are designed to meet or exceed all the requirements of MIL-P-13949.

■ **Consistent performance in conventional processes**

■ **Very low warpage at high temperatures**

■ **U.L. File No. E3486**

■ **MIL-P-13949 qualified**

GRADE 65M38
TYPICAL PROPERTIES [1]

PROPERTY	UNIT	TYPICAL VALUE [2]
Peel Strength		
As received	lb./in.	11.0
After thermal stress	lb./in.	11.0
Volume Resistivity		
As received	megohm-cm.	1×10^8
At elevated temperature	megohm-cm.	1×10^7
Surface Resistivity		
As received	megohm	5×10^7
At elevated temperature	megohm	6×10^5
Permittivity @ 1 MHz		4.7
Loss Tangent @ 1 MHz		0.021
Arc Resistance	sec.	115
Flammability		V-0
Burn Time	sec.	3
Water Absorption	%	0.09
Dielectric Breakdown	KV	>60
Glass Transition	°C	130

1. TYPICAL PROPERTIES OF A 0.059" LAMINATE, CLAD 1/1. PROPERTIES OF OTHER THICKNESSES MAY VARY.
2. EXCEPT AS NOTED, IPC-TM-650 TEST METHODS WERE USED.

12/88

Fortin

AVAILABILITY:

Thickness: 0.031, 0.047, 0.059, 0.062, 0.093 and 0.125

Thickness tolerance: Class 2 (per MIL-P-13949) is standard

Claddings: Class 1 copper - 1/2, 1 and 2 ounce

Laminate Size: Standard full sheets: 48 x 36
                                          48 x 48
                                          48 x 72

Other sizes available on special order
Panels cut to size with specified grain direction

For availability of other thicknesses and/or copper cladding, please consult your sales representative.

PROCESSING AND HANDLING:

Grade 65M38 laminates withstand normal board fabrication and assembly processes, including thermal stressing, plating and the use of stripping solvents, fluxes and flux removers.

Grade 65M38 laminates will respond to standard desmear processes.

Textured finish on the unclad side is available.

ORDER INFORMATION:

When ordering or requesting quotations on this product, specifiy the following:

1. Grade or MIL-P-13949 designation.

2. Core thickness and tolerance.

3. Copper cladding.

4. Sheet or panel size and quantity.

5. Applicable standards and specifications.

6. Marking, packaging, shipping and billing instructions.

WESTINGHOUSE ELECTRIC CORPORATION
Copper Laminates Division
12840 Bradley Avenue
Sylmar, California 91342-3887
(818) 362-4350, Fax: (818) 362-5310

Final Report

Part II

Electrical Contacts to $YBa_2Cu_3O_{7-x}$ Superconductor

submitted to

National Aeronautics and Space Administration

Langley Research Center

Submitted by

Chi-Shiung Hsi

Principal Investigator

Gene H. Haertling

Dept. of Ceramic Eng.

Clemson University

Contract No. NAG-1-820

Sept., 1990

Abstract

Several methods of measuring contact resistance between metal electrodes and $YBa_2Cu_3O_{7-x}$ superconductors were investigated; i.e., two-point, three-point, and lap-joint methods. The lap-joint method was found to yield the most consistent and reliable results and is proposed as a new technique for this measurement. Silver, gold, platinum, and palladium metals were used as electroding materials. Painting, embedding, and melting techniques were used to apply the electrodes to the $YBa_2Cu_3O_{7-x}$ Superconductors. Low resistivity contacts were found from silver and gold electrodes. Silver, which made good ohmic contact to the $YBa_2Cu_3O_{7-x}$ superconductors with contact resistivity as low as 1.9×10^{-9} Ω-cm^2, was found to be the best electroding material among the materials used in this research.

I. Introduction.

High resistivity in the contact area between the electrode and the superconductor influences critical current measurements and limits the applications of the superconductor. Hence, obtaining low resistivity and reliable contact between the electrode and the superconductor is quite important for basic considerations and actual device development. Since $YBa_2Cu_3O_{7-x}$ was reported as a high T_c superconductor material in 1987, many investigators have worked on lowering the contact resistivities between the electrodes and the $YBa_2Cu_3O_{7-x}$ superconductor[1-5].

Noble metals, which usually produce low resistance ohmic contacts, are the most common materials used to apply electrodes to the surface of the $YBa_2Cu_3O_{7-x}$ superconductor. Gold and silver are especially advantageous in that they are relatively inert chemically with strongly positive standard reduction potentials[6]. Silver has other advantages in that its oxides dissociate at fairly low temperatures. This allows oxygen permeability at moderate temperatures, and diffusion into the $YBa_2Cu_3O_{7-x}$ superconductor. For the above reasons, silver was interesting to the investigators. Ekin et. al.[1] sputtered silver and gold onto the superconductor surfaces. Contact resistivities were obtained in the range of 10^{-6} Ω-cm^2. Suzuki et. al. deposited platinum onto the $YBa_2Cu_3O_{7-x}$ superconductor pellet and acquired contact resistivities in the 10^{-4} Ω-cm^2 range at 80k. Tzeng et al.[2] evaporated a silver film on the $YBa_2Cu_3O_{7-x}$ superconductor surface and achieved contact resistivity in the 10^{-8} Ω-cm^2 range after annealing in oxygen at 500ºC. Painting silver epoxy on the $YBa_2Cu_3O_{7-x}$ superconductor surface also produced good contact with contact resistivity in the 10^{-7} Ω-cm^2 range[3]. A contact resistance in the range of 10^{-10} Ω-cm^2 was obtained by sputtering gold or silver onto the $YBa_2Cu_3O_{7-x}$ superconductor surface and annealing at 500~600ºC in an oxygen atmosphere[4].

Contact resistivities in the range of 10^{-12} Ω-cm^2 were obtained by embedding silver wire in the $YBa_2Cu_3O_{7-x}$ superconductor before sintering[5].

The two-point and three point methods are the traditional techniques used to measure the contact resistance between the electrodes and $YBa_2Cu_3O_{7-x}$ superconductors. Jing et. al.[7] found that the measuring electrode, in the three-point method, was not in an equipotential state. In their results, contact resistance could not be directly determined from the three-point measurement. Some correcting factors had to be considered to calculate the contact resistance. A measuring configuration similar to the three-point method was used in the two-point measurement. The same problems might be found in this method.

In this work, a direct contact resistance measuring method was proposed after the evaluation of different measurement techniques. Using the new measuring configuration, various electroding materials and application methods were investigated.

II. Experimental Procedure.

The $YBa_2Cu_3O_{7-x}$ superconductor tape, made by a tape casting process[8], was used as a starting material in this research. The tape was cut into strips with the dimensions 25.4mm x 2.0mm x 0.5mm. Silver, gold, platinum, and palladium metals were used as electroding materials. The electrodes were applied by painting, embedding, and melting techniques.

Silver electrodes were applied by a single or double firing process. In the single firing process, the electrodes were applied by the painting or embedding method before sintering the strips. In the embedding method, the strips were wet with toluene, and silver foils were embedded onto the wet strip surfaces. The thickness of the silver foils was 0.025mm. In the painting method, a high density silver paste (Cermalloy C8710) was painted onto the strip surfaces. After electroding, the strip and the electrodes were co-sintered together. In the double firing process, the strips were sintered before the electrodes were applied. These electrodes were applied by the painting or melting method. In the melting method,

the silver foils were put on the sintered strip surfaces and fired at 950°C for 12 min.. In the painting method, the silver paste was painted onto the strip surfaces and fired from 840 to 920°C for 0 to 48 min.. Gold electrodes were applied by the single fire/painting or single fire/embedding methods and fired at 920°C for 12 hours. Platinum and palladium electrodes were applied by the single fire/embedding method and fired at 920°C for 12 hours. All samples were annealed at 450°C for 12 hours after firing the electrodes.

After the samples were prepared, contact resistivities and I-V characteristics were measured at liquid nitrogen temperature. Contact resistances were calculated from the slopes of the I-V characteristics at a current of 0.1 A. The contact resistivity equals the contact resistance times the contact area between the electrodes and the $YBa_2Cu_3O_{7-x}$ superconductors. A Keithley 148 nanovoltmeter was used to measure the voltage difference between the two voltage leads.

III. Contact Resistance Measurement.

Table 1 lists the investigators and the configurations of the two-point, three-point, and four-point methods. In the two-point method, each electrode had one current lead and one voltage lead on its surface. In three point method, one current lead and one voltage lead were applied on an electrode (measuring electrode), and contact resistance was measured from the this electrode. The three-point method is the most common method used by investigators to measure contact resistances between the metal electrodes and the superconductors. In one instance, the four-point method was also used to measure the contact resistance of Ag doped Bi-Sr-Cu-Ca-O superconductor[23].

Figure 1 shows the I-V characteristics of a sample measured by the three-point method. Three different voltage connections, VA, VB, and VC, with different distances between the voltage lead and the current lead were applied to the measuring electrode. Different I-V characteristics were measured from the different voltage connections. The lowest contact resistance was obtained from the VA connection which had the largest distance between the voltage lead and the

unit: $\mu\Omega \cdot cm^2$

Double Firing	Painting of silver paste					
	Time (min)	Temperature (degree C)				
		840	860	880	900	920
	0		8.6		0.22	
	12	7.9	0.91	0.094	0.02	0.02
	24				0.016	
	48		0.11		0.013	
	Melting					
	Time (min)	Temperature (degree C)				
		950				
	12	0.0026				
Single Firing	Painting of silver paste					
	Time (hour)	Temperature (degree C)				
		900	910	920	930	
	12	0.0078	0.0024	0.0032	0.0027	
	24		0.0035	0.0023		
	Embedding					
	Time (hour)	Temperature (degree C)				
		920				
	12	0.05				
	24	0.0019				

Table 2: Resistivities of silver-YBCO contacts via different electroding mtthods, using the lap-joint configuration.
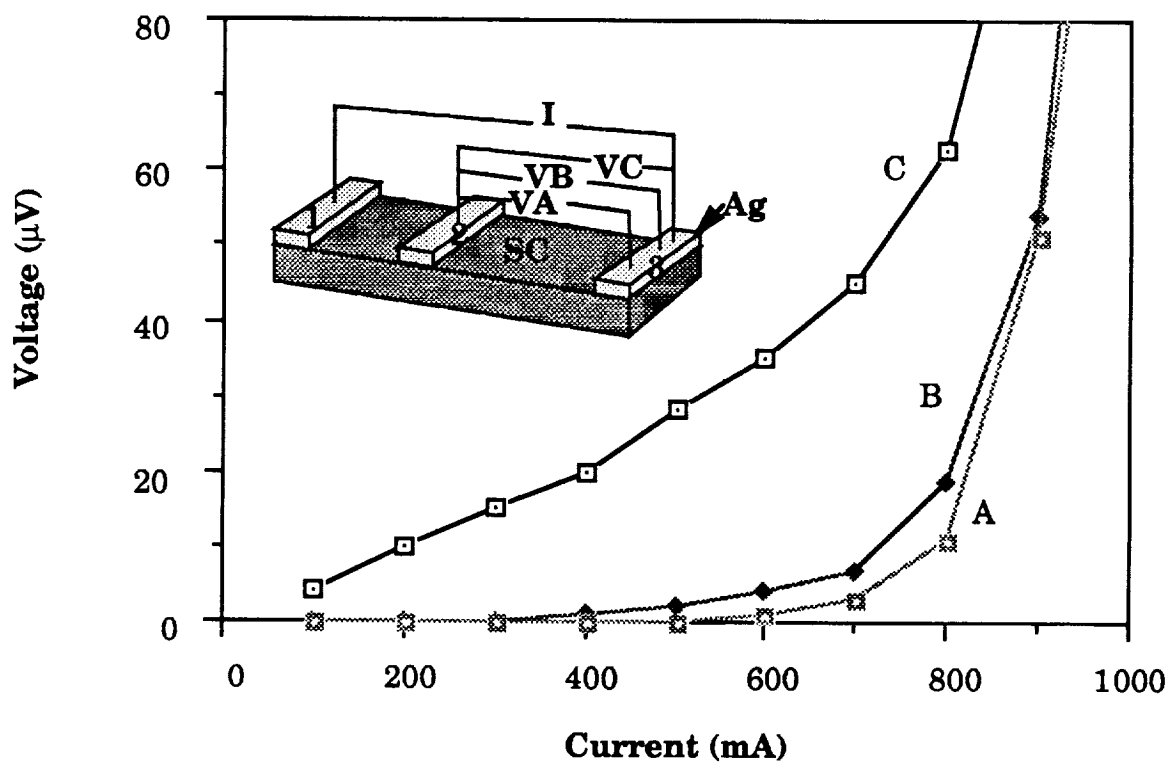
Figure 1: I-V Characteristics of a sample prepared by the three-point method. The sample had three different voltage connections with different distances between the voltage lead and the current lead(VA= 1.4mm, VB= 0.4 mm, VC= 0.0mm). The silver electrodes were co-fired with the superconductor at 920 degrees C for 12 hours.

current lead at the measuring electrode. When the voltage lead and the current lead were connected together, the highest contact resistance was obtained. Since the contact resistance measured by this method and this particular configuration was influenced by the distance between the voltage lead and the current lead at the measuring electrode, the measuring electrode was not in an equipotential state and the contact resistance might not be measured correctly.

Figure 2 shows the configuration for a two-point measuring method, prepared by embedding silver wires inside the $YBa_2Cu_3O_{7-x}$ superconductor strips, and the I-V characteristics of the sample. The three different kinds of voltage connections as shown in Figure 2 are VA, VB, and VC. Very low contact resistivity in the $10^{-12}\Omega\text{-cm}^2$ range was obtained from VA connection; however, the contact resistivities for the VB and VC connections were more than three orders of magnitude higher than that of the VA connection. Therefore, the silver wires inside the $YBa_2Cu_3O_{7-x}$ superconductors were not in an equipotential state and great care must be taken in order to obtain reliable results.

When measuring the contact resistance, if one voltage lead and one current lead are applied to the measuring electrode then it is difficult to determine the appropriate location for the voltage lead and the current lead because the measuring electrode is not in an equipotential state. In order to avoid this problem and to measure the contact resistance properly, the voltage lead and the current lead should not be applied on the same electrode while measuring the contact resistance.

Figure 3 shows the configuration and the equivalent electrical circuit of the lap-joint method which has the voltage lead and the current lead on separate electrodes. There was a joint electrode applied between the two superconductor strips. In this method the total resistance, R, measured from the voltage lead is:

$$R = R_s + R_c + R_{Ag} + R_s + R_c$$

Where R_s is the resistance of superconductor, R_c the contact resistance, and R_{Ag} the resistance of the silver electrode. At 78K, $2R_s \ll R_{Ag} + 2R_c$, then

Figure 2: I-V characteristics of a silver wire embedded sample. The sample was fired at 920 degrees C for 12 hours.
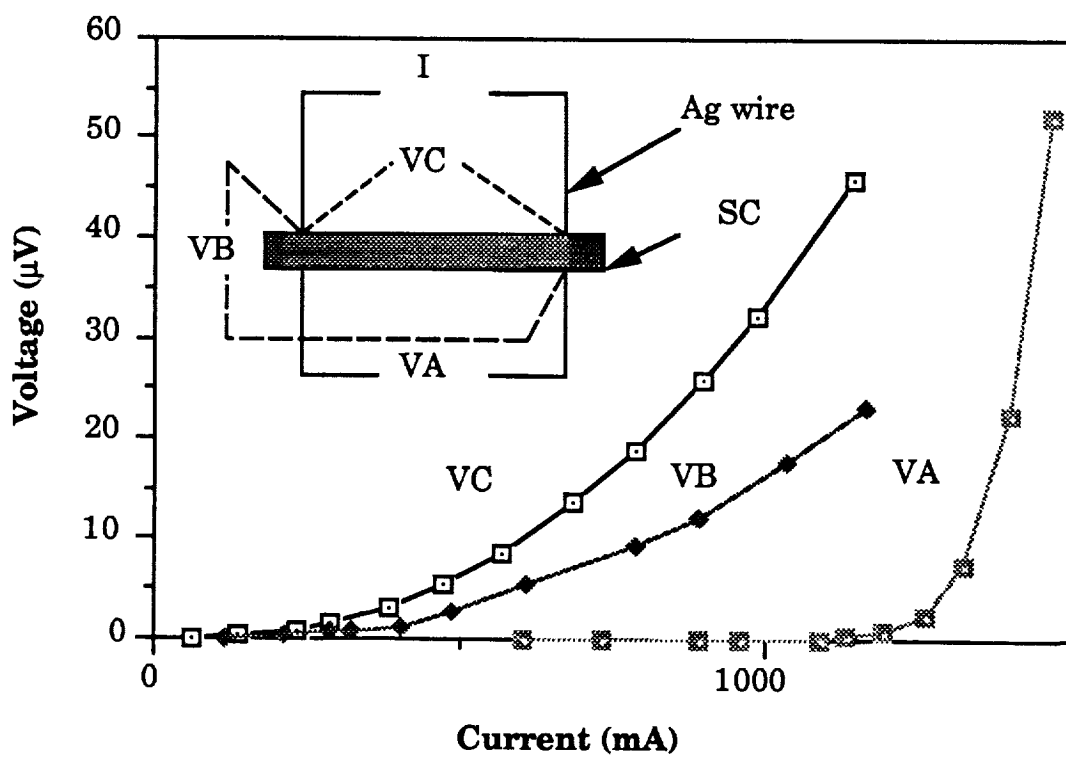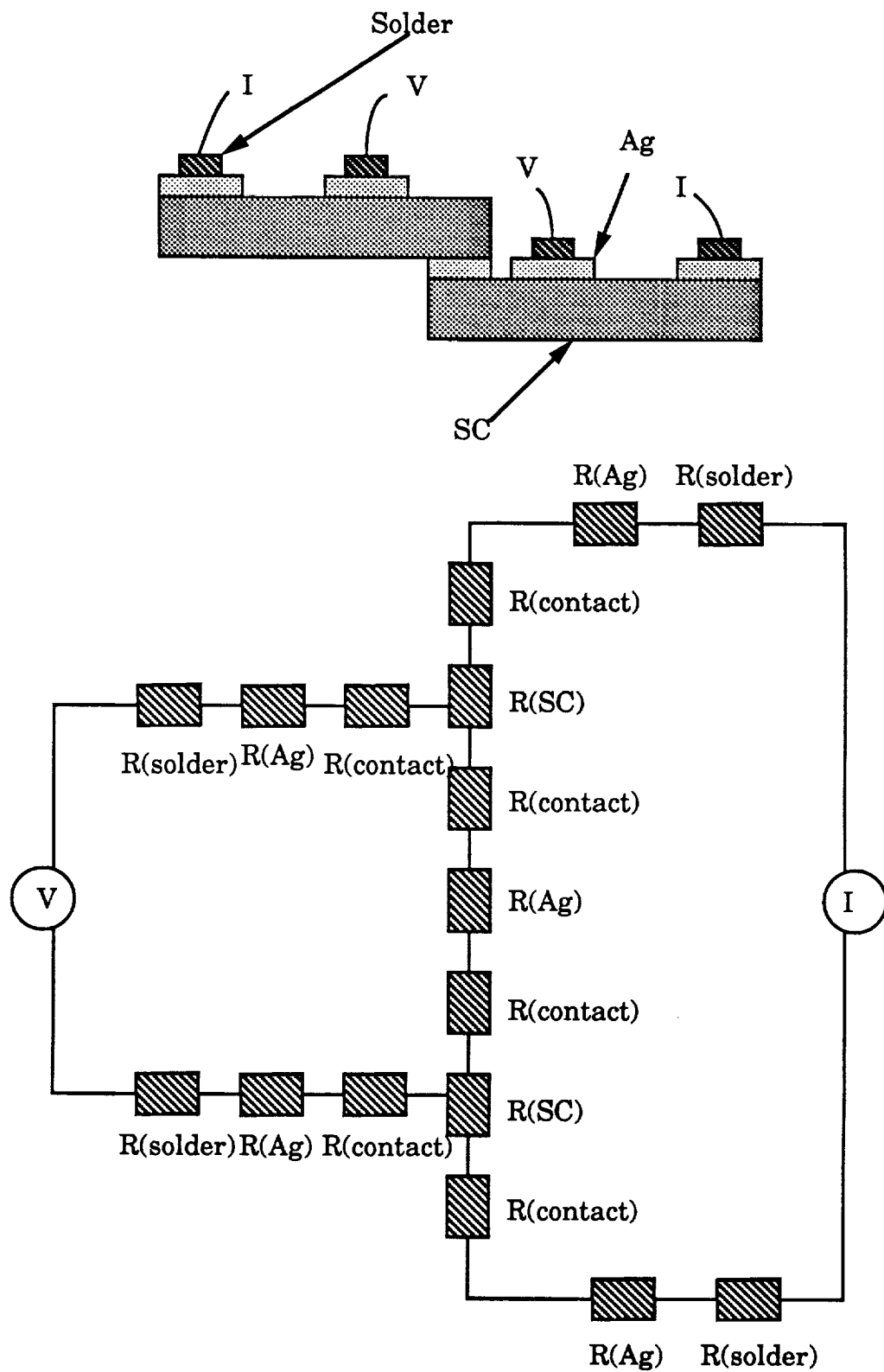
Figure 3: Configuration and equivalent electrical circuit of the four point
lap-joint method

$$R = 2R_c + R_{Ag}$$

The thickness of the measuring electrode was approximately 10 μm. The resistivity of silver at 78K is about 3×10^{-7} Ω - cm. Therefore, the limitation of this method is about 3×10^{-10} Ω - cm^2, which is the resistance of silver at a thickness in the 10 μm range. Because the resistance of the superconductor is five orders of magnitude, or more, lower than the resistance of the silver at 78K, and the measuring electrode carries no current, the contact surface between the voltage electrodes and the YBa$_2$Cu$_3$O$_{7-x}$ superconductors does not contribute to R.

Figure 4 shows the I-V characteristics of a sample made by the lap-joint method with the four different voltage connections. As can be seen, the same I-V characteristics were obtained from the VA, VB, and VC connections before the sample became normal. Contact resistances of both sides of the measuring electrode were determined from VA, VB, and VC connections but only one side was measured from the VD connection. Thus, only half of the contact resistance determined from VA, VB, or VC was obtained from the VD connection. The contact resistivity measurement by this method was not influenced by the location of the voltage leads within the sensitivity of the nanovoltmeter(20 nV). Samples used in this measuring procedure can be prepared by painting, embedding, and melting, and all of these are practical methods for applying the electrodes to YBa$_2$Cu$_3$O$_{7-x}$ superconductors. Therefore, this method provides a more reliable contact resistance measurement than the methods which connect the voltage lead and the current lead to same electrode.

IV. Results and Discussions.

In the last report, the three point method was used to measure the contact resistance between the electrodes and YBa$_2$Cu$_3$O$_{7-x}$ superconductor. This did not represent the real contact resistivities as previous discussed. Therefore, in this report, contact resistivities of the electrode and YBa$_2$Cu$_3$O$_{7-x}$ superconductor contact
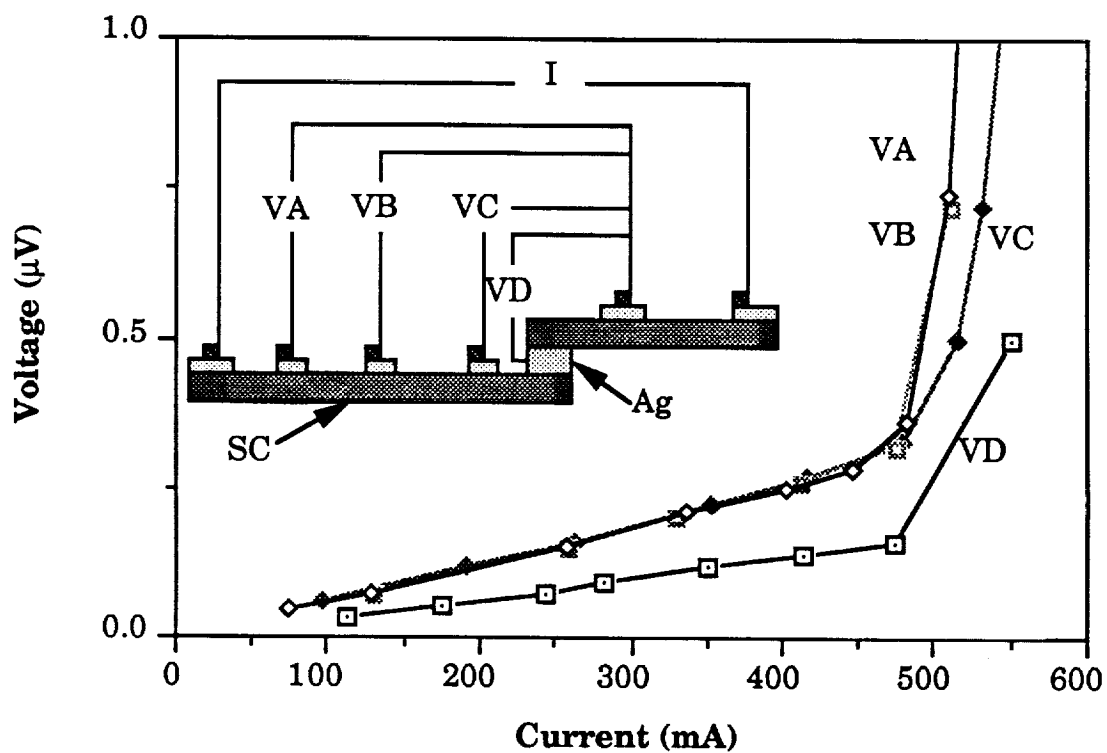
Figure 4: I-V characteristics of a lap-joint sample with different voltage connections. The silver electrodes were co-fired with the superconductor at 920 degrees C for 12 hours.

were measured by the lap-joint method.

IV. 1 Silver Electrode.

Table 2 lists the contact resistivities determined by the lap-joint method, of the samples prepared by the different electroding methods. Contact resistivities of the samples prepared by the double fire/painting method varied from the 10^{-6} Ω-cm^2 range to the 10^{-8} Ω-cm^2 range, when the samples were fired from 840 to 920°C. The dwell time and the firing temperatures were important in decreasing the resistivities of the silver and the YBa$_2$Cu$_3$O$_{7-x}$ superconductor contacts. The contact resistivity of the electrode prepared by melting silver at 950°C for 12 min. was 2.5 x 10^{-9} Ω-cm^2. The contact resistivities of the single fired/painted samples, which were prepared by painting the silver paste onto the YBa$_2$Cu$_3$O$_{7-x}$ superconductor strips and sintering the strips at 900 to 930°C for 12 hours, were in the 10^{-9} Ω-cm^2 range. Sintering temperatures and times did not have much influence on the contact resistance when the samples were prepared by this method. When the samples were prepared by embedding silver foil and sintering with the YBa$_2$Cu$_3$O$_{7-x}$ superconductor strips at 920°C for 24 hours, the contact resistivity was as low as 1.9 x 10^{-9} Ω-cm^2.

Figure 5 shows the I-V characteristics of four lap-joint samples with different joint preparations.. Linear I-V characteristics were obtained from single fired samples before they became non-superconducting. The double fired samples did not have a linear I-V relation. The voltage of the double fired samples increased rapidly at a lower current range than those of the single fired samples. This might be caused by the lowering of the critical current of the samples after double firing, since it has generally been observed that double firing the superconductor material can lead to a reduction in critical current density.

Figure 6 shows the contact resistivities of the double fired/painted silver electrodes and the critical current density ratios of the samples compared with the single fired/painted sample. The electrodes were fired at different temperature for 12
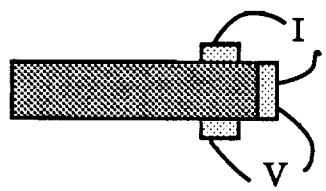
Method	Measuring Configurations	Reference
Two-point		(2), (5), (9), (10), (11) (12), (13)
Three-point		(1), (3), (5), (14), (15) (16), (17), (18), (19) (20), (22)
		(7), (21)
Four-point		(23)

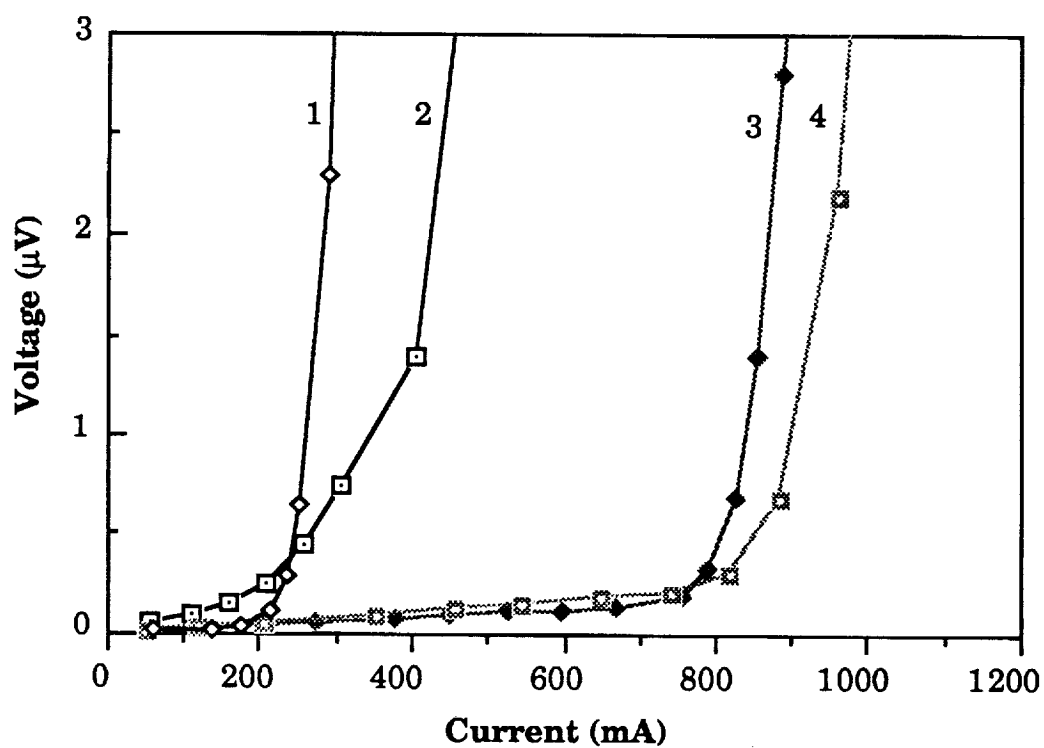Table 1: The configurations and reference of the two-point, three-point, and four-point methods.

Figure 5: I-V characteristics of different silver electrodes. (**1**. double fired/ painted electrode at 900 degrees C for 12 minutes, **2**. double fired/melted electrode at 950 degrees C for 12 minute, **3**. Single fired/painted electrode at 920 degrees C for 12 hours, **4**. single fired/ embedded electrode at 920 degrees C for 12 hours)
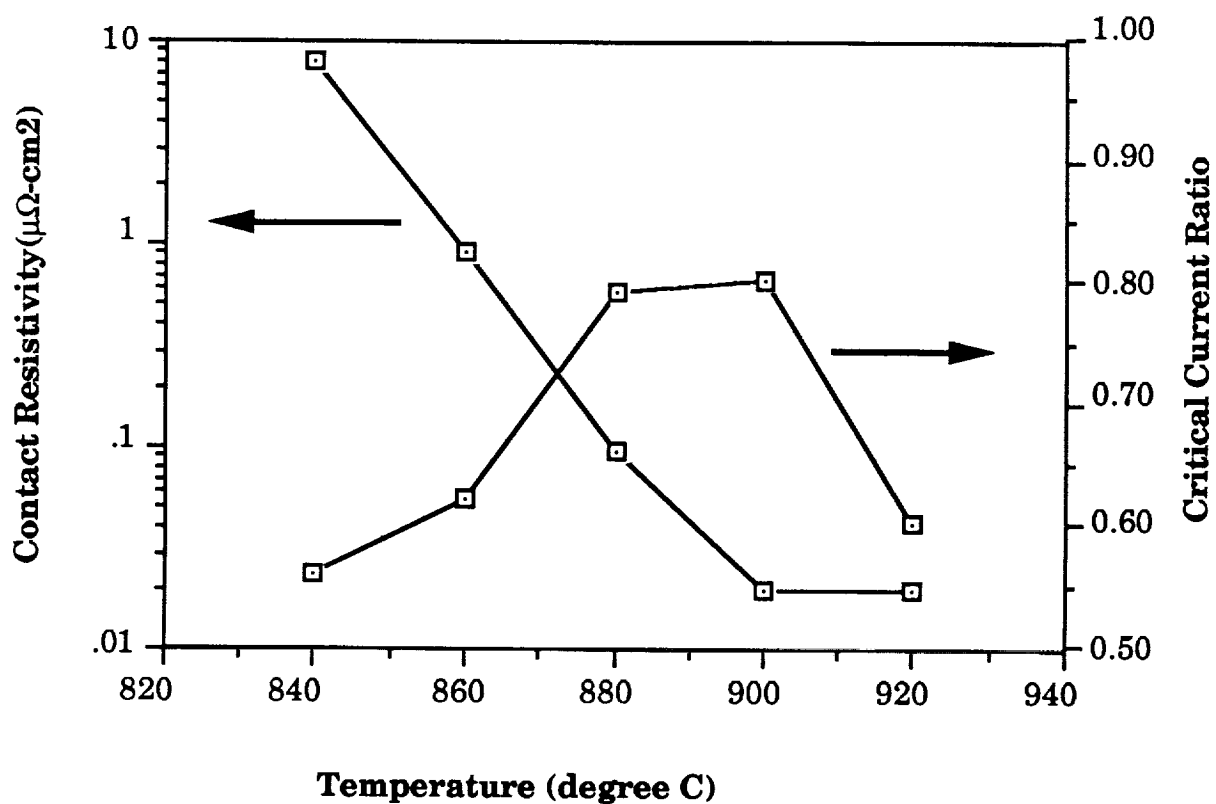
Figure 6: Contact resistivity of the double fired/painted silver electrodes and the critical current change of the samples after firing the electrode. The electrodes were fired at different temperatures for 12 minutes.

minutes after sintering the $YBa_2Cu_3O_{7-x}$ superconductors. The contact resistivities of the samples, which were fired at temperatures lower than 900°C, exponentially decreased with increasing firing temperature. When the firing temperatures reached 900°C or higher, the contact resistivities were in the 10^{-8} Ω-cm^2 range. Low critical current density ratios were obtained from the samples fired at 880°C or lower. The contact resistivities of these samples were in the 10^{-6} Ω-cm^2 range, which were one to two orders magnitude higher than those fired between 880° to 900°C. Critical current density ratios higher than 0.80 were obtained from the samples fired between 880° to 900°C while the contact resistivities were lower than $10^{-7}\Omega$-cm^2 in these samples. Higher contact resistivities accounted for the lowing of the critical current density ratios of these samples. When the electrodes were fired at temperatures higher than 900°C, the critical current density ratios of the samples decreased despite the fact believed to be that the contact resistivities of the samples were lower than those fired at 880°C. This was caused by the degradation of the superconductor materials.

Contact resistivities of the double fired/painted samples, which were fired at 900°C for different amounts of times, are shown in Figure 7. This Figure also shows the critical current density ratios of the double fired/painted samples compared with the single fired/painted sample. Dwell time was important in decreasing the contact resistivities of the samples. Samples with zero dwell time showed contact resistivities one order magnitude higher than those which had a dwell time greater than zero. After firing at 900°C with some dwell time, the contact resistivities of the samples were in the $10^{-8}\Omega$-cm^2 range. The length of the dwell time did not have much influence on the contact resistivity.

The critical current density ratios of the double fired/painted samples decreased with increasing of dwell time. The contact resistivities were not influence by the critical current of the samples, but rather, by the preparation conditions of the electrodes. Figure 8 shows the I-V characteristics of these samples. Linear I-V characteristics were obtained from the samples fired at 900°C for 12 minutes or
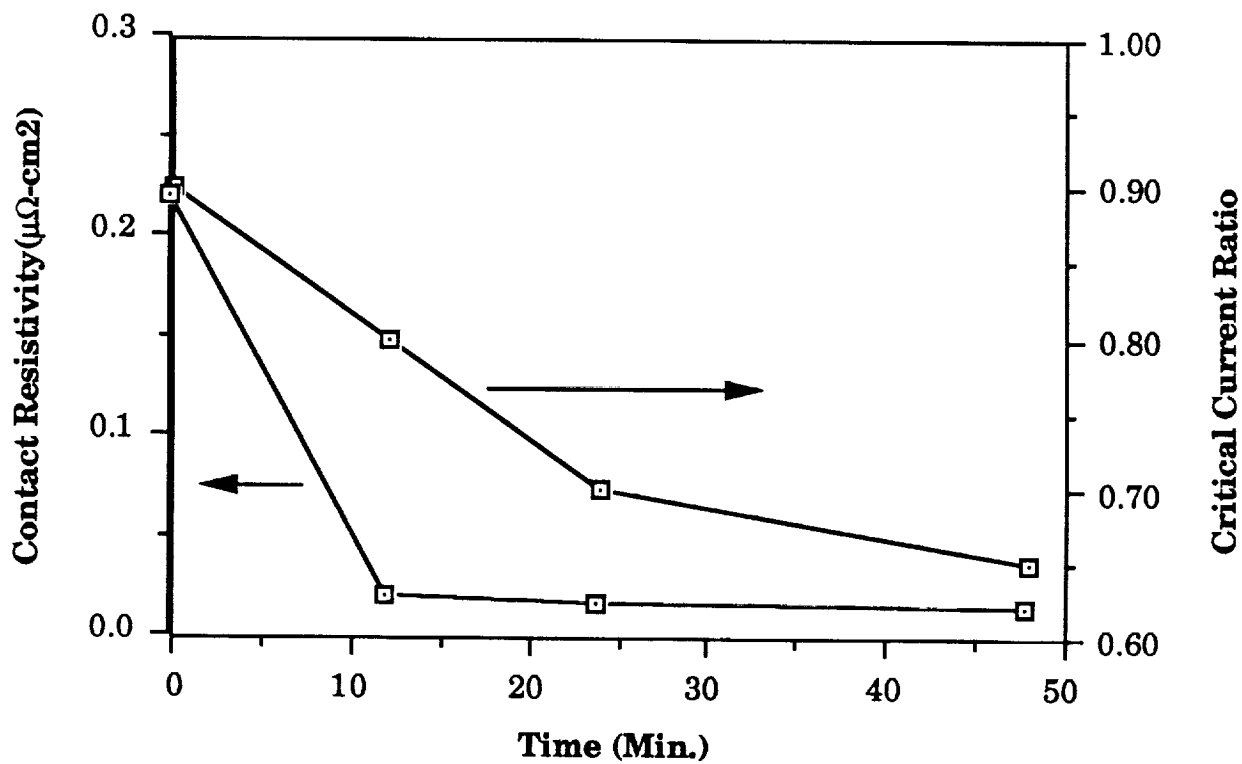
Figure 7: Contact resistivity of the double fired/painted silver electrodes and the critical current change of the sample after firing the electrodes. The electrodes were fired at 900 degrees C for different times.
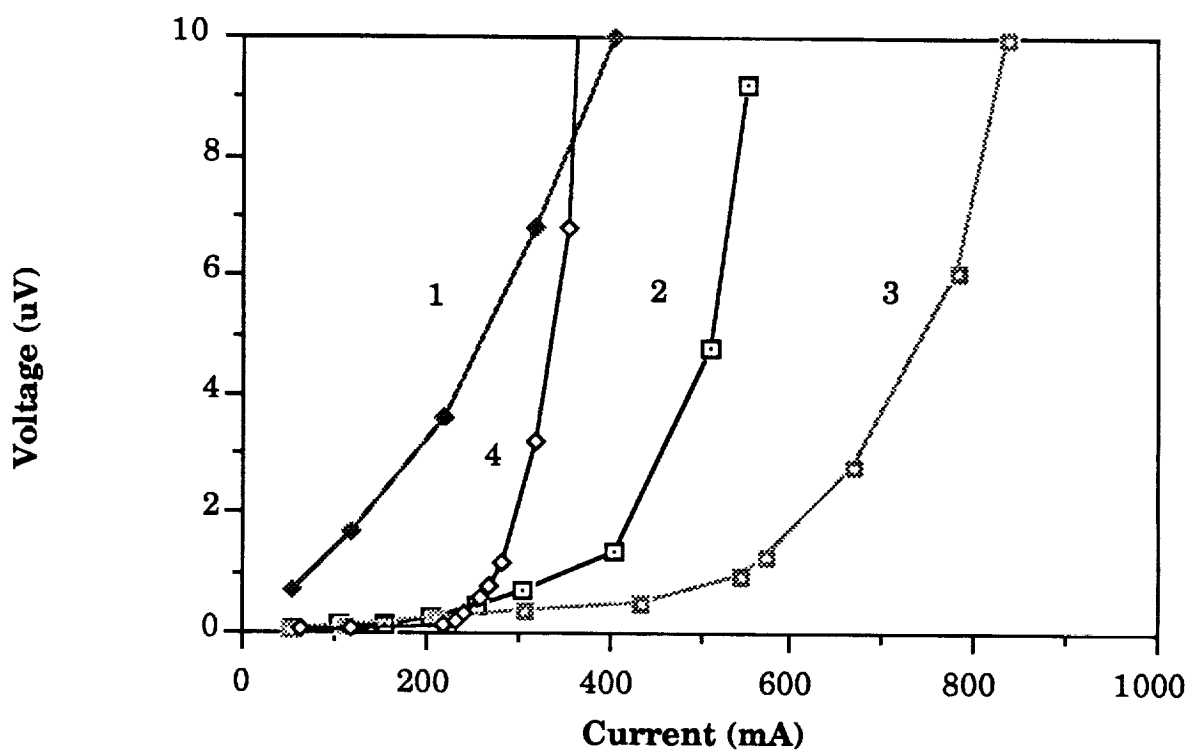
FIgure 8: I-V characteristics of double fired/painted silver electrodes, the electrodes were fired at 900 degrees C for different times.(1. 0.0 minute, 2. 12 minutes, 3. 24 minutes, 4. 48 minutes.)

longer. The samples fired at 900°C for 24 minutes showed the longest linear range in the I-V curves, and these presented more stable contacts than the others. When the samples were fired for 48 minutes, the linear range in the I-V curve decreased. However, the contact resistivities of this sample at 100mA current was lower than those fired for shorter times. The decreasing of the current range of the linear I-V relation might be caused by the degradation of the superconductor.

IV.2 Gold Electrodes.

Figure 9 shows the I-V characteristics of gold electrodes. The electrodes were prepared by the single fired/painted and single fired/embedded methods. The contact resistivity was 1.8×10^{-8} Ω-cm^2 for the painted electrode and 1.1×10^{-8} Ω-cm^2 for the embedded electrode. Linear I-V characteristics were found from the gold embedded sample. It exhibited a more stable electrode than those prepared by the gold paste painted method.

It was noted that there was a second phase black in color, which formed on the electrode surface after firing the electrode. An X-ray diffraction pattern of the second phase is shown in Appendix I but has not yet been identified. This black phase made soldering wires onto the samples difficult.

IV.3 Platinum and Palladium Electrodes.

When the platinum and palladium electrodes were prepared by the single fired/embedded method, there was a green phase at the interface of the electrodes and the $YBa_2Cu_3O_{7-x}$ superconductors. A X-ray diffraction pattern of the green phase, as shown in Appendix II, included $Y_2Ba\,CuO_x$ and other phases. Those phase formed a high resistance layer between the metal electrode and the $YBa_2Cu_3O_{7-x}$ superconductor.
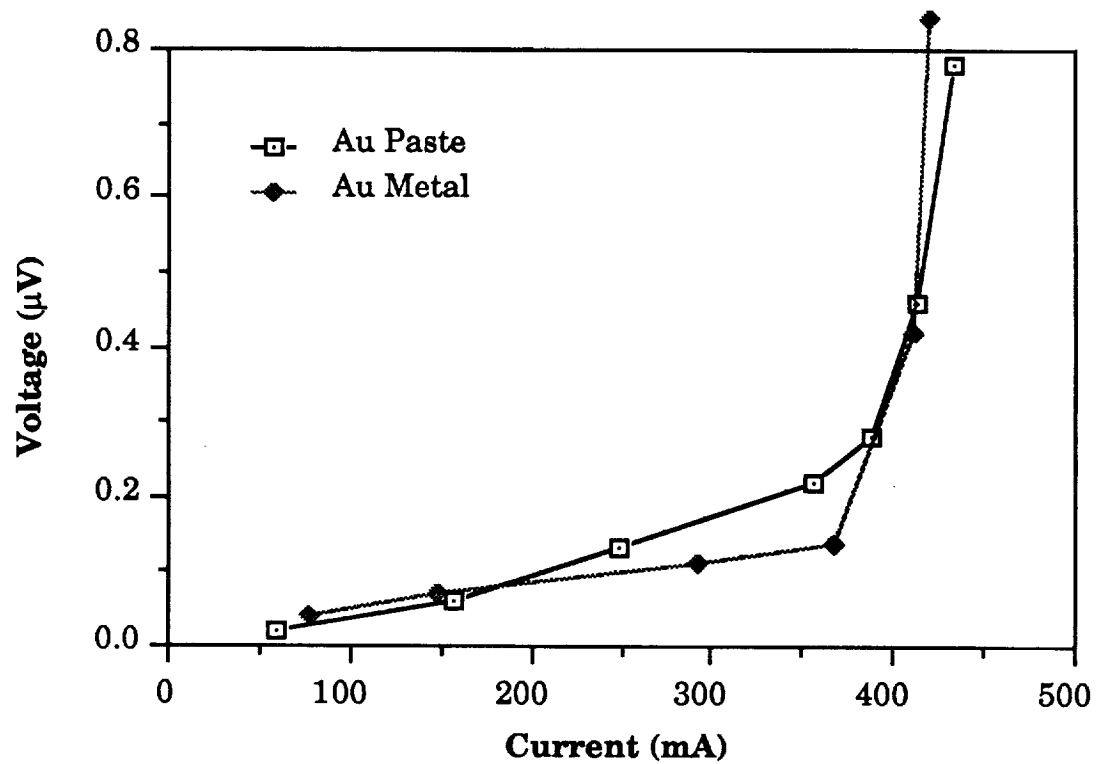
Figure 9: I-V characteristics of gold paste and gold metal contacts. The electrode were prepared at 920 degrees C for 12 hours

V. Conclusions.

A new, more reliable contact resistance measuring method was developed. Silver was found to be the best electroding material to make electrical contacts with the $YBa_2Cu_3O_{7-x}$ superconductors. The following conclusions can be reached from this research.

1. A new lap-joint configuration has been developed for measuring contact resistivities, which is not influenced by the location of the current lead or the voltage lead on the measuring electrode.

2. Contact resistivities were significantly influenced by the electroding conditions; i. e., the electroding materials and the firing conditions.

3. Silver, making clean contact surfaces and low resistivity contacts , is the best electroding material for the $YBa_2Cu_3O_{7-x}$ superconductors.

4. The silver electrode has been found to produce good ohmic contacts to the $YBa_2Cu_3O_{7-x}$ superconductor with a contact resistivity as low as 1.9×10^{-9} $\Omega\text{-cm}^2$.

5. Several techniques for applying the electrodes to the $YBa_2Cu_3O_{7-x}$ superconductors were successful: painting, melting, and embedding.

6. The painting method, which can be applied in single firing and double firing procedures, is more practical than the other methods. The best electroding conditions for double fired/painted silver electrodes were a firing temperature of $900^\circ C$ and a dwell time of 12 minutes.

VI. Reference.

1. J. W. Ekin, A. J. Panson and B. A. Blankenship, Appl. Phys. Lett., 52, 331 (1988)
2. Y. Tzeng, A. Holt and R. Ely, Appl. Phys. Lett., 52, 155 (1988)
3. J. van der Mass, V. A. Gasparov and D. Pavuna, Nature, 328, 603 (1987)
4. J. W. Ekin, T. M. Larson, N. F. Bergren, A. J. Nelson, A. B. Swartzlander, L. L. Kazmerski, A. J. Panson, and B. A. Blankenship, Appl. Phys. Lett., 52, 1819 (1988)
5. S. Jin, M. E. Davis, T.H. TIefel, R. B. van Dover, R. C. Sherwood, H. M. O'Bryan, G. W. Kammlott, and R. A. Fastnacht, Appl. Phys. Lett., 54, 2605 (1989)
6. CRC Hand Book of Chemistry and Physics, R. C. Weast ed. (CRC, Bocaratom, FL, 1987)
7. T. W. Jing, Z. Z. Wang, and N. P. Ong, Appl. Phys. Lett., 55, 1912 (1989)
8. Introduction to the Principles of Ceramic Processing, J. S. Reed (John Wiley & Son, New York, 1988)
9. L. R. Tesser, U. Dai, N. Hess, and G. Deutscher, J. Phys. D, 21, 1652 (1988)
10. Y. Tzeng, J. Electrochem. Soc., 1310 (1988)
11. M.Suzuki, T. Fujii, K. Mori, K. Muta, and T. Watari, Jpn. J. of Appl. Phys., 27, (1988)
12. K. Mizushima, M. Sagoi, T. Miura, and J. Yoshida, Appl. Phys. Lett., 52, 1011(1988)
13. A.D. Wieck, Appl. Phys. Lett., 52, 1017(1988)
14. J. W. Ekin, T. M. Larson, N. F. Bergen, A. J. Nelson, A. B. Swartzlander, L. L. Kazmerski, A. J. Panson, and B. A. Blankenship, Appl. Phys. Lett., 52, 1819(1988)
15. Q. X. Jia and W. A. Anderson, J. Phys. D, 22, 1565(1989)
16. Y. Suzuki, T. Kusaka, A. Aoki, T. Aoyama, T. Yotsuya and S. Ogawa, Japn. J. of Appl. Phys., 28, 2463(1989)
17. I. Sugimoto, Y. Tajima and M. Hikta, Japn. J. of Appl. Phys., 27, L864(1988)
18. S. Yokoyama, T. Yamada, Y. Kubo, K. Egawa and Y. Simizu, Cryogenics, 28, 734(1988)
19. R. Caton, R. Selim, A. M. Buoncristian and C. E. Byvik, Appl. Phys. Lett., 52, 1014(1988)
20. S. Jin, J. E. Graebner, T. H. Tiefel and G. W. Kammlott, Appl. Phys. Lett., 56, 186(1990)
21. T.W. Jing, Z. Z. Wang, and N. P. Ong, Physica C, 162-164, 1061(1989)
22. S. T. Lakshmikumar and A. C> Rastogi, Appl. Phys. A, 48, 325(1989)
23. N. Shimizu, K. Michishita, Y. Higashida, H. Yokoyama, Y. Hayami, Y. Kubo, E. Inukai, A. Saji, N.Kuroda, and H. Yoshida, Japn. J. of Appl. Phys., 28, L1955(1989)

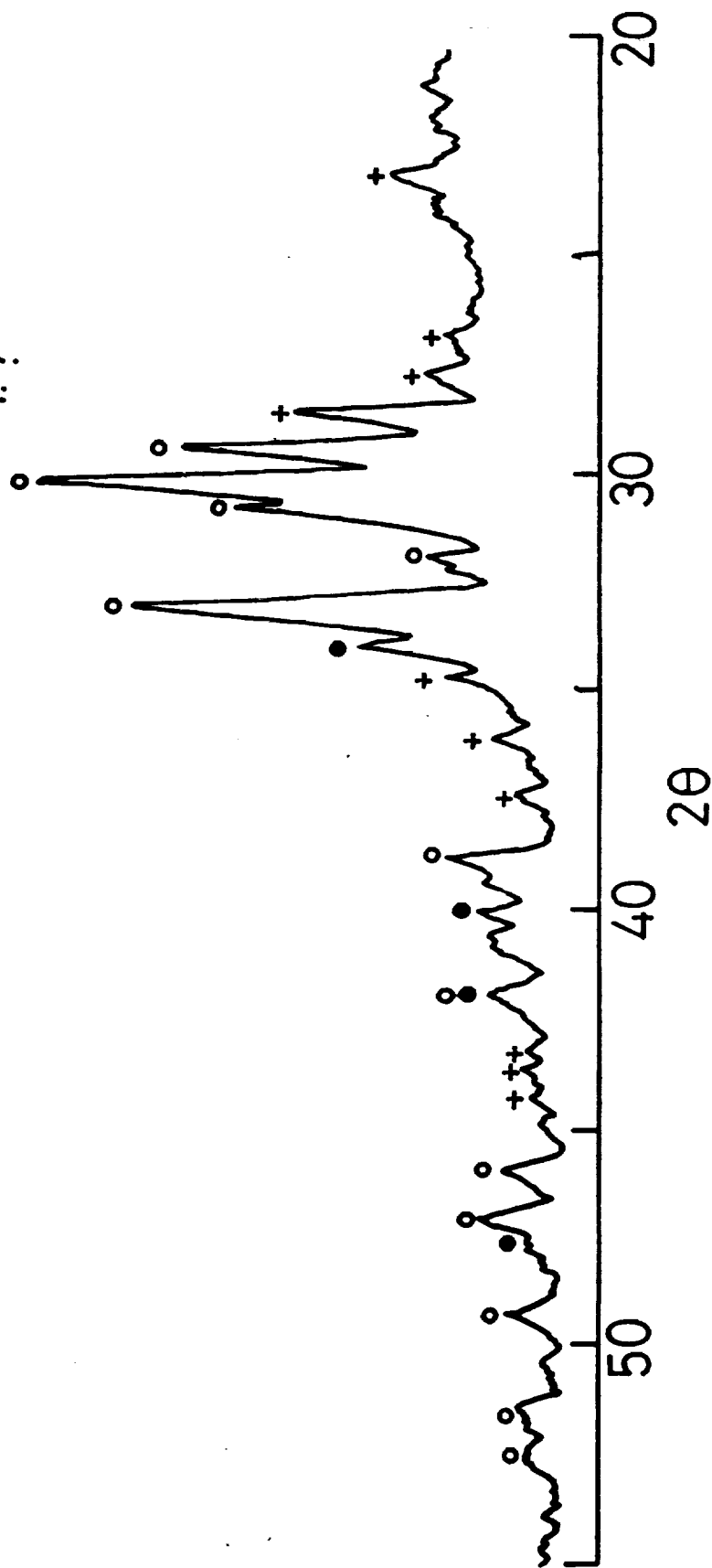Appendix I: X-ray diffraction pattern of gold electrode with the black phase.

o: Au
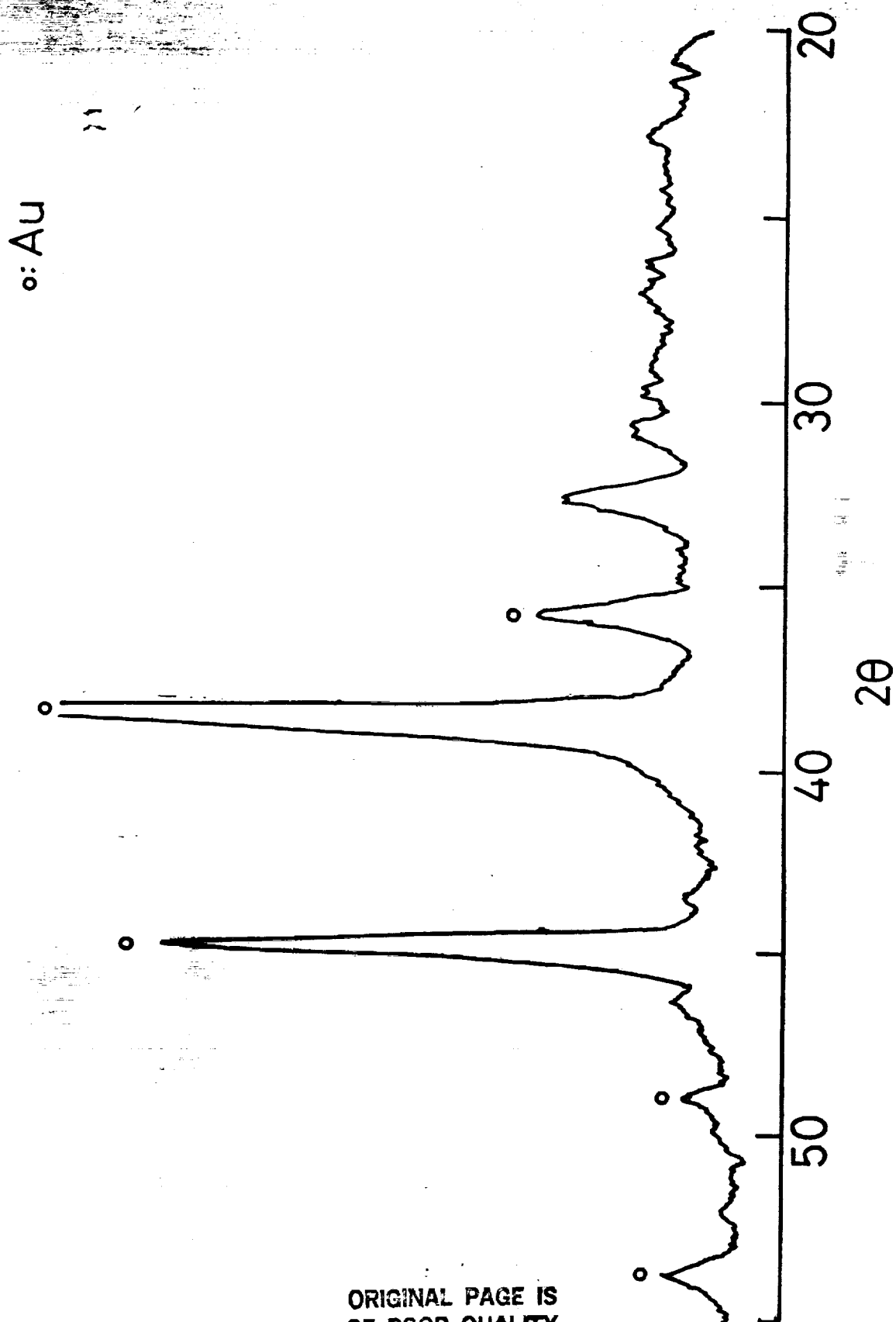
Appendix II: X-ray diffraction of the green phase between the palldium electrode and the superconductor.

$\bullet$: $YBa_2Cu_3O_{7-x}$

$\circ$: Y_2BaCuO_x

$+$: ?

2θ

FINAL REPORT

PART III

DEVELOPMENT AND CHARACTERIZATION OF HIGH CURRENT DENSITY YBa$_2$Cu$_3$O$_{7-x}$ CIRCUIT ELEMENTS

SUBMITTED TO

SUBMITTED BY
Vibhakar Modi

PRINCIPAL INVESTIGATOR
Gene Haertling
Department of Ceramic Engineering
Clemson University

DEVELOPMENT OF HIGH CURRENT DENSITY $YBa_2Cu_3O_{7-x}$ CIRCUIT ELEMENTS

1 INTRODUCTION

The transport critical current density in bulk polycrystalline samples of high-T_c superconductors is three to four orders of magnitude lower than the same observed in single crystal and thin film samples. That, combined with the relative difficulty of fabrication has impeded rapid introduction of useful devices based upon these superconductors. The promise these materials offer largely relies on the ability of researchers to form bulk, intricate, high current carrying devices.

The research effort in this project is focused on fabrication and characterization of high critical current circuit elements from the ceramic superconductor $YBa_2Cu_3O_{7-x}$. Tape casting and die pressing have been used to make pre-fired bodies of $YBa_2Cu_3O_{7-x}$ which were later processed under varying conditions and characterized. The goal was to fabricate bulk $YBa_2Cu_3O_{7-x}$ specimens showing a critical current density (J_c) of at least 1,000 A/cm^2 at 77 K in the absence of an applied magnetic field. Solid state sintering, liquid phase assisted sintering using silver, and melt processing have been employed and extensively studied during the course of fabricating the desired circuit elements. Electrical characterization was peformed using the standard four probe method. Powder samples have been analyzed using both x-ray and scanning electron microscopy. Bulk specimens were also characterized using SEM. Some other characterizations performed on the samples include differential thermal analysis, density measurement, and particle size analysis.

The electrical measurements conducted on both tape cast and die pressed specimens have yielded interesting results. The maximum J_c measured on the tape cast products has been 120 A/cm^2. On the other hand the die pressed samples which were melt processed have shown J_c in excess of 3,000 A/cm^2. It is believed that only

the lower estimate of the actual J_c has been measured on the melt processed samples due to instrumental limitations. The die pressed samples prepared with silver addition have exhibited maximum J_c of 766 A/cm^2. More testing and characterization is underway to establish the process parameters for achieving optimum results with regard to the current density.

A discussion on the major factors responsible for low J_c in bulk polycrystalline samples and the ways to overcome these factors is presented in the next section. The powder preparation technique has been described in detail in Section 3. Details on experiments conducted on the tape cast products have been described in Section 4, followed by similar discussions on the die pressed and silver doped specimens in Sections 5 and 6 respectively. The summary of results has been presented in Section 7.

2 FACTORS RESPONSIBLE FOR LOW J_c IN BULK YBCO

In spite of the fact that current densities in excess of 10^6–10^7 A/cm^2 have been reported for single crystal $YBa_2Cu_3O_{7-x}$, the values measured in bulk polycrystalline samples that are prepared by the solid state route have J_c typically less than 10^3 A/cm^2.[1] Many factors have been identified for the low J_c values reported. A discussion on these factors is presented below.

I POROSITY

Bulk, polycrystalline $YBa_2Cu_3O_{7-x}$ products have been known to contain residual porosity after sintering. Figure 1 shows pores in a sintered YBCO sample. Excessive porosity results in weak links in the path of the supercurrent. A small amount of porosity is desirable since it facilitates oxygen transport during annealing.
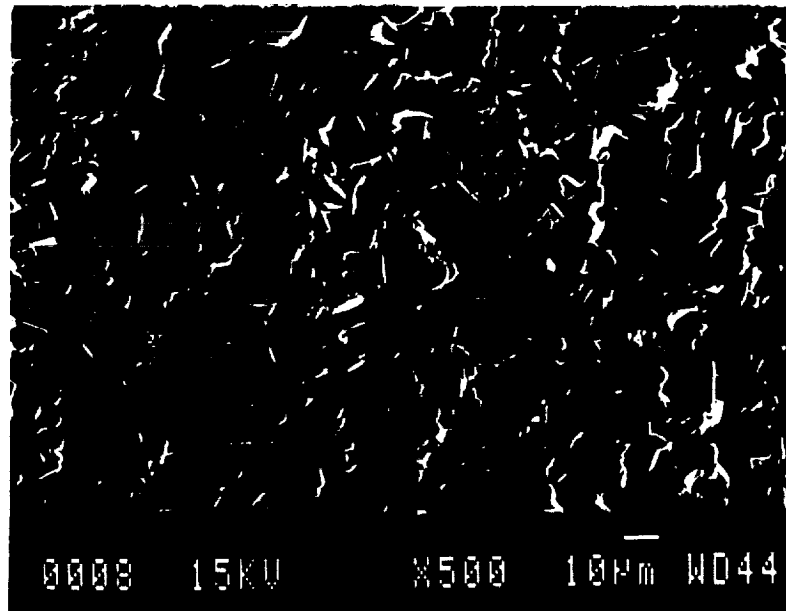
Figure 1. Porosity in a sintered specimen of $YBa_2Cu_3O_{7-x}$

Sintered $YBa_2Cu_3O_{7-x}$ which was 90% dense theoretically has been reported to show higher current density than denser samples processed identically.[2] The density of sintered YBCO tapes may be increased by techniques such as blending different particle size

distributions, liquid phase sintering with addition of $Ag/AgO/Ag_2O$, re-sintering at a higher temperature, and melt processing.

II SECONDARY PHASES

A variety of secondary phases could be present in bulk superconductors that, besides reducing the overall content of the superconducting phase, act as barriers to the flow of supercurrent. Chief among the secondary phases are Y_2BaCuO_5, $BaCuO_2$, $BaCO_3$, and CuO. Some impurities come from the raw materials and others are incorporated during handling (ball milling, dusty environment etc.). Some of these inclusions may act as sites for secondary grain growth, resulting in abnormally large grains. The presence of large grains may increase porosity and may result in random orientation during melt-texturing. Thus efforts must be made to produce phase-pure $YBa_2Cu_3O_{7-x}$ calcined and sintered products.

III MICROCRACKING

Microcracks in $YBa_2Cu_3O_{7-x}$ occur due to anistropy in thermal expansion and contraction behaviour. They act as discontinuities in the path of the supercurrent, forcing it to find alternate paths which may not always be available. Figure 2 shows a microcrack in a tape cast sample. Microcracks could be critical
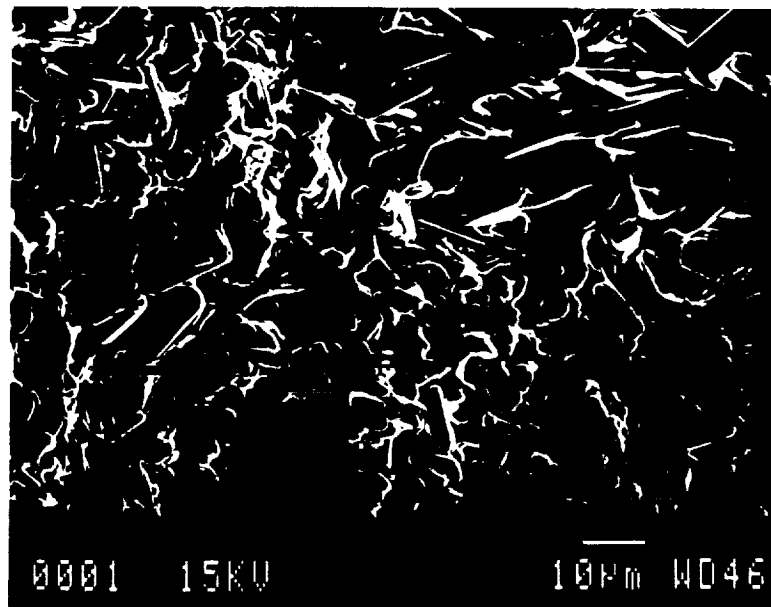
Figure 2. A microcrack in sintered sample of $YBa_2Cu_3O_{7-x}$.

during thermal cycling (room temperature to 77 K). They could be removed by forming $YBa_2Cu_3O_{7-x}$-Ag composites. The silver-rich matrix is known to withstand thermal and mechanical shocks better than $YBa_2Cu_3O_{7-x}$ alone. Alignment of grains can also reduce random thermal expansion or contraction.

IV   INSUFFICIENT OXYGEN CONTENT

The superconducting properties of $YBa_2Cu_3O_{7-x}$ are greatly affected by the amount of oxygen present. Ideally there should be 6.98 atoms of oxygen per molecule of $YBa_2Cu_3O_{7-x}$. The amount of oxygen may be lower than desired due to incomplete annealing. It is very important to establish the optimum annealing conditions for $YBa_2Cu_3O_{7-x}$ products.

V   RANDOM ORIENTATION OF GRAINS

By far, random orientation is the most critical of all factors that reduce J_c in bulk, polycrystalline $YBa_2Cu_3O_{7-x}$. It is now known that J_c in the a-b plane of orthorhombic $YBa_2Cu_3O_{7-x}$ lattice is an order of magnitude higher than the same in the direction of the c-axis. The current travels in a tortorous path of
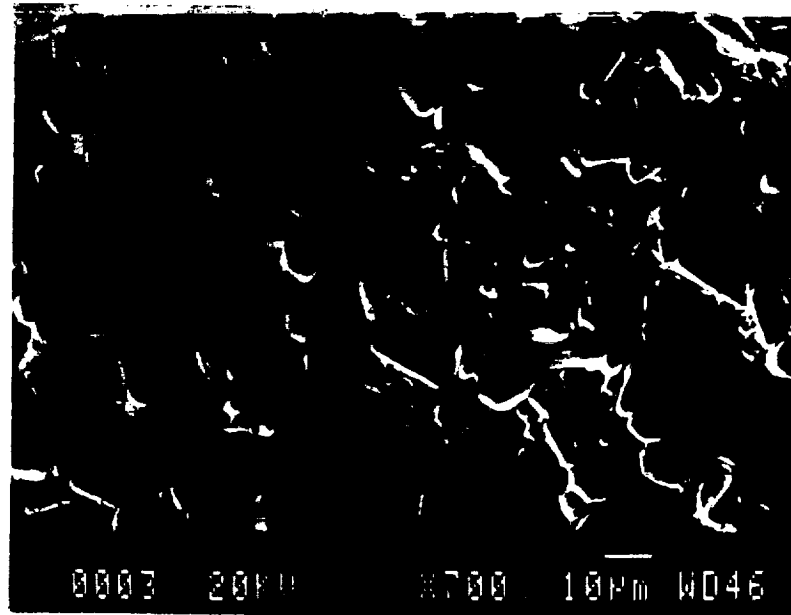
Figure 3. Microstructure of $YBa_2Cu_3O_{7-x}$ showing randomly oriented grains

fortuitously aligned grains in randomly oriented $YBa_2Cu_3O_{7-x}$. Figure 3 shows a surface of a tape that was solid state sintered. It is clearly evident that grains of widely varying sizes and orientation are present.

Alignment of $YBa_2Cu_3O_{7-x}$ single crystals has resulted in significantly higher current densities than normal.[3,4] Grain alignment can be performed by techniques such as melt-texturing, application of magnetic[5,6] or electric field, or using compressive stress during the tetragonal to orthorhombic transformation.

Many of the suggestions mentioned in this section have been tried and improvements have been made in the overall process of making $YBa_2Cu_3O_{7-x}$ samples. A detailed discussion of the techniques used is presented in following sections, together with their effect on the measured transport J_c of $YBa_2Cu_3O_{7-x}$ samples.

3 IMPROVEMENTS IN POWDER SYNTHESIS METHOD

Solid state preparation of $YBa_2Cu_3O_{7-x}$ powder is the most widely followed method for obtaining the precursor for further processing. In this method, $Y2O3$, $BaCO3$, and CuO are mixed in stoichiometric proportion to yield $YBa_2Cu_3O_{7-x}$ after calcining. Typically the powder mix is calcined at 900 C for 5 hr followed by a 12 hr anneal in air at 450 C. This process is repeated two more times to get homogeneous powder. Figure 4 shows the x-ray diffraction pattern of a powder synthesized from oxides as mentioned. The pattern is compared with the Joint Committee on Powder Diffraction Standards (JCPDS) database patterns for $YBa_2Cu_3O_7$ (the orthorhombic phase), $YBa_2Cu_3O_{6.56}$, and $YBa_2Cu_3O_6$ (tetragonal). This diffraction pattern is marked by low overall intensities of the characteristic peaks.

Although simple, the solid state route has several limitations that leave room for investigation of utilizing other techniques for powder synthesis. The principal disadvantages of the solid state route are; long calcining schedules due to low precursor reactivity, relatively higher processing temperatures compared to chemical methods, lower phase purity and homogeneity, and a coarser particle size distrbution. To form $YBa_2Cu_3O_{7-x}$ products, the solid state derived powder has to be ball milled to break down the coarser particles. This may add to the contamination problem and may result in a decreased J_c.

To eliminate the difficulties faced in synthesizing solid state derived $YBa_2Cu_3O_{7-x}$, a chemical co-precipitation route was investigated. In this method, dilute solutions of nitrates of Y, Ba, and Cu prepared and assayed. Dimethyl formamide is added to increase the solubility of barium nitrate in water.The chemicals are mixed together in a borosilicate glass beaker to yield stoichiometric $YBa_2Cu_3O_{7-x}$ precursor solution. A specific amount of oxalic acid (calculated on molar basis) is added to the solution to precipitate the nitrates. The following reactions take place:
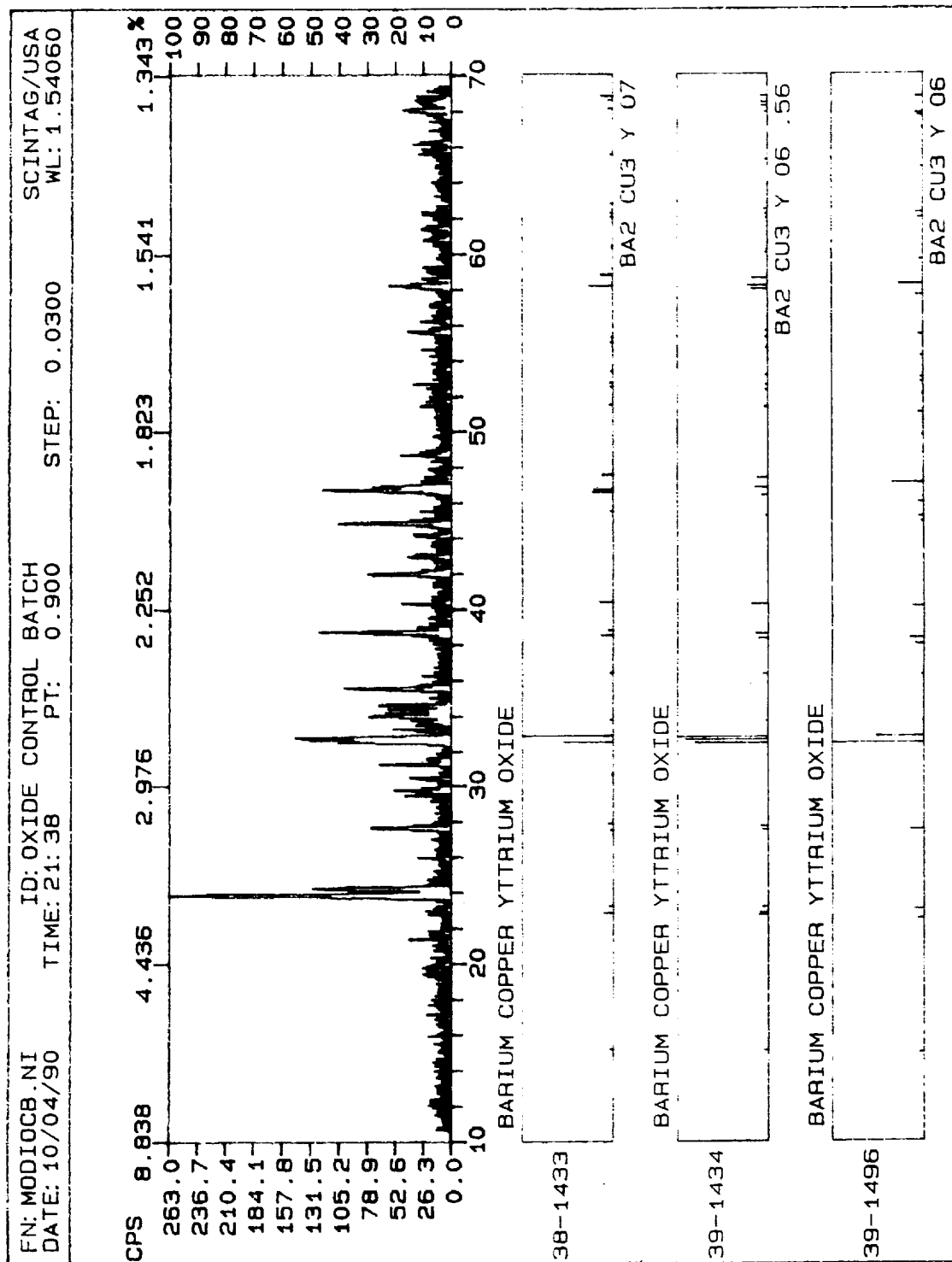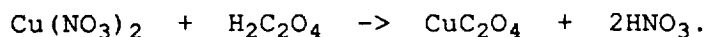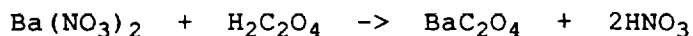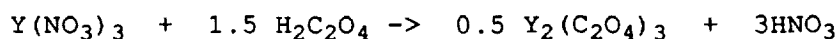
FN: MODIOCB.NI   ID: OXIDE CONTROL BATCH
DATE: 10/04/90   TIME: 21:38   PT: 0.900   STEP: 0.0300   SCINTAG/USA
                                                                     WL: 1.54060

Figure 4. X-ray diffraction pattern of sintered YBa$_2$Cu$_3$O$_{7-x}$ powder derived from oxide precursors.

$$Y(NO_3)_3 \ + \ 1.5 \ H_2C_2O_4 \ -> \ 0.5 \ Y_2(C_2O_4)_3 \ + \ 3HNO_3$$

$$Ba(NO_3)_2 \ + \ H_2C_2O_4 \ -> \ BaC_2O_4 \ + \ 2HNO_3$$

$$Cu(NO_3)_2 \ + \ H_2C_2O_4 \ -> \ CuC_2O_4 \ + \ 2HNO_3.$$

The metal oxalates have very low solubility in water, thus they precipitate. The precipitates are dried till a thick paste is obtained. During drying, the nitric acid in the top liquid reacts with metal oxalates and forms some amount of nitrates back. This happens towards the end of drying, when the concentration of nitric acid is high. Thus, the paste obtained is a mixture of oxalates and nitrates. The paste is pyrolyzed at 600 C for 30 minutes. An exothermic reaction takes place which increases the local temperature much higher than 600 C. The pyrolyzed powder is crushed and later calcined at 850-875 C for 5 hours, followed by annealing in air at 450 C for 12 hours. Figure 5 shows the x-ray diffraction pattern for powder that was sintered at 925 C for 12 hours and annealed in air at 450 C for 12 hours. It may be noticed that all the major peaks of the pattern match very closely with the peaks on the JCPDS pattern of $YBa_2Cu_3O_7$. Figure 6 shows the diffraction pattern for a powder calcined at 875 C for 5 hr and annealed in air at 450 C for 5 hr. It is evident from this figure that a considerable amount of orthorhombic phase is present. When Figures 4 and 6 are overlapped for comparison as in Figure 7, the difference in the intensities of the peaks is apparent.

The advantages of chemically derived powders are as follows:

(1) better homogeneity and phase purity compared to the oxide derived powder. This is revealed by the x-ray diffraction pattern comparison shown in Figure 7. The code OCB refers to oxide control batch. A differential thermal analysis was performed on sintered specimens of the chemically derived powder (Figure 8). The curve shows behaviour of the melting of a single phase material if the effect of instrumental noise is disregarded;

(2) lower calcining and sintering temperatures, and single step calcining as opposed to three times in solid state route;
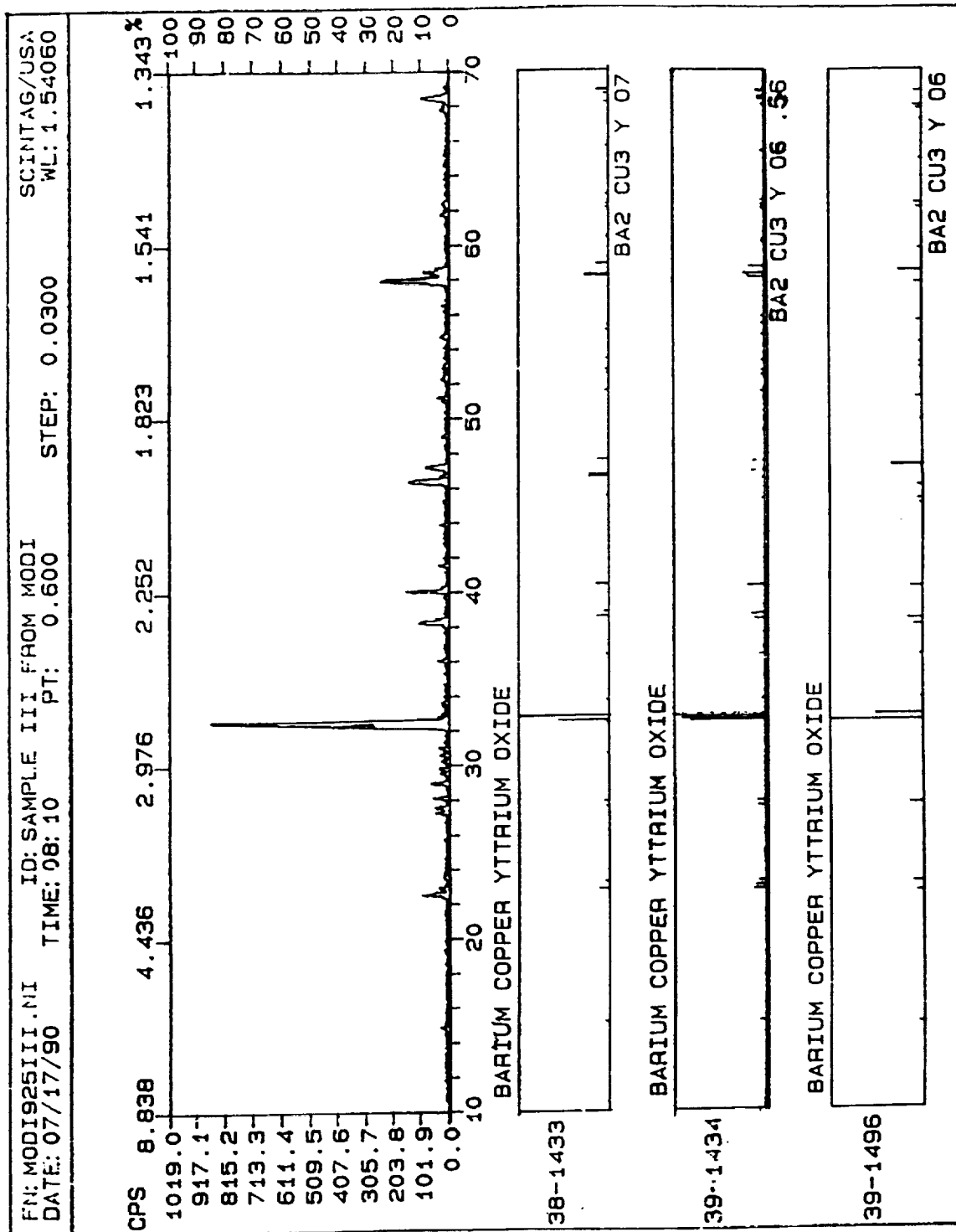
FN: MODI925III.NI   ID: SAMPLE III FROM MODI
DATE: 07/17/90   TIME: 08:10   PT: 0.600   STEP: 0.0300

SCINTAG/USA
WL: 1.54060

CPS

BARIUM COPPER YTTRIUM OXIDE

38-1433   BA2 CU3 Y O7

BARIUM COPPER YTTRIUM OXIDE

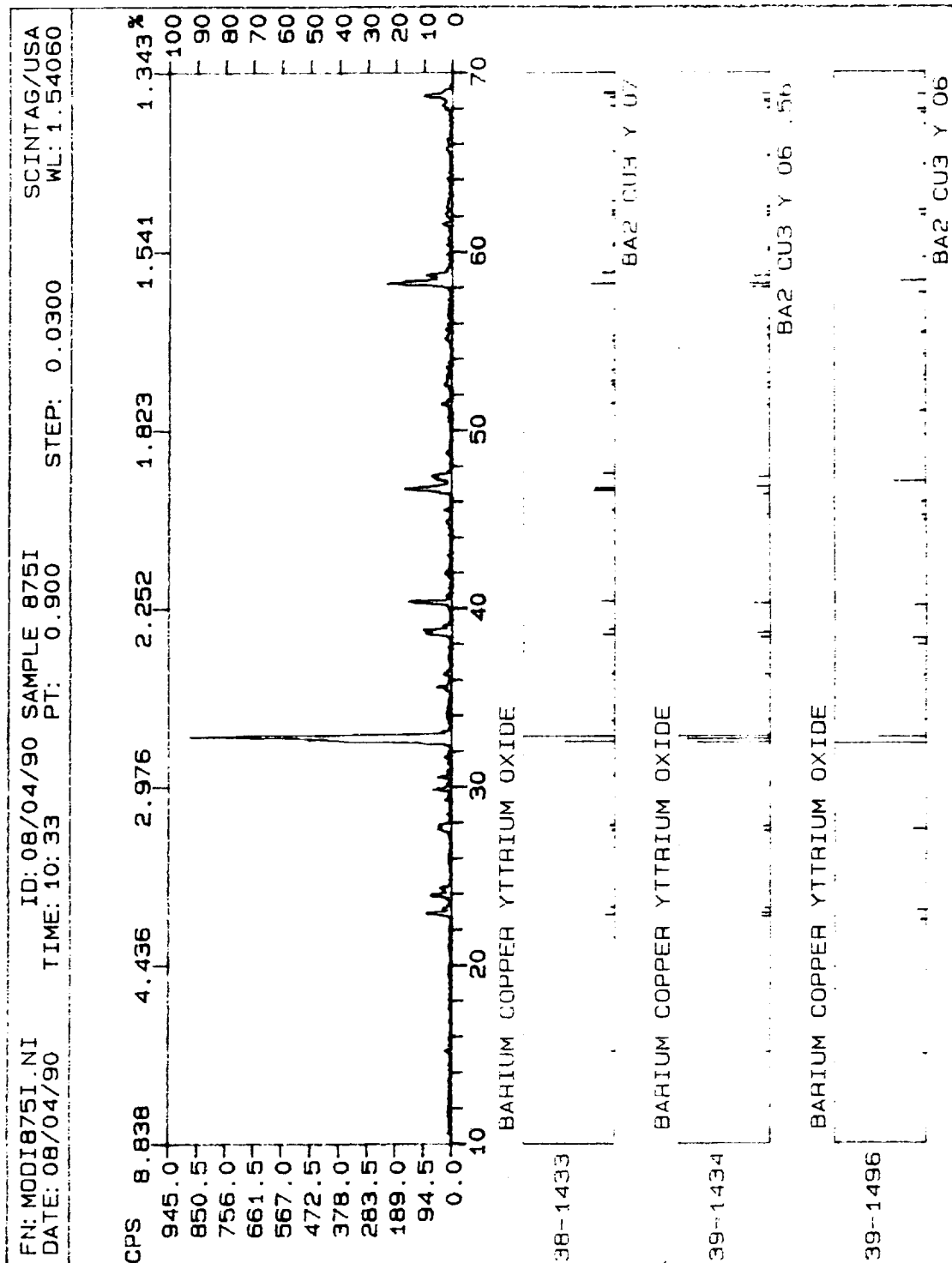39-1434   BA2 CU3 Y O6 .56

BARIUM COPPER YTTRIUM OXIDE

39-1496   BA2 CU3 Y O6

Figure 5. X-ray diffraction pattern of sintered $YBa_2Cu_3O_{7-x}$ powder derived from the co-precipitation of nitrate solutions. The pattern shows a very good match with the JCPDS

Figure 6. X-ray diffraction pattern of calcined $YBa_2Cu_3O_{7-x}$ powder derived from the co-precipitation of nitrate solutions. The pattern shows a good match with the JCPDS database pattern for $YBa_2Cu_3O_7$.
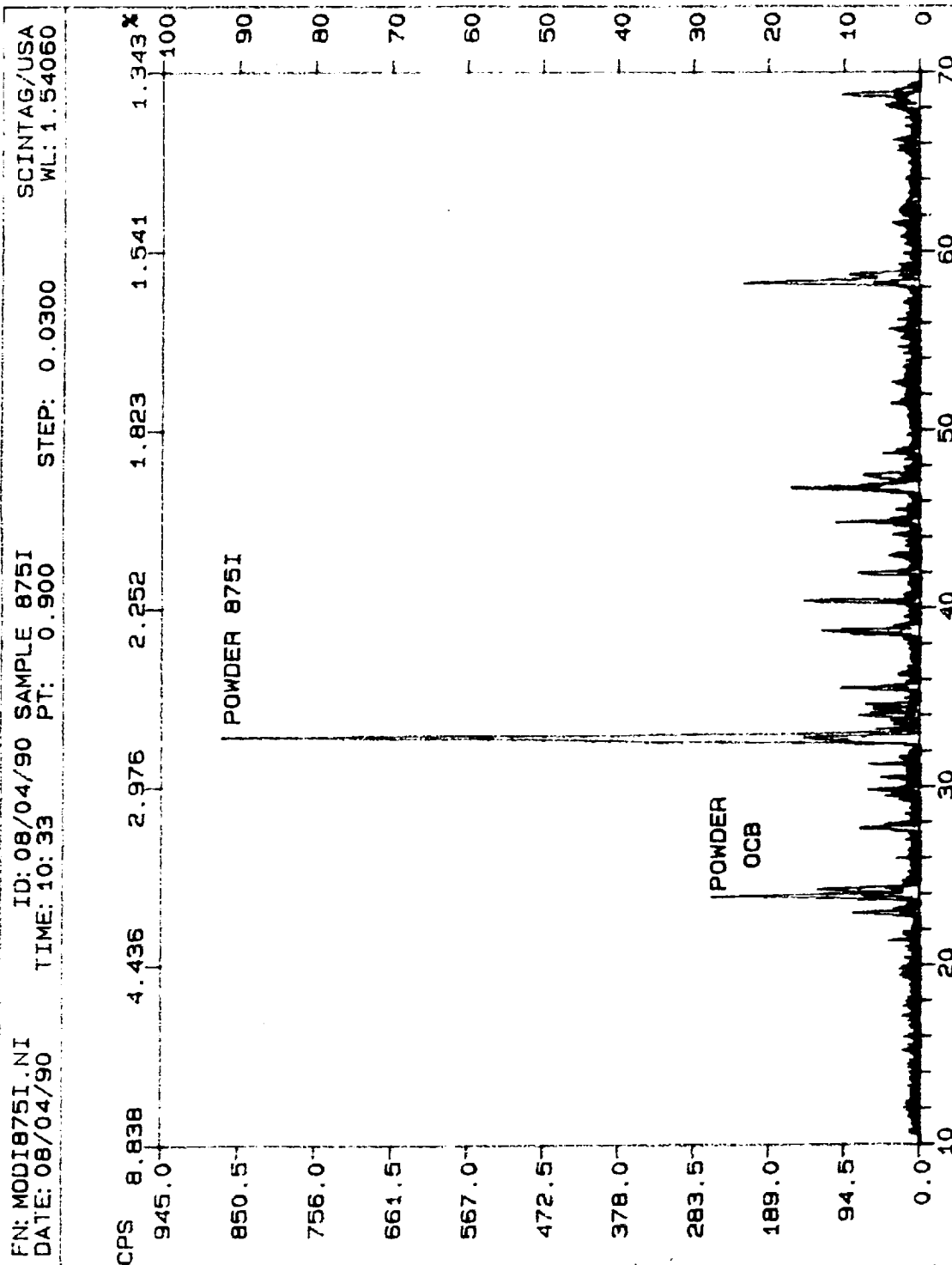
Figure 7. The x-ray patterns in Figures 4 and 6 are overlapped to show the difference in the quality of powders obtained by the solid state and co-precipitation routes. Notice the large difference in the intensities of the characteristic (1 1 0) peak at 32.8 degrees.
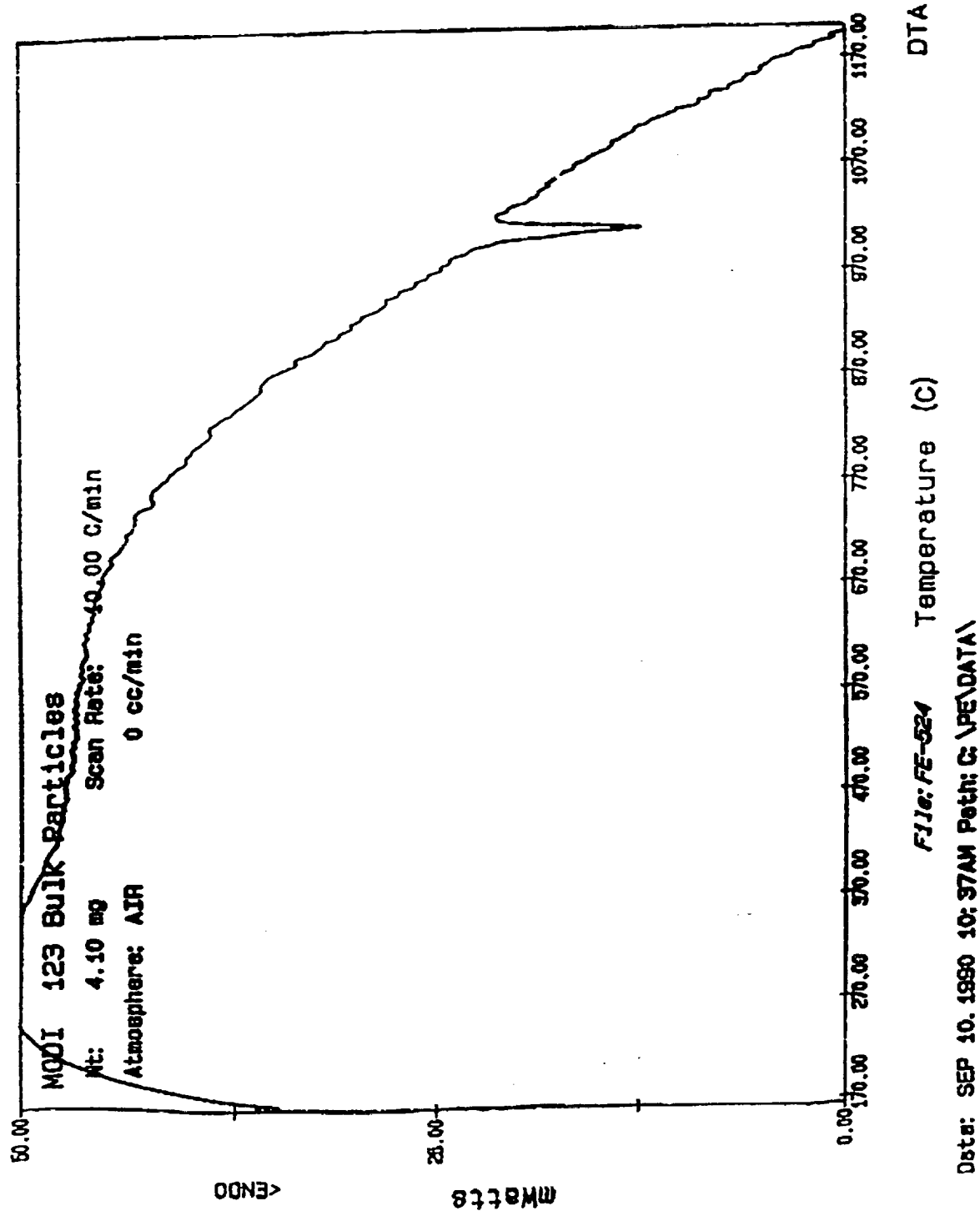
Figure 8. DTA analysis performed on sintered pellet of $YBa_2Cu_3O_7-x$ prepared by the co-precipitation method. The curve displays melting characteristics of a single phase material (courtsey John Buckley).

(3) finer calcined powder, finer than what is obtainable by ball milling the oxide derived powder for an hour. In a particle size analysis performed on both the thrice calcined and ball milled powder and the once calcined chemically derived powder, the median particle size was found to be 4.91 μm and 4.12 μm, respectively.

The elimination of the ball milling step in processing is very important since contamination from the media and ball jar could adversely effect the superconduting properties. In fact a small increase in J_c was noticed in nitrate derived tapes in comparison to the ones prepared from oxide derived powder (the J_c goes up from 80 A/cm^2 to about 120 A/cm^2).

4 EXPERIMENTS PERFORMED ON TAPE CAST PRODUCTS

A significant portion of the research effort was directed at attempts to fabricate high J_c tape cast products. In contrast to other fabrication techniques tape casting is a versatile method when formation of intricate shapes is required.

The initial experiments involved using ball milled powder derived from the oxide precursors. The powder is mixed with an organic binder (B-73305, Metoramic Sciences Inc.) in 65-35 weight ratio, respectively. The resulting slurry is cast in the form of tape using the doctor blade process. Typical thicknesses of as-cast tapes are 25-50 mils. Upon evaporation of the solvent, the green tape is removed from the casting substrate and cut into required shapes. The green tape bodies are then sintered between 925-950 C for 5 hr or more and cooled to 450 C where they are annealed in air of oxygen for 12-24 hr. Silver paint electrical contacts are sintered on the processed tapes at 925 C for 0.5 hr and the samples are oxygenated again at 450 C for 12-24 hr. Current density is measured on the specimen using the four contact method and a criterion of $1\mu V/mm$ of distance between the potential measuring leads on the samples.

The typical J_c values measured on oxide derived tapes are less than or equal to 80 A/cm^2. Low bulk density of tape cast products is considered to be responsible for the low J_c values. Low density is associated with high porosity which in tape cast $YBa_2Cu_3O_{7-x}$ may act as weak links in the path of supercurrent. It is imperative to reduce the porosity not just for current density improvement, but also for getting higher strength. Four methods have been tried for densification of tapes. These methods have been described in detail below:

I BLENDING PARTICLES WITH VARYING SIZE DISTRIBUTIONS

Particles tend to pack together densely if they are of varying size since the smaller of them can fit in the interstices between the larger ones. In a particular experiment, three particle size distribution were blended together to achieve higher packing. The size distributions were obtained by milling the oxide derived calcined powder for 1 hr, 2 hr, and 3 hr respectively. The optimum

fraction of each distribution in the blend was calculated using the Dinger-Funk[7] distribution analysis software. Tapes could be cast with reduced amount of binder (from nearly 35% by weight to less than 25% by weight). The sintered tapes were far stronger than normally processed tapes and were denser in appearance also. Actual bulk density measurements on the tapes gave misleading results because of the volatility of media used for suspension (toluene and trichloroethylene). Measuring the specific surface area of the samples is suggested to get a reliable estimate of the relative bulk densities of samples prepared by using different methods.

Although the samples obtained by the particle blending method seemed to be denser than the ones obtained by using a single distribution, there was no improvement in the current density of the tapes. The J_c of the denser tapes ranged from 5 to 25 A/cm^2. Two reasons were considered responsible for this behaviour, namely lower oxygen content due to higher density, and the contaminants introduced during ball milling. Of the two, the latter seems to be more likely the cause for low J_c.

Varying size distributions can be obtained from the chemically derived powders by calcining at different temperatures. It is believed that the median particle size of the calcined powder would be higher with higher calcining temperature. This study is being conducted presently and the results will be reported later.

II RESINTERING OF TAPES

Density of ceramics can be improved by sintering less denser compacts at higher temperatures. This technique was used for densification of $YBa_2Cu_3O_{7-x}$ tapes. Initial compacts were sintered at 930-950 C and re-sintered at 970 C or higher. Figure 9 shows a surface view of a re-sintered tape. There was no improvement in current density of the tapes in spite of improvement in the density of the material. Partial meltdown of the tapes and formation of second phases are considered to be responsible for the lower J_c of re-sintered tapes.

III LIQUID PHASE ASSISTED SINTERING

Silver additions have been made to $YBa_2Cu_3O_{7-x}$ in order to improve the density. Silver may assist in liquid phase sintering and also provide a high electrical conductivity matrix. A batch with approximately 15% by weight Ag_2O was tape cast and sintered at
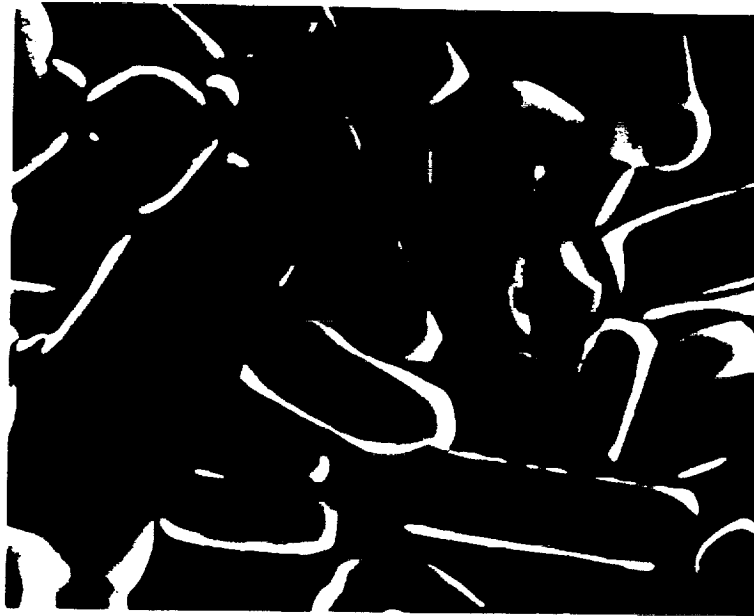
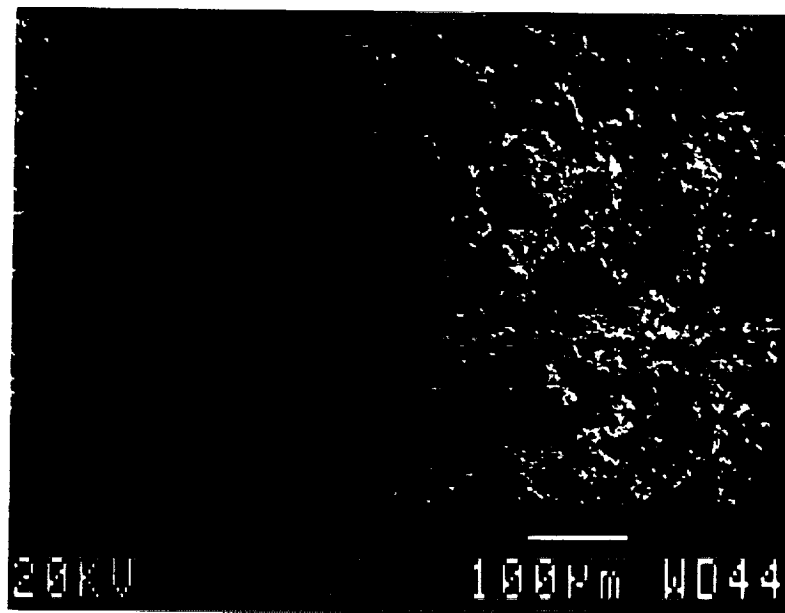**Figure 9. Microstructure of a re-sintered tape**

Figure 10. Microstructure of a sintered tape doped with Ag₂O. The dark regions are silver rich

935 C for 5 hr. Figure 10 shows a SEM micrograph of the tape surface. A careful look at the picture reveals dark silver rich portions. There seems to be no visible sign of pores in the sample.

No appreciable increase in J_c has been observed with this batch yet. Reasons other than the amount of silver are considered responsible for the lower J_c. Decomposition of a large fraction of $YBa_2Cu_3O_{7-x}$ due to presence of silver in excess of the solubility limit (~ 0.1 atomic percent)[8] may be responsible for low J_c of the composite in spite of the high density. The processing conditions of $YBa_2Cu_3O_{7-x}$-Ag composites are being evaluated presently.

III MELT PROCESSING

Processing $YBa_2Cu_3O_{7-x}$ from melt has yielded close to theoretical density bulk specimens. In the case of the tapes however the same results have not been noticed due to lower density of the starting compacts. Considerable melting occurs due to the particles not being able to hold together. It is essential to have compacts of high starting density in order to perform melt processing. Typically, samples are introduced rapidly in a furnace maintained at 1050-1100 C, melted for 2-5 min, and slow cooled to 980 C. The samples are soaked at 980 C for 8-16 hr and slow cooled to room temperature thereafter. Figures 11 and 12 reveal the effect of melt processing on grain alignment in small regions of the tape.
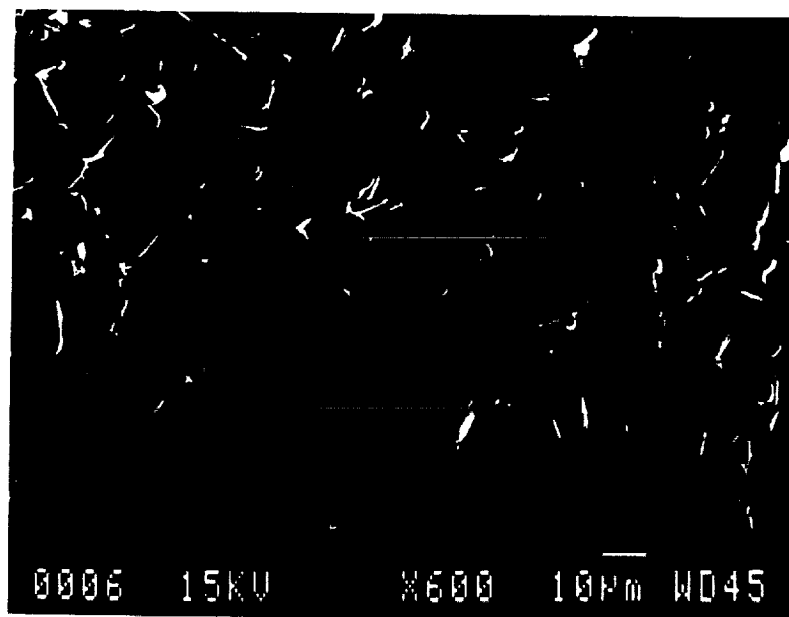

Figure 11. Microstructure of a melt processed tape showing randomly oriented grains with high aspect ratio.

The four methods tried above have not produced higher J_c products. Other publicatioons have reported low J_c also.[9,10,11] Two reasons are considered responsible for the low J_c. The first is absence of compressive stress during casting of tapes. Unlike die pressed specimens the powder is in a compacted, relatively dense state the tape casting slurry is held together by an organic binder which volatilizes at 400 C or higher. After the binder burnout the particles are very weakly held together by collapsing on one another till the temperature is high enough for sintering. Thus tape cast products exhibit a lower bulk density compared to die pressed products. As mentioned earlier in this section, lower density is a major reason for low J_c due to the weak link problem attributed to porosity. The second reason is the large amount of binder that has to be included to form the slurry, after burnout, leaves a proportional amount of open space behind. This open volume between particles results in pores in the sintered compacts.
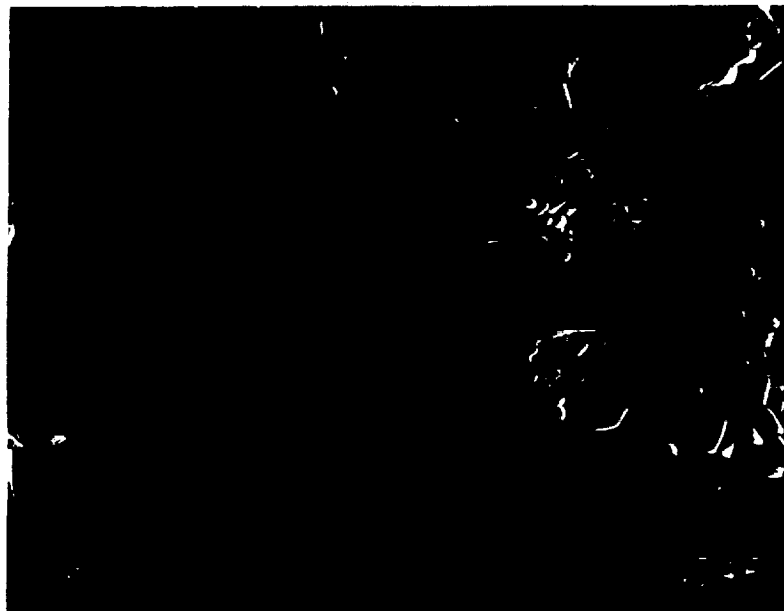

Figure 12. Microstructure of a melt processed tape showing grain alignment in a small region.

5 MELT PROCESSING OF DIE PRESSED SPECIMENS

After several attempts at increasing the J_c of tape cast specimens it was felt that a better understanding of many of the processes employed would be gained if the initial compacts had higher green density and lower binder content. Dies of various shapes were used to press pellets from $YBa_2Cu_3O_{7-x}$ powder. The pellets were sintered at 925 C for 5-24 hours. Sections from these pellets were cut for melt processing experiments.

It is a well known fact that one way of increasing the J_c of superconductors is to reduce the cross sectional area through which the current passes. Hence the need for fabricating a die that would give small cross section, high green density compacts was felt. Such a die, shown in Figure 13, was fabricated from A2 tool steel. The small area of the mold enables generation of high pressures at relatively low applied loads.
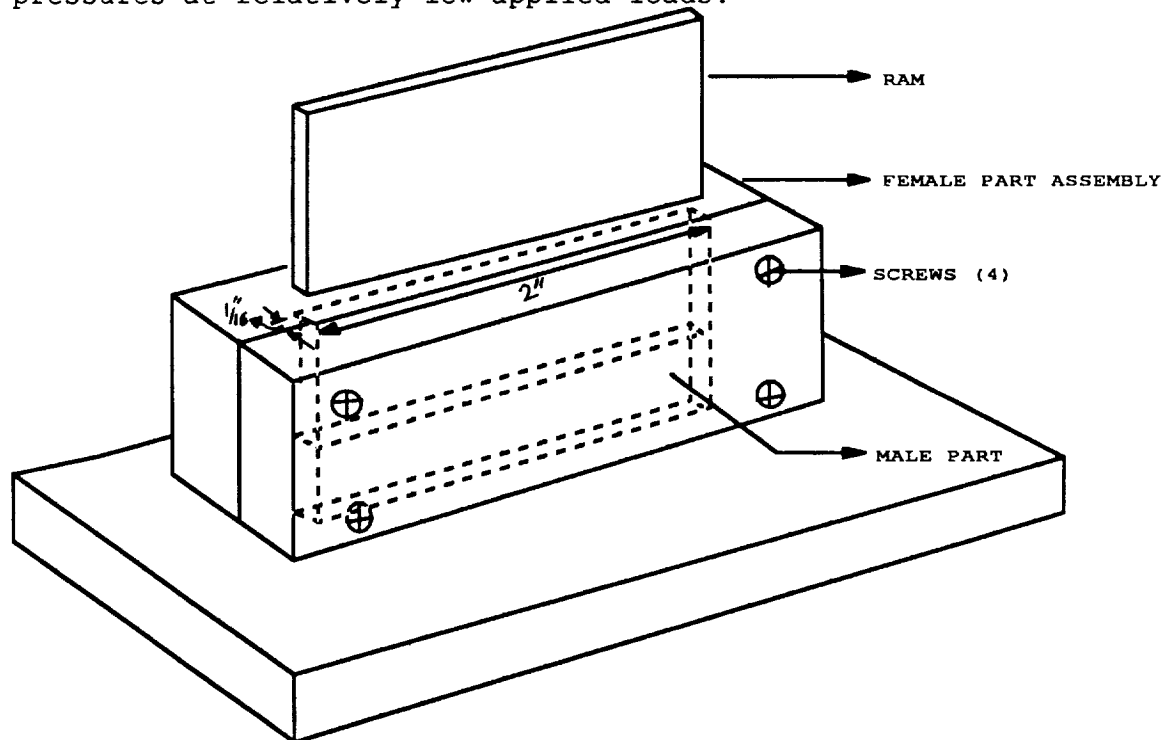

Figure 13. Schematic diagram of the die used for pressing small cross section bars from $YBa_2Cu_3O_{7-x}$ powder. The mold dimensions are 2"x 1/16".

The most widely followed melt growth procedure is as follows. A box furnace is pre-heated to 1,050-1,100 C and a crucible containing sintered bars of $YBa_2Cu_3O_{7-x}$ embedded in flux of the same material is rapidly introduced into the furnace. This is done to avoid formation of low melting eutectic phases in the Y_2O_3-BaO-CuO system during heating. The bars are melted for 5-10 min and the furnace temperature is rapidly reduced to 1030 C, the peritectic point, by keeping the door open. The samples are then cooled at a very slow rate (from 6 C/hr to less than 1 C/hr) to 980 C where they are soaked for 8-16 hr. A slow cooling to room temperature follows after the soak. Salama et al.[4] have reported J_c in excess of 18,500 A/cm^2 using this technique. Figure 14 shows the temperature profile of the process.
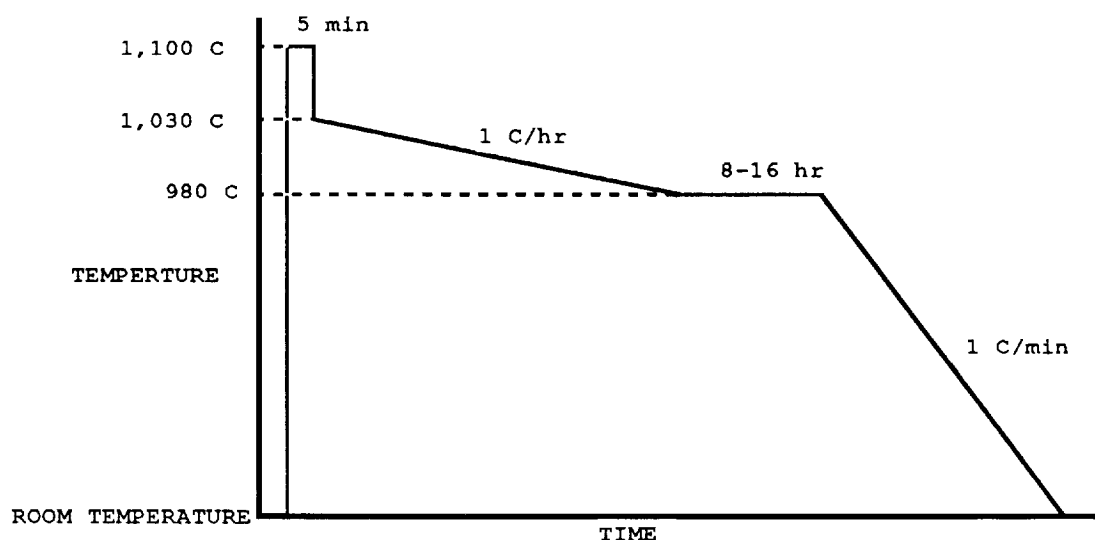

Figure 14. The temperature profile of a typical melt processing experiment. The units are arbitrary.

The purpose of performing melt processing on $YBa_2Cu_3O_{7-x}$ samples is to get preferred orientation of the grains in the a-b crystallographic plane. $YBa_2Cu_3O_{7-x}$ melts incongruently to Y_2BaCuO_5 and a $BaCuO_2$ rich liquid. Upon cooling the products of melting react to form $YBa_2Cu_3O_{7-x}$ again. Following peritectic reactions take place during the transformation;

$YBa_2Cu_3O_{7-x}$ -> Y_2BaCuO_5 + $BaCuO_2$ rich liquid

Y_2BaCuO_5 + liquid -> $YBa_2Cu_3O_{7-x}$
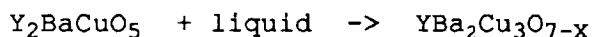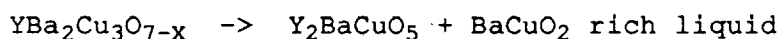
The intial runs made on sections cut from pellets did not

The intial runs made on sections cut from pellets did not show grain alignment. The large mass of the samples prevented rapid dissociation of $YBa_2Cu_3O_{7-x}$ according to the peritectic reaction. Only very small areas of the pellet seemed to show grain alignment as evidenced in Figure 15. Most of the samples were cooled at a rate of 0.1 C/min from 1,030 C to 980 C.
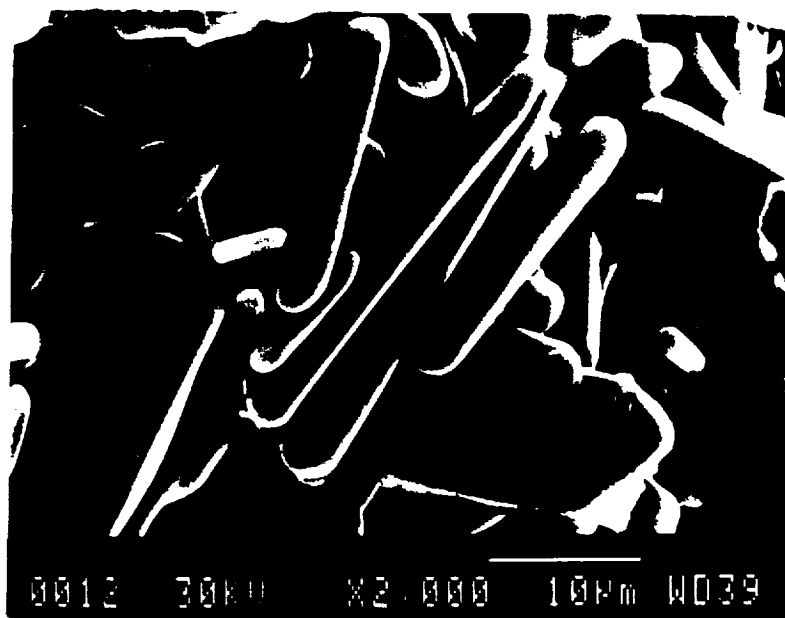

Figure 15. Microstructure of a melt processed pellet showing grain alignment in a very small region

An experiment involving sample MT231 resulted in very apparent grain alignment in an area measuring ~ 50-80 μm in thickness and ~ 0.8mm in width. The aligned region was 3-4 mm long. Figure 16 shows a large single crystal of $YBa_2Cu_3O_{7-x}$ that grew from the flux which did not get a chance to grow to the superconductor. The alignment of grains is displayed in Figure 17.

Silver paint contacts were applied to this specimen in such a way that the voltage sensing contacts were in the region of alignment, approximately 1 mm apart. The current leads were attached both to the aligned and the random region. The sample carried 1.65 A in this configuration at 77 K before it went normal. Similar measurement performed with all contacts on the randomly oriented region resulted in the sample carrying 0.58 A. The

same superconductor proves the fact that the grain aligned region has a higher J_c than the randomly oriented region.

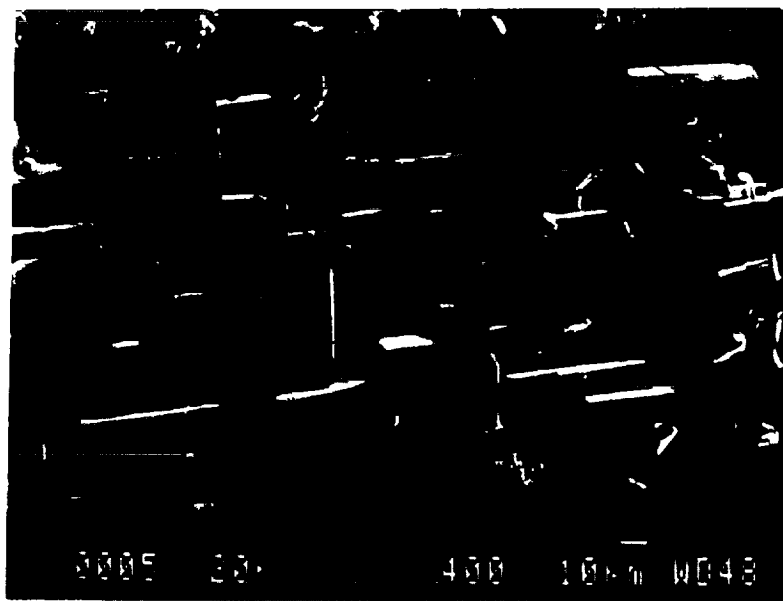Figure 16. A large single crystal of $YBa_2Cu_3O_{7-x}$

Figure 17. Microstructure of the grain aligned region of sample MT231

The situation can be modelled by considering an equivalent circuit where two regions, 1 and 2, in a superconductor having current densities J_{c1} and J_{c2} are connected in parallel. If J_c is lower than J_{c1}, the current in excess of $J_{c2}A_2$ (0.58 A in this case) will flow through region 1. The current density of region 1 can be computed by passing the current and sensing the voltage drop across region 1. Thus the current density of the aligned region in sample MT231 would be approximately 1.65/(0.005x0.1) or 3,300 A/cm^2.

In spite of success in achieving grain alignment the method of using a box furnace had to be abandoned due to certain drawbacks. The most serious concern is safety, since the furnace door has to be opened and closed at high temperatures several times before the temperature stabilizes. The damage the furnace heating elements and refractory may undergo due to rapid changes in temperature could shorten the furnace life.

A vertical tube furnace was designed and fabricated to create the conditions of melt processing as depicted by the time temperature profile shown in Figure 14. The process can be carried out very smoothly without the problems mentioned above. Figure 18 shows the schematic diagram of the two zone vertical tube furnace.
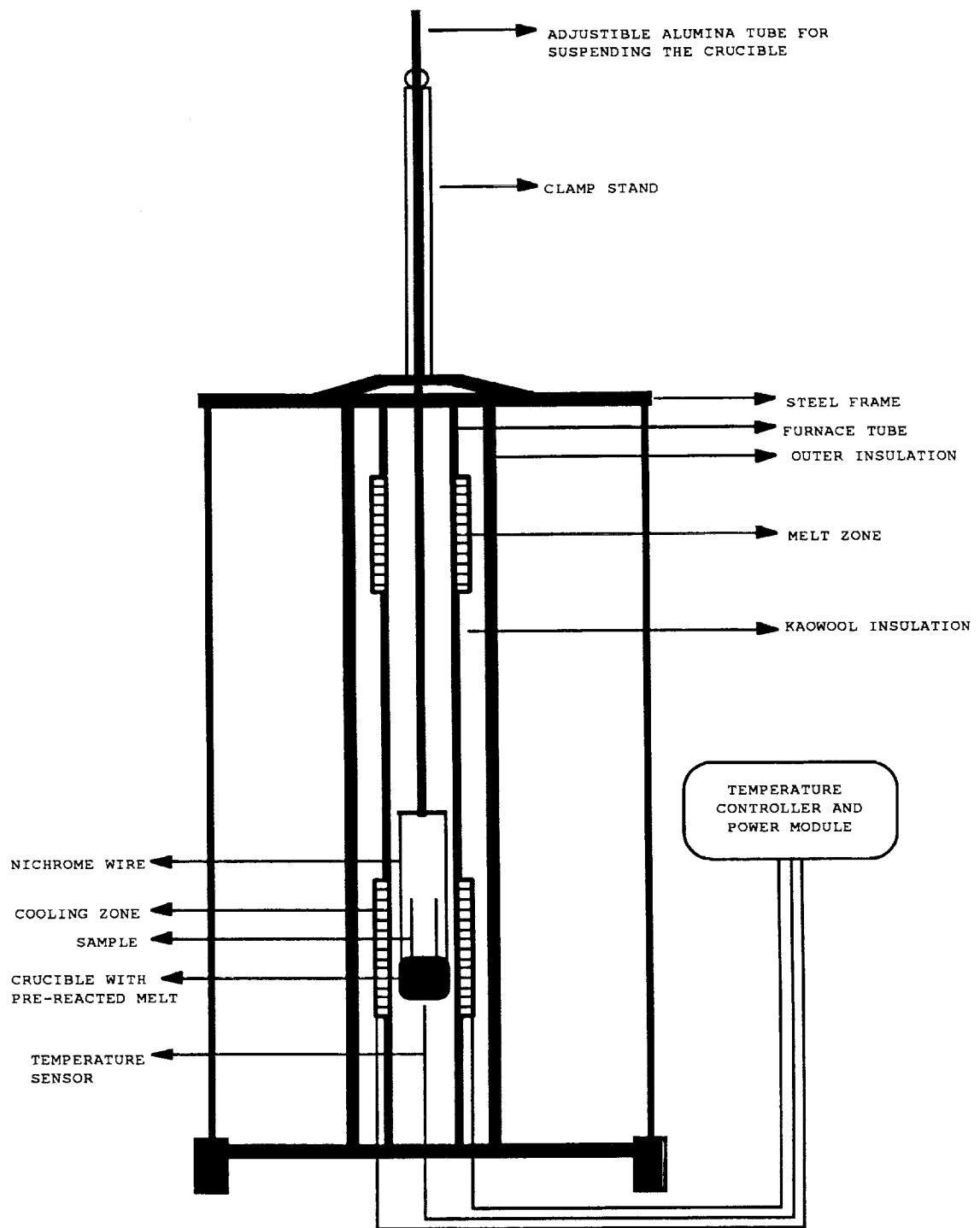
ADJUSTIBLE ALUMINA TUBE FOR
SUSPENDING THE CRUCIBLE

CLAMP STAND

STEEL FRAME
FURNACE TUBE
OUTER INSULATION

MELT ZONE

KAOWOOL INSULATION

TEMPERATURE
CONTROLLER AND
POWER MODULE

NICHROME WIRE

COOLING ZONE

SAMPLE

CRUCIBLE WITH
PRE-REACTED MELT

TEMPERATURE
SENSOR

**Figure 18. Schematic diagram of the two zone
vertical tube furnace designed and fabricated for melt
processing of $YBa_2Cu_3O_{7-x}$ bars.**

$YBa_2Cu_3O_{7-x}$ powder is melted in an alumina crucible,
approximately 0.5" in internal diameter at 1,150 C. Pre-sintered

fused. Thus further testing could not be performed on the sample. The J_c of the sample amounted to 1,944 A/cm^2 using the 52.5 A current value and a cross section of 0.12x0.225 cm^2. The length of the sample before the fusion of the current contact was 0.5 cm.

Figure 19 shows the grain aligned texture of sample MT242A. Figure 20 shows the I-V characteristics of the sample up to 52.5 A. The fluctuations on voltage axis are due to instrumental noise and the step like character of the analog output of the microvoltmeter that was employed for measuring the potential developed on the sample. It may be noticed that the noise level is less than 1 μV in absolute value.

The fabrication of high critical current specimens by melt processing has not been easily reproducible. The reason for difficulty in obtaining reliable, repeatable results is the need to start cooling exactly at the peritectic transformation point. If the slow cooling is started at a temperature even a few degrees higher than the peritectic point, the liquid phase may stay in the liquid form for too long a time. During this time large amount of liquid may flow away from the sample. This could upset the phase stoichiometry required for YBa$_2$Cu$_3$O$_{7-x}$ formation. On the other hand if the cooling is started at a temperature lower than the peritectic point, rapid nucleation and growth of YBa$_2$Cu$_3$O$_{7-x}$ can occur due to faster kinetics of reaction. In such a situation the texture development cannot be controlled and a randomly oriented sample will result. Thus for successful melt processing the peritectic point of each batch must be precisely established.

The most common method for determining the peritectic transformation point is DTA/DSC. A sharp drop in the DTA/DSC curve is noticed in the immediate vicinity of the transition. The sharp peak in Figure 8 for die pressed and later sintered YBa$_2$Cu$_3$O$_{7-x}$ is magnified in Figure 21 for detail. As mentioned on the curve the transformation occurs at 1009.3 C. Thus the cooling for that particular batch must start at no higher than 1,010 C or below 1,009 C.

Melt processing is a promising technique for fabricating high J_c products from die pressed samples. Experimention is in progress to establish the parameters for melt processing.

bars of $YBa_2Cu_3O_{7-x}$ pressed using the die in Figure 13 at 100,000 psi are embedded in the melt in the crucible after the latter is rapidly removed from the furnace. Up to four bars are embedded in the crucible per run. The crucible with the sample bars is then attached to the adjustible alumina tube with a nichrome wire. The alumina tube is mounted on a clamp stand. The melting zone (Zone 1) is maintained at 1,100 C and the cooling zone (Zone 2) at 1025-1030 C. The crucible is lowered in the Zone 1 where the samples melt for 2-5 min, after which it is quickly lowered in Zone 2. The samples are slowly cooled through the peritectic range in Zone 2. After completion of the cycle Ag-paint contacts are applied to the samples and annealing is performed in oxygen.

Sample MT242A, prepared as above, could carry 30 A (the maximum current available from the power supply) without going normal at 77 K. Further testing was performed using a larger power
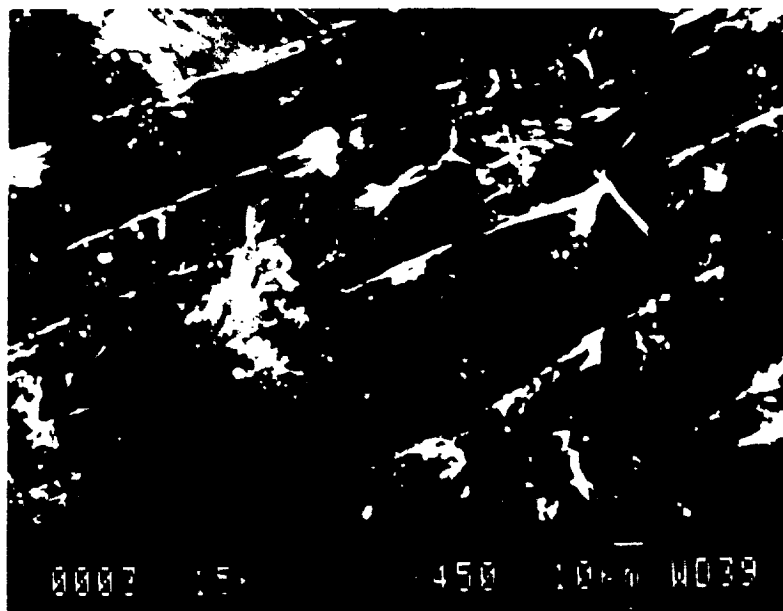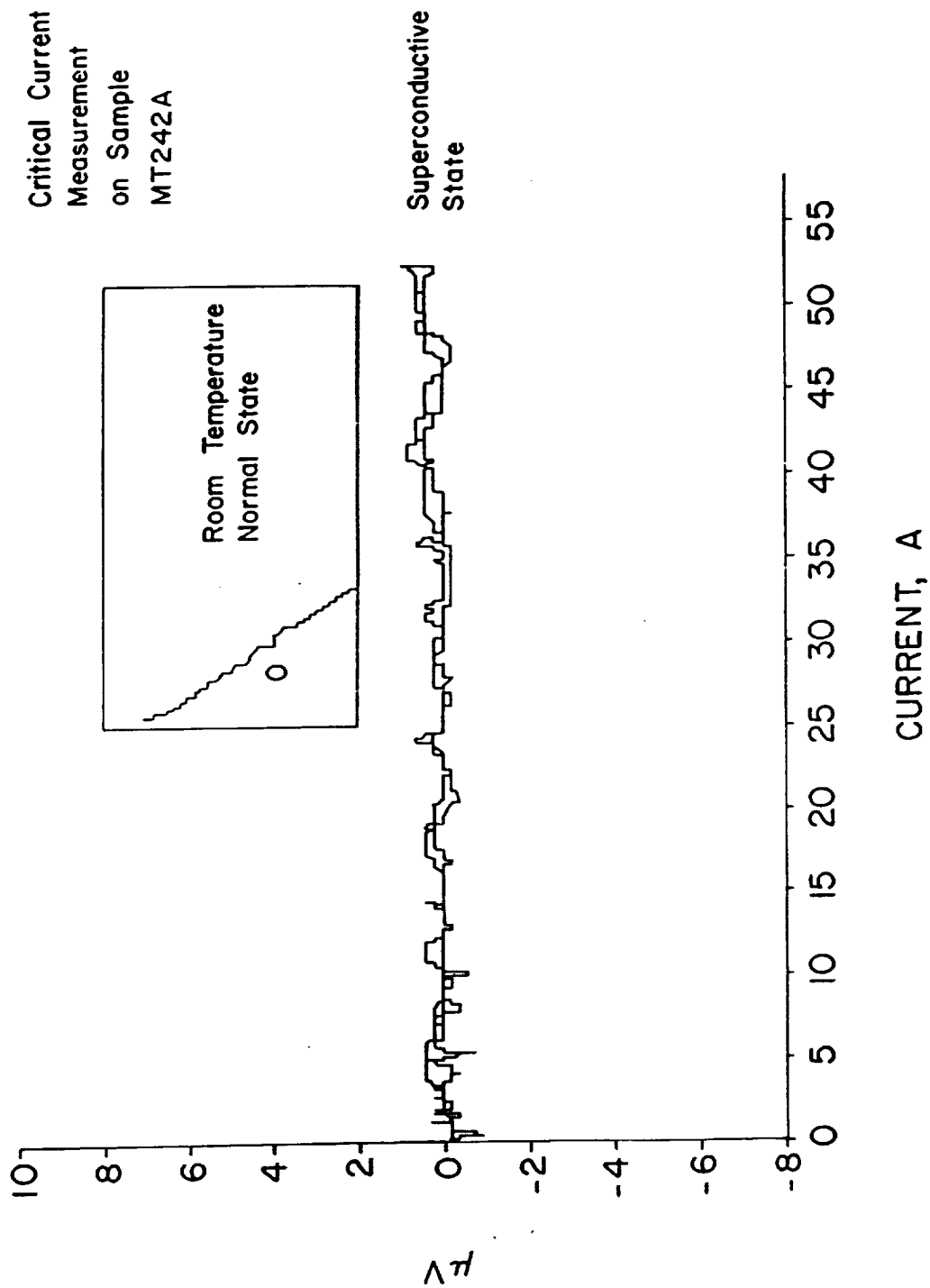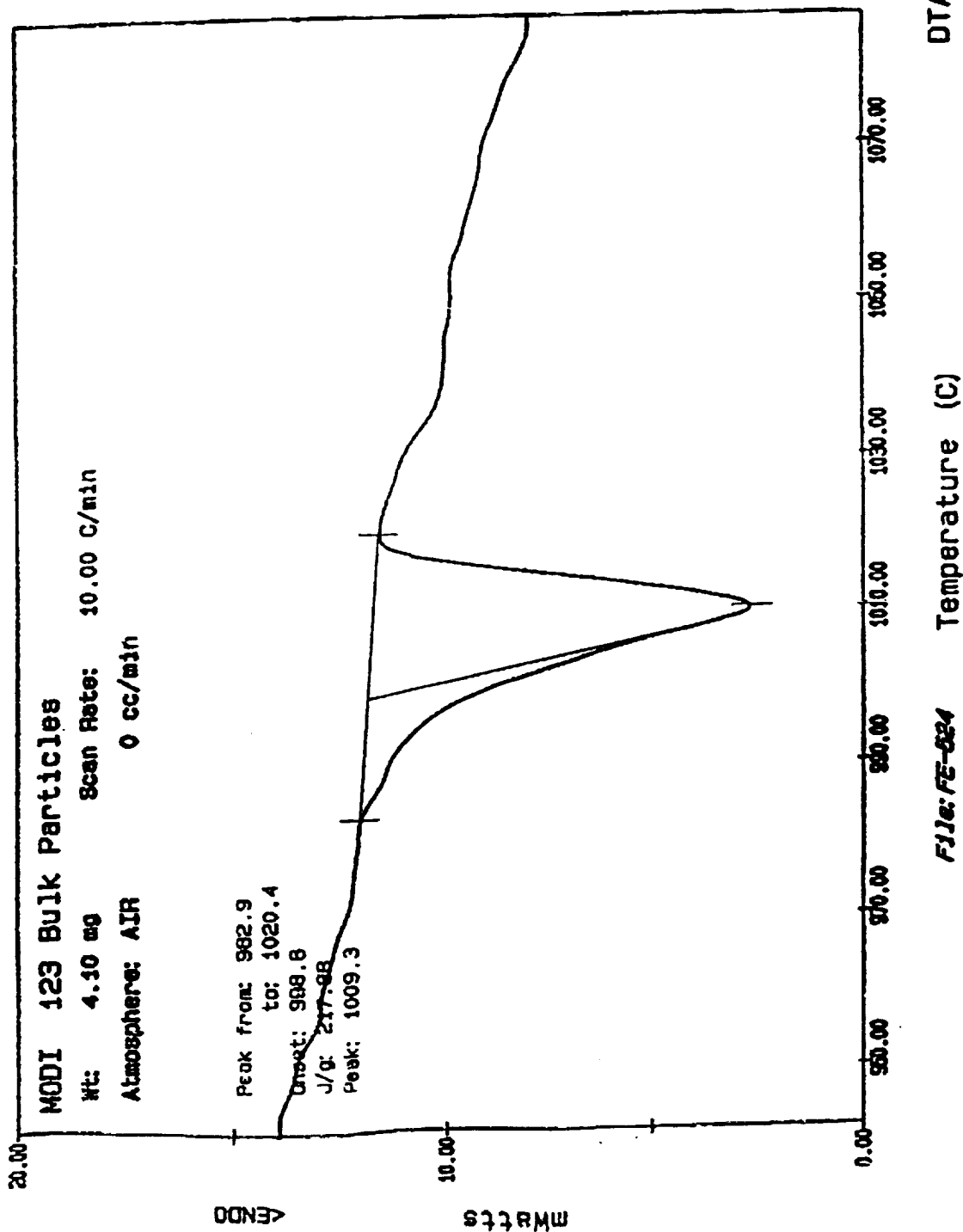

Figure 19. Microstructure of melt processed sample MT242A showing an aligned surface texture.

supply. The sample exceeded the limit of this power supply also, 52.5 A. Yet another power supply with capacity of 80 A was used. During testing with this source, a spike of current in excess of 60 A was generated and as a result one of the current contacts was

Fig 20 Transport Critical Current Measurement on Melt
Processed Sample MT242A

Critical Current
Measurement
on Sample
MT242A

Superconductive
State

Room Temperature
Normal State

μV

10

8

6

4

2

0

-2

-4

-6

-8

0   5   10   15   20   25   30   35   40   45   50   55

CURRENT, A

MODI 123 Bulk Particles

Wt: 4.10 mg   Scan Rate: 10.00 C/min

Atmosphere: AIR   0 cc/min

Peak from: 982.9
       to: 1020.4
Onset: 998.8
J/g: 217.88
Peak: 1009.3

FILE: FE-624   Temperature (C)

DTA

Date: SEP 10. 1990 10: 37AM Path: C: \PE\DATA\

Figure 21. An enlarged view of the peak of the curve shown
in Figure 8. This analysis can be used for exact
determination of the peritectic point of $YBa_2Cu_3O_{7-x}$
(courtsey John Buckley).

6 $YBa_2Cu_3O_{7-x}$-Ag COMPOSITES FORMED BY LIQUID PHASE ASSISTED SINTERING

It is now well established that large amount of silver can be added to $YBa_2Cu_3O_{7-x}$ without severely damaging the superconducting properties. Although silver has less than 1 atomic percent solid solubility in $YBa_2Cu_3O_{7-x}$, the excess silver can form a strong, stable, and highly conductive matrix. The transition temperature is depressed as a result of a silver addition, and J_c is improved due to silver carrying part of the current. Silver also assists in liquid phase sintering of the superconductor. The melting point of silver, 960 C, is ideally close to the processing temperature of the superconductor.

There have been conflicting reports about the amount of silver that should be added for achieving the best results. The reports suggest inclusion of silver from an insignificant amount to 30 percent by weight. In order to understand the role of silver in increasing the J_c, a new set of experiments was planned and is presently being executed. Twenty gram batches of nitrate solutions were mixed and added to these batches was silver nitrate to yield 1, 3, 5, 10, 15, and 30 % of silver by weight of the superconductor with nominal composition $YBa_2Cu_3O_{6.5}$. The powders were calcined at 925 C for 12 hr followed by an anneal at 450 C for 24 hr. Bars were pressed from the powders at 100,000 psi and processed under varying conditions of sintering temperature, soaking time, and cooling rate. Figure 22 shows the R vs T diagrams of silver doped samples. The samples were sintered at 940 C for 24 hours. It is observed from the plot that the transition temperature of the composite superconductors is reduced with an increase in the amount of silver. The room temperature resistance is in general lower for the specimens containing higher amounts of silver. This is due to the low resistivity of silver in the matrix. Following variables were used in processing the composites:

Sintering temperature; 925 C, 940 C, and 955 C

Soaking time; 5 hr, 24 hr.
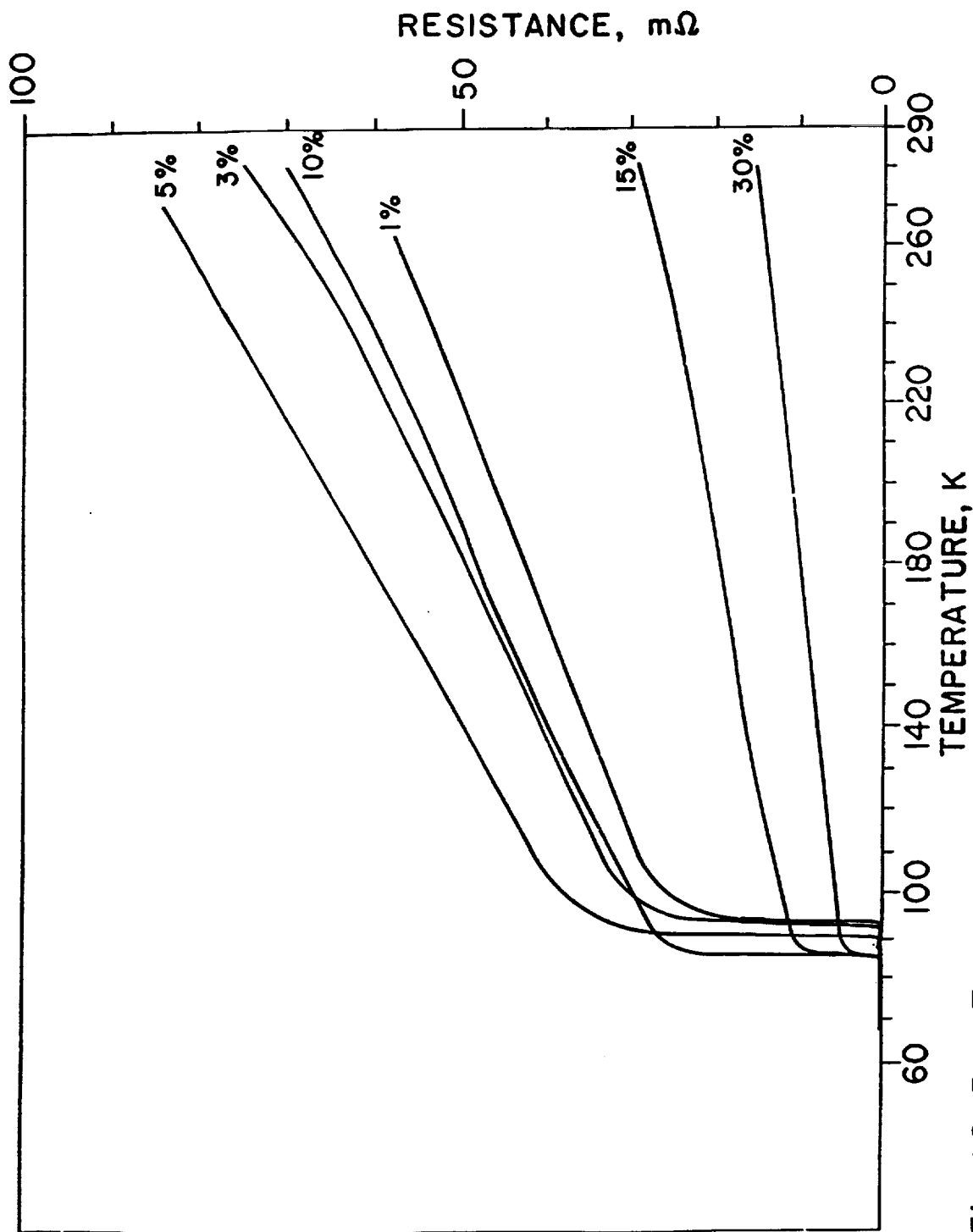
Cooling rate; 5 C/min, 2 C/min.

Fig 22 R vs. T measurements on $YBa_2Cu_3O_{7-x}$ -Ag composites.

The numbers at the begining of the curves refer to the

amount of silver in weight percent

Twelve possible combinations of processing conditions can be arrived at using the above variables. The numbers refer to sintering temperature, soaking time, and cooling rate, respectively. The combinations are listed below:

925,5,5	925,24,5	925,5,2	925,24,2
940,5,5	940,24,5	940,5,2	940,24,2
955,5,5	955,,24,5	955,5,2	955,24,2

The current densities measured on samples in batch (955,24,5) were very low so it was decided to avoid processing the last batch, i.e. (955,24,2). Silver paint contacts were sintered on the processed bars which were annealed in flowing oxygen for 24 hr at 450 C. The current densities were measured using the standard four point method. Figures 23, 24, and 25 depict the J_c values as function of processing conditions.
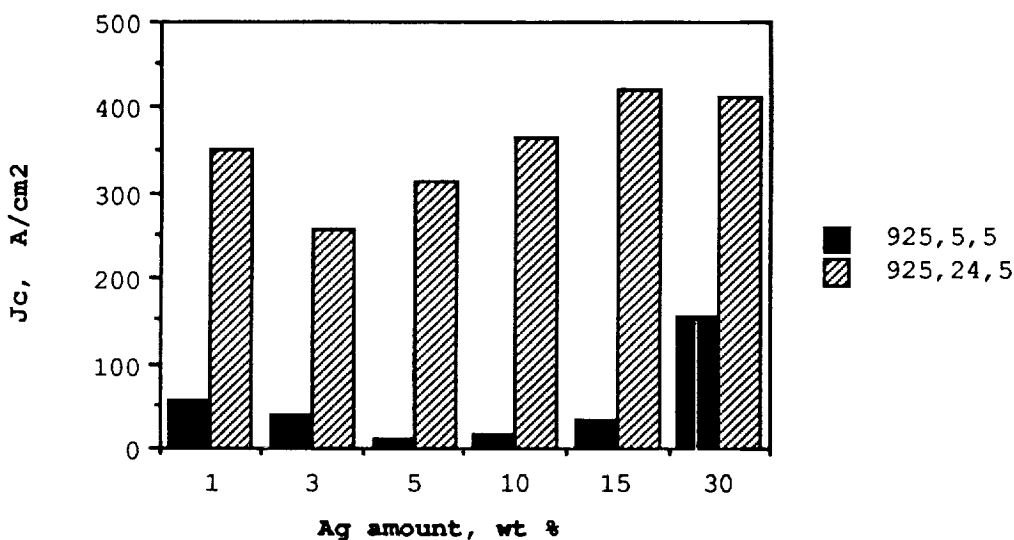

Figure 23. Effect of processing conditions on the current density of $YBa_2Cu_3O_{7-x}$-Ag composites.

The significance of processing at the right temperature can be understood by comparing the J_c values for the following batches;

Ag 1%, (925,5,5)   57 A/cm^2

Ag 1%, (940,5,5)   391 A/cm^2.

A look at the micrographs of the above two batches, as represented in Figures 26 and 27 respectively, shows that the 940 C
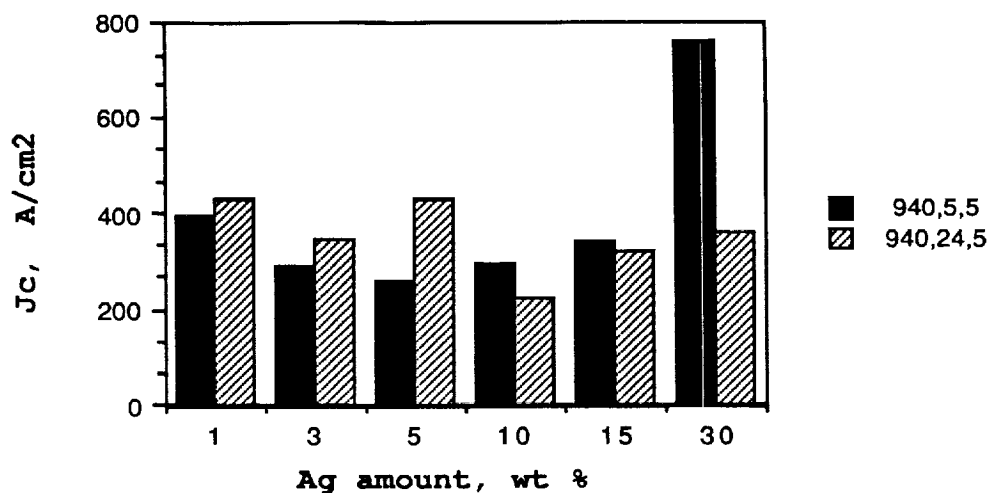
C-2

Figure 24. Effect of processing conditions on the current density of $YBa_2Cu_3O_{7-x}$-Ag composites.

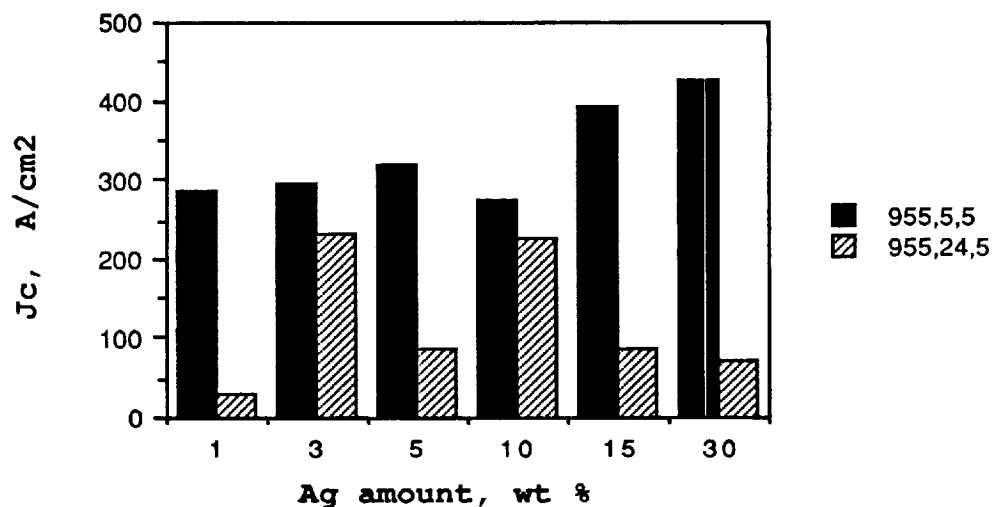**Figure 25. Effect of processing conditions on the current density of $YBa_2Cu_3O_{7-x}$-Ag composites.**

batch has less porosity and consequently higher J_c for the same amount of silver added.

The highest recorded J_c in $YBa_2Cu_3O_{7-x}$-Ag composites is 766 A/cm^2 in the batch containing 30% silver and processed under the conditions (940,5,5). Other batches are being sintered and will be evaluated.
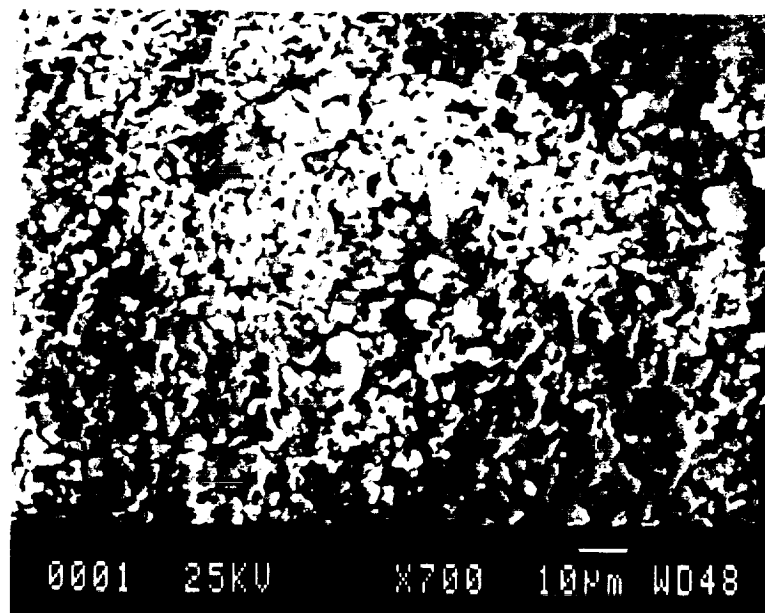
Figure 26. Microstructure of $YBa_2Cu_3O_{7-x}$-Ag sample containing 1% by weight Ag, processed at 925 C for 5 hr.
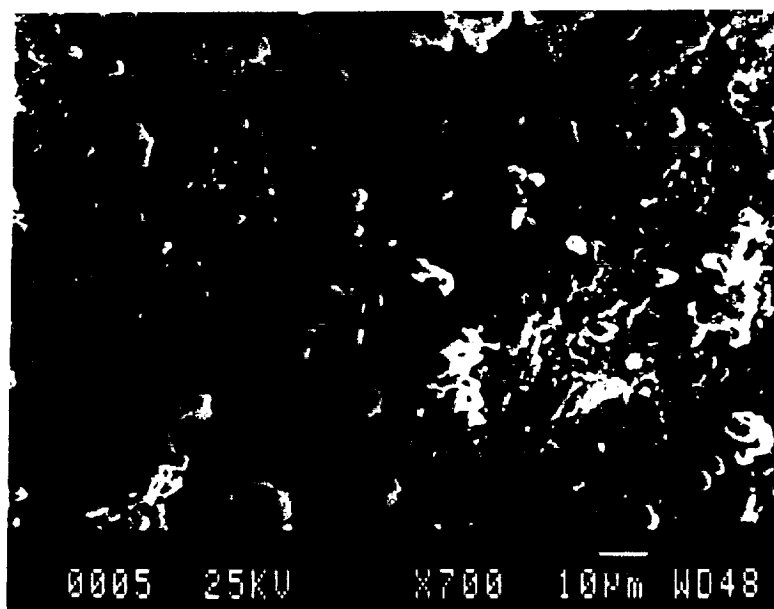

Figure 27. Microstructure of a sample from the same batch as in Figure 26 processed at 940 C for 5 hr

7 SUMMARY OF RESULTS

A variety of techniques and processes have been tried to fabricate high J_c circuit elements from the superconductor $YBa_2Cu_3O_{7-x}$. It has been possible to show J_c of up to 3,300 A/cm^2 in bulk $YBa_2Cu_3O_{7-x}$ samples. Following points summarize the results observed so far;

(1) the powders prepared by chemical co-precipitation of nitrate solutions of Y, Ba, and Cu are superior in terms of homogeneity, phase purity, calcining temperature and time, and particle size

(2) the current density of tape cast products is not very likely to reach higher than the presently observed level of 120 A/cm^2. The major reasons for low current density in such products are absence of compressive stress during the forming operation and the large scale void structure left behind by the burnt-off binder.

(3) addition of Ag/AgO/Ag$_2$O in the tape casting slurry may help in reducing the amount of porosity and may result in higher J_c values.

(4) melt processing of die pressed $YBa_2Cu_3O_{7-x}$ has resulted in grain alignment and consequently, high J_c. The highest J_c recorded on grain aligned specimens is 3,300 A/cm^2.

(5) precise information about the temperature at which the peritectic transformation of $YBa_2Cu_3O_{7-x}$ into Y_2BaCuO_5 and liquid occurs is required for getting the best results with the melt processing technique.

(6) silver addition to $YBa_2Cu_3O_{7-x}$ results in increase in J_c. The highest J_c recorded with silver addition,766 A/cm^2, is for the batch containing 30% by weight of silver and processed at 940 C for 5 hr. The samples were cooled to room temperature at .5 C/min and annealed in flowing oxygen for 24 hr.

REFERENCES

1. Laibowitz, R.B., et al.; Phys. Rev. B, 35, 8821(1987).

2. McN Alford, N., et al.; "The Effect of Density on Critical Current and Oxygen Stoichiometry of $YBa_2Cu_3O_x$ Superconductor"; Nature, Vol 332, No 6159, pp 58-59.

3. Jin, S., et al.; " High Critical Currents in Y-Ba-Cu-O Superconductors"; Appl. Phys. Lett. 52(24), pp 2074-2076.

4. Salama, K., et al.; "High Current Density in Bulk $YBa_2Cu_3O_x$ Superconductor"; Appl. Phys. Lett. 54(23), pp 2352-2354.

5. Knorr, D.B., et al.; " Texture Analysis of Magnetically Aligned $RBa_2Cu_3O_{7-x}$ by Pole Figure Technique"; Supercond. Sci. Technol. 1(1989) 302-306.

6. Farreira, J.M., et al.; " Magnetic Field Alignment of High-Tc Superconductors $RBa_2Cu_3O_{7-x}$ (R=Rare Earth)"; Appl. Phys. A, 47, 105-110(1988).

7. Dinger, D.R., et al.; "Particle Packing: I-Review of Packing Theories"; Presented at Fine Particles Society, 13th Anuual Meeting, Spring 1982, April 12-14, Chicago.

8. Simmins, J.J., et al.; "The Effect of Silver Substitution for Copper on the Crystal Structure of $Ba_2YCu_3O_{7-x}$ Superconductor"; Proceedings of The Second Annual Conference on Superconductivity and Applications, New York State Institute on Superconductivity, April 18-20, 1988, Buffalo, pp 89-93.

9. Ishii, Mamoru, et al.; " Fabrication of Superconducting $YBa_2Cu_3O_{7-x}$ Films by a Tape Casting Method"; Jap. Jour. Appl. Phys., vol 26, No 12, December 1987, pp L1959-L1960.

10. Beckers, G.J.J., et al.; " Critical Current Density in Tape Cast $YBa_2Cu_3O_{7-x}$ Superconductors"; J. Mater. Sci. Lett., 7(1988), pp 703-704.

11. Ishii, Mamoru, et al.; "Critical Current Density and Microstructure of Superconducting $YBa_2Cu_3O_{7-x}$ Films Prepared by a Tape Casting Method"; Jap. Jour. Appl. Phys., vol 27, No 8, August 1988, pp L1420-L1421.